MICROWAVE FREEZE-DRYING OF AQUEOUS SOLUTIONS

By

James P. Dolan

THESIS

Submitted to
Virginia Polytechnic Institute & State University
in fulfillment of the requirements
for the degree of

MASTER OF SCIENCE

in

Department of Mechanical Engineering

APPROVED:

Elaine P. Scott, Chairperson

James R. Thomas

William C. Thomas

September 20, 1994
Blacksburg, Virginia

MICROWAVE FREEZE-DRYING OF AQUEOUS SOLUTIONS

by

James P. Dolan

Committee Chairperson: Elaine P. Scott
Mechanical Engineering

(ABSTRACT)

The freeze-drying process has been plagued with problems, such as long drying times and inefficiency. Microwave freeze-drying has proven its potential as way of reducing long drying times associated with freeze-drying, and as a result, there has been a considerable amount of work done to increase its use in industrial applications. However, it is not widely utilized for drying of pharmaceuticals, which appear to be better suited to microwave freeze-drying than foods.

This paper discusses the results of applying microwave freeze-drying to an aqueous solution, as well as how various freezing rates affect freeze-drying characteristics. Results show that microwave freeze-drying can greatly reduce the time required to freeze-dry an aqueous solution while maintaining a high product quality. The investigation into the effects of different freezing conditions shows that different physical characteristics in the dried product can be achieved through varying the freezing rate.

ACKNOWLEDGEMENTS

I would like to thank all the people who made it possible for me to achieve this milestone, and I would especially like to thank everyone who has helped me along the way.

I would like to thank Dr. Elaine P. Scott for all her guidance and technical assistance over the last two years and for making my experience as a graduate research assistant a pleasurable one.

I would also like to thank my friends in the lab for make the days I spent there a little more enjoyable: Zoubeir Saad, John Ludman, Debbie Moncman, Joe Hanak, Sandrine Garcia, Kasey Lee, and Greg Walker.

I would like thank all my friends outside the lab who made Blacksburg Virginia a great place to be. Most of all I would like to thank Robert Bennett, Anne-Claire Christiaen, Benoit Girardin, Delphine Justin, Diane Peters, Anne Vilette and the New River United FC.

I would like to give a special thanks to my parents, Thomas and Sandra Dolan, for all their love, support and constant encouragement.

In addition, I would like to say that the financial support provided by the Creative Match Grant of Virginia Tech and the Witaker Foundation is greatly appreciated.

TABLE OF CONTENTS

LIST OF TABLES

LIST OF FIGURES

NOMENCLATURE

C	Moisture concentration (g/cm^3)
E	Electric field strength (V/cm)
E	Rate of energy consumption (W)
G	Volumetric heat generation (W/cm^3)
h_{ig}	Enthalpy of sublimation (kJ/kg)
L	Sample thickness (cm)
L_C	Cavity length (cm)
L_P	Coupling probe length (cm)
m	Sublimation rate (g/h)
$\langle P \rangle$	Time averaged absorbed power density (W/cm^3)
P_{eq}	Equilibrium vapor pressure (Torr)
P_i	Incident power (W)
P_{min}	Minimum measured pressure (Torr)
P_r	Reflected power (W)
P_{sat}	Saturation pressure (Torr)
P_t	Total Power (W)
P_{tot}	Total pressure (Torr)
P_v	Vapor pressure (Torr)

$\boldsymbol{r}$	Location vector
R_p	Mass transfer resistance of the dried product (Torr*h/g)
S	Freezing rate (°C/min)
t	Time (h)
$t_{0.85}$	Time required to achieve the temperature difference $T_{0.85}$ (°C)
T^*	Temperature of the cooling medium (°C)
T_0	Initial sample temperature (°C)
$T_{0.85}$	Eighty-five percent of the difference between T_0 and T^* (°C)
$T_{measured}$	Temperature measured in the sample (°C)
T_{sat}	Saturation temperature (°C)
w	Weight of the sample (g)
X	Sublimation front position (cm)
x_v	Mole fraction of water vapor
ε''	Effective material loss factor
ε_0	Dielectric constant of free space (F/m)
ω	Excitation frequency (Hz)

Subscripts

D	Dried layer
F	Frozen layer
s	Surface
i	Interface

Chapter 1

Introduction

Freeze-drying (lyophilization) is a process which removes water from a moisture laden product, usually for the purpose of preservation. By removing the water, the product becomes more stable at room temperature. The final product is light and porous and maintains its original shape. The process consists of three stages: freezing, primary drying and secondary drying. During the primary drying stage, frozen water is sublimated. This stage is the most time consuming part of the process. The secondary drying stage is the desorption of bound water. Bound water is attached to the dried material by electrostatic forces or hydrogen bonds and removed by evaporation after the ice has been sublimated.

Freeze-drying is a common process in both the food and pharmaceutical industries. In the pharmaceutical industry, the production of biochemicals involves many processing steps including extraction, precipitation, fractionation, and purification. The end result is an aqueous solution that is usually very dilute. The water must then be removed from solution leaving the dried product to be further processed or packaged. A common

application in the food industry is freeze-dried coffee. Freeze-drying of coffee greatly extends its shelf life and preserves flavor and aroma. Another common and important use of freeze-drying is in the preservation of biomedical material, such as blood plasma. In fact, since freeze-drying stops the growth of microorganisms, it is generally considered that freeze-dried blood plasma is superior to stored liquid plasma (Mellor, 1978).

The advantages to freeze-drying are: the product is protected against chemical decomposition, the distribution of components in the dried product remains unchanged, processing temperatures are low, and the moisture content can be reduced to very low levels. Generally, the lower the moisture content, the more stable the material. In most cases, the final product is stored at room temperature, thus eliminating the high energy costs associated with storage of products in freezers. However, the cost of freeze-drying is very high compared to other drying processes because of high equipment costs and long drying times (Pikal, 1983). Reduction of the high cost of freeze-drying is the motivation behind much of the freeze-drying research that has been done in the past.

Another advantage to freeze-drying, particularly pertaining to foods, is that the process maintains the structural integrity of the material. This allows the material to be rehydrated and returned to nearly its original state at a later time. Thus, freeze-drying can not only aid in preservation of food, but also facilitate its transportation by reducing is weight.

Although the basic concepts of freeze-drying are known, the details are far from being well understood. Fundamental knowledge in some areas concerning the physical processes of freeze-drying are not complete. As a result, freeze-drying equipment often

lacks the ability to produce high quality dried products for a range of product types. The optimum parameter settings are usually found by trial and error, and some manufacturers will even suggest that a product be stored in a freezer *after* it has been freeze-dried!

There have been many attempts to improve the efficiency of the freeze-drying process. It has been determined that the processing time can be decreased by improving the transfer of heat to the sublimation front in the material. Experiments with pulsing pressure and various mechanical devices for improving heat transfer have been semi-successful, but the most promising method of improving heat transfer is by the use of microwave energy to supply heat directly to the material.

The use of microwave energy to facilitate the freeze-drying process has been studied by many previous investigators (Copson, 1957; Hoover et al., 1966; Ma and Peltre, 1975; Ang et al., 1977). It has been demonstrated that microwave energy has a great advantage over conventional types of heating. Microwaves have the ability to generate heat volumetrically throughout the sample, overcoming heat transfer resistances associated with the conventional process (Copson, 1958; Hoover et al., 1966). Previous studies have focused on the application of multimode microwave cavities to freeze-dried bulky foods and the development of mathematical models (Ma and Peltre, 1973, 1975a and 1975b; Ang et al. 1975).

One accomplishment of previous research is the development of a combined radiant and microwave freeze-drying system by Ma and Chang (1985). A similar system is currently being used in an industrial application to freeze-dry coffee (Owusu-Ansah, 1991). However, in the case of food, there are often problems associated with the

nonhomogeneous material and odd geometric shapes that can cause uneven heating. Since aqueous solutions are more uniform and frozen in cylindrical vials, they are easily adaptable to microwave freeze-drying, suggesting that microwave freeze-drying could be more suitable to the pharmaceutical industry. However, there is little evidence that there has been any significant research activity into this application of microwave freeze-drying.

The goals of this research are to apply microwave freeze-drying to aqueous solutions typical of those encountered in the pharmaceutical industry and to demonstrate how this technology can be used as a fundamental research tool. The specific goals of this project are to:

1. Develop an experimental microwave freeze-drying apparatus and procedures,
2. Study the feasibility of applying microwave freeze-drying to aqueous solutions, and
3. Study the effects of freezing rates on the freeze-drying characteristics of pharmaceuticals.

Once an apparatus capable of producing the required conditions for freeze-drying has been developed, experiments are needed. The results of these experiments will help produce a more detailed description of the heat and mass transfer present in the process. This fundamental knowledge can then aid in the design of improved freeze-drying equipment and better procedures for determining the optimum operating conditions of the equipment.

Chapter 2

Literature Review

Many previous studies have been performed that pertain to microwave freeze-drying. However, there appears to be no published research into the application of microwave freeze-drying to aqueous solutions. On the other hand, there are many studies on freezing and conventional freeze-drying of aqueous solutions. Freezing is a dominant factor in determining the physical characteristics of the dried product. This chapter contains a review of work relevant to: freezing of aqueous, conventional freeze-drying of aqueous solutions and microwave freeze-drying of foods.

2.1 The Effects of Freezing Rates

The freezing rate can be an important parameter in the freeze-drying process. However, many freeze-drying studies, especially microwave freeze-drying studies, do not include investigations into freezing rates. However, there have been studies dealing with the physical chemistry of freezing and how the physical changes caused by varying the freezing rate can affect freeze-drying characteristics.

One study on the influence of the freezing rate on product quality was made by Thijssen and Rulkens (1969). Specifically, the study focused on the effect of the freezing rate on the rate of sublimation and flavor retention in freeze-dried dextrin solutions. Using dextrin solutions with concentrations between ten and forty percent by weight, it was found that with a decrease in the freezing rate, the mean pore size increased in the dried material. The increase in pore size resulted in an increase in wall thickness between the pores and an increase in the drying rate. The recommendation of Thijssen and Rulkens is that the freezing rate should be kept as low as possible for the best aroma retention.

An overview of the basic principles of freeze-drying was made by Franks (1989). Here, Franks discusses the importance of understanding the freezing process. He also explains how the quality of the final product can often be improved by simple changes in the formulation or the freezing and drying conditions.

Kochs et al. (1993) studied the influence of the freezing process on vapor transport during sublimation in vacuum freeze-drying of macroscopic samples. The vapor transport properties varied with local differences in the freezing conditions. It was found that there could be large differences in the local diffusion coefficients for a single macroscopic drying sample. Also, it was noted that a decrease in the freezing rate lead to a significant shift in diffusion coefficients to higher values and a corresponding decrease in drying times.

2.2 Conventional Freeze-Drying of Pharmaceuticals

Vial freeze-drying of aqueous solutions is a common processing step in the pharmaceutical industry. Here, freeze-drying usually involves vials of a solution placed on a tray which is then placed on a shelf in a freeze-drier. The shelf provides both cooling to freeze the liquid and heating to sublimate the ice. There has been significant research on this type of freeze-drying. Like freeze-drying of foods, freeze-drying of pharmaceuticals is slow and expensive. A better understanding of the heat and mass transfer that takes place during the drying process can lead to the design of improved equipment and economical processing costs.

2.2.1 Heat and Mass Transfer

In an attempt to gain a better understanding of the physical chemistry of freeze-drying, Pikal et al. (1983) measured sublimation rates for freeze-drying of aqueous solutions. In this study, an attempt was made to determine the relation between mass transfer resistance and the thickness of the dried product. It was found that there were two basic type of curves; one showed a generally linear relationship between mass transfer resistance and thickness and the other was concave toward the thickness axis. For each of these two basic types of curves there were two variations:

A) linear

Type I) linearly increasing for the entire drying process

Type II) initial sharp decrease in resistance from a high value to a low value and then a constant positive slope for the rest of the drying process

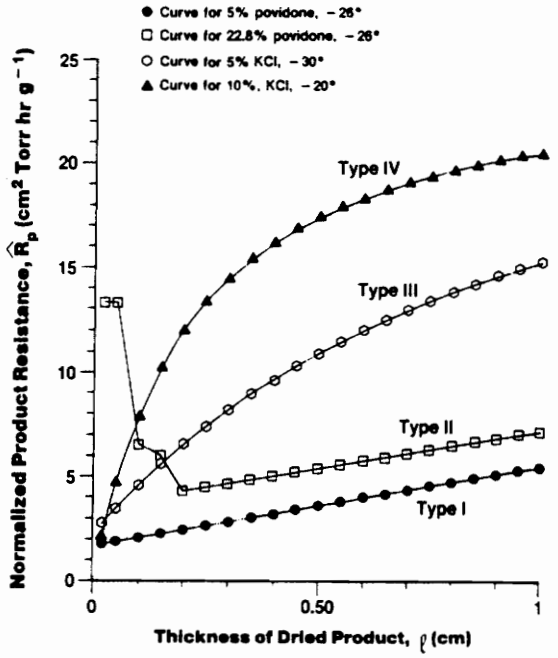

Figure 2.1 Product resistance vs. dried product thickness

B) concave toward the thickness axis

Type III) gradual curve

Type IV) sharp curve

Figure 2.1 shows the four types of curves found by Pikal et al. These results do not confirm the notion that resistance is independent of temperature and directly proportional to the thickness. However, the sample was very small compared to typical vial samples.

Subsequent work focused on heat and mass transfer in vial freeze-drying using slightly modified conventional vials (Pikal et al., 1984). This experimental study evaluated the mass transfer coefficients for several different semi-stoppered vials, the mass transfer resistance of the chamber-to-condenser pathway in a laboratory freeze-drier

and vial heat transfer coefficient as a function of chamber pressure for several types of vials. It was determined that the temperature distribution in the frozen product is adequately described by a constant temperature gradient in the vertical direction and the thermal conductivity of ice.

The previous studies focused on the primary drying stage. Pikal et al. (1990) studied the secondary drying stage, particularly the investigation focused on the dependance of the drying rate on temperature and pressure. It was found, for the materials used, that the drying rate during the secondary drying stage did not depend on pressure, but on temperature. In fact, it was recommended that the common practice of using pressures as low as possible during secondary drying not be used because of the possibility of transferring stopper components to the product.

2.2.2 Process Control

Control of the freeze-drying process requires knowing how the product will behave with respect to pressure, temperature and product size. Temperature is often limited by a eutectic or glass transition temperature and pressure can be limited by the allowable degree of solid entrainment. However, pressure and temperature are coupled, and it is difficult to predict how one will react to a change in the other. As a result, determining the optimum operating conditions is often a trial and error procedure.

Pikal (1985) described the use of laboratory data in freeze-drying process design. A computer program was written that would use certain experimental data to determine the optimum control strategy for a given product. Sublimation rates, temperatures and

pressures as a function of time are predicted for trial processes not studied experimentally.

An attempt to clarify some ambiguities on the subject of chamber pressure was made by Livesey and Rowe (1987). In their discussion, they argue that the reduced drying times observed when system pressure is increased in vial freeze-drying are a consequence of improved heatflow between the shelf and vial base. When the process is heat transfer limited, a higher pressure can improve heat flow to the frozen product. When the dried layer thickness becomes large, the process becomes limited by mass transfer and lower pressures can improve the rate of vapor flux leaving the material.

Roy and Pikal (1989) investigated the use of an electronic moisture sensor to determine the end point of sublimation in vial freeze-drying of aqueous solutions. It was found that the moisture sensor has the sensitivity and the precision to provide an unambiguous criterion for the end of primary drying. The moisture sensor is useful since the common method of endpoint determination is by the use of temperature sensors and often the vials with the temperature sensors will dry faster than the vials without temperature sensors. Removal of vials that still contain ice will result in product loss and will lower the efficiency of the equipment.

2.3 Microwave Freeze-Drying

The primary reason for use of microwave energy in freeze-drying is that the removal of the heat transfer limitation by using microwave heating is superior to conventional accelerating methods (Peltre et al., 1977). With radiant or conductive heat transfer, heat transfer is dependant on the temperature gradient between the phase front

and the heat source. Since the material is usually heat sensitive, high temperatures can not be tolerated and thus temperature gradients are small and the process is rate limited by heat transfer. Microwave heating eliminates problems associated with heat transfer and the process becomes one limited by mass transfer. However, this is a result that has been determined primarily through experimentation with microwave freeze-drying of food. This section discusses previous microwave freeze-drying research based on experiments with food.

Arsem and Ma (1980) published a brief review of microwave freeze drying. This review covers experimental, mathematical and economical studies. Sunderland (1982a) also presented a review of microwave freeze-drying. This review included an evaluation of past work and recommendations for future work. In addition, Peltre et al. (1977) and Sunderland (1982b) published economic studies of microwave freeze-drying and made a comparison to conventional freeze-drying. The results show that the use of microwave energy offers a significant cost reduction over a conventional process.

2.3.1 Analytical Studies

This section discusses analytical studies of microwave freeze-drying. It starts from early attempts to analytically predict temperature gradients and drying times for microwave freeze-drying of certain foods, primarily beef. Models have been developed based on pseudo-steady state and transient conditions. Also, some computer simulations have produced data that compares well with experimental data (Arsem and Ma, 1990).

Ma and Peltre (1973) presented a mathematical model to describe the freeze-

drying process with volumetric heating. This model is derived from a one-dimensional unsteady state analysis. The calculations made were for beef. Comparisons were made between two different microwave power inputs, two initial temperatures and two values of diffusivity in the dried layer. They plotted typical temperature and moisture concentration profiles and determined that drying times could be reduced by four times over conventional freeze-drying. Later, this model was improved by allowing for the transport and dielectric properties to vary with both time and location in the sample as a function of temperature and pressure (Ma and Peltre, 1975b). This study was the first detailed theoretical study of microwave freeze drying accompanied by an experimental investigation (Ma and Peltre, 1975c).

Ang et al. (1977) also conducted a theoretical and experimental investigation into microwave freeze-drying of beef. The model presented by Ang differs from the one developed by Ma and Peltre (1975b). Ang's model is a two dimensional model that takes into account the directionality of conduction in the meat due to the grain structure. It was found that anisotropy has a strong influence on the quality of the freeze-dried beef. The temperature profiles found by Ang et al. (1977a) are very similar to those found by Ma and Peltre (1975b).

A computer simulation of the freeze-drying of beef was presented by Ma and Arsem (1982). This simulation involved a freeze-drying system that combined both radiant heating and microwave heating. The new model included multicomponent sublimation in order to account for solids entrained in the vapor flux. Good agreement was found between the simulation and experimental data when solid entrainment was

included in the model.

A review of mathematical models of freeze-drying, as well as a mathematical analysis of a combined microwave and radiant freeze-drying was presented by Arsem and Ma (1990). They compared three drying curves. One was experimental data, one was a prediction without entrainment and one with entrainment, for three different conditions for drying beef. In all three cases, the prediction with entrainment gave much better agreement with the experimental data.

In another analytical study, Scott (1994) produced an exact one dimensional solution to a problem involving sublimation with volumetric heating within a semi-infinite porus medium. A sensitivity study was also performed.

2.3.2 Experimental Investigations

In 1957, Copson and Decareau demonstrated that the heat of sublimation can be provided by microwave energy. This effort demonstrated that the use of microwave energy at 2450 MHz permits the rapid dehydration of some foods not easily handled by conventional freeze-drying. Also, it was noted that the application of microwave energy seemed to be limited by mass transfer and not heat transfer. Copson (1958) examined some of the operating parameters of microwave freeze-drying. This research involved an explanation of dielectric properties and an attempt to describe microwave heating during the freeze-drying process in terms of the dielectric properties. The results show a 75 percent reduction in drying time for beef compared to the same product dried by conventional freeze-drying.

Hoover et al. (1966a) found drying rates to be 3-13 times faster than radiant freeze-drying for chopped beef patties, potato patties, shrimp, peas and coffee extract. These experiments were conducted using frequencies of 915 and 632 MHz. These frequencies were used, because lower frequency equipment provided economic advantages. In Hoover et al. (1966b), the results of the previous paper were discussed and it was determined that engineering data derived from these results show that microwave energy can possibly provide cost savings over conventional processes. Also, these data were used to develop and test an intermediate-sized microwave cavity. These tests demonstrated the feasibility of microwave freeze-drying for several types of food and that the use of thick bed depths can increase food-handling capability by about one order of magnitude over that possible with conventional freeze-drying.

Gould and Kenyon (1971) studied the relationship between microwave gas breakdown and microwave field strength. They concluded that frequency has a strong effect on the economics of microwave freeze-drying and 2450 MHz appeared to be better than 915 MHz from a theoretical standpoint. Many parameters affect the point at which breakdown is most likely to occur in the freeze-drying process. Some of these are input power, the gas temperature, pressure and composition, sublimation rate, dielectric constants and loss factors for the material.

In the experimental investigation by Ma and Peltre (1975c), several significant points were brought out. First, it was demonstrated that for beef meat slabs, significant reductions in drying time could be achieved. Also, there was some investigation of the controlling parameters. It was found that shorter drying times could be achieved if the

pressure was higher, 1 Torr rather than 0.2 Torr, for the same microwave power. Also noted was that the diffusivity will vary significantly depending on the choice of meat and most of all the rate of freezing.

Ang et al. (1977b) also made an effort to determine experimentally how the freeze-drying process and the final outcome was affected by field strength, sample size and chamber pressure. They suggest a low pressure and a high field strength to ensure low temperatures in the sample and enable the use of high field strengths to shorten the drying time.

The optimization of microwave freeze-drying was investigated by Ang et al. (1978). It was determined that the drying rate cannot be increased by simply increasing the power over the entire run. However, higher field strengths could be achieved, compared to previous investigations (Ang et al., 1977b; Ma and Peltre, 1975c). This was done by initially using a high field strength and decreasing the power over time, thus increasing the magnitude of the average field strength.

In the comparison of analytical and experiment data, it was found that drying rates were sometimes higher than what was theoretically possible (Arsem and Ma, 1985). Arsem and Ma found that solid entrainment was the cause of this phenomena. A detailed investigation of the solid entrainment phenomena and the formation of aerosols during microwave freeze-drying of beef was conducted. It was discovered that the low pressure conditions combined with higher processing temperatures of microwave freeze-drying promoted the generation of an aerosol. An evaluation of the microstructure and flavor of the conventional and microwave freeze-dried beef was conducted. There was a

noticeable difference in texture and microstructure was observed, but no significant difference in sensory characteristics.

2.3.3 Process Control

Ang et al. (1978) studied the optimal modes of operation for microwave freeze-drying of beef. It was found that higher field strengths and corresponding shorter drying times can be achieved with the use of a simple field strength feedback control unit. It was also noted that faster drying can be achieved though higher temperatures and the best way to maintain high drying rates is to keep the pressure as low as possible and the field strength high.

An optimal control strategy was applied to a hybrid microwave and radiant freeze-drying system by Chang and Ma (1985). This project stressed practical application and as such the apparatus used was developed by converting a conventional radiant freeze-drier into one that would also accept microwave energy. This is the same apparatus used by Arsem and Ma (1985). The results agreed well with the experimental data and suggests that microwave and radiant freeze-drying can improve energy efficiency and reduce the cost of freeze-drying. The model used is one dimensional and based on an unsteady state analysis.

2.3.4 Apparatus

There have been several types of devices used for coupling microwaves to the material to be heated. Copson and Decareau (1957) used a microwave cavity fitted with

a 6-station manifold constructed of copper tubing placed inside a vacuum chamber. Hoover et al. (1966) used a resonant mode microwave cavity placed inside a vacuum chamber.

A multimode cavity was part of the apparatus, shown in Fig. 2.2, that was used by Ma and Peltre (1975b). The cavity was placed inside a larger vacuum chamber. The sample was suspended inside the cavity making it possible to measure weight during drying. The magnetron was capable of providing 1200 Watts to the cavity. In the experiments by Ma and Peltre (1975b), there were experiments to measure weight and separate experiments to measure temperature.

Ang et al. (1977b) used a waveguide instead of a cavity applicator, as shown in Fig. 2.3. In this case, the sample was suspended inside a tube that was passed through the waveguide. The apparatus was also equipped to measure weight like the others. This apparatus, like the one used by Ma and Peltre (1975b), also required separate temperature and weight runs.

In an attempt to overcome the difficulty of coupling microwaves with the material during the start-up phase of microwave freeze-drying, Ma and Arsem (1982) combined radiant and microwave heating in an experimental freeze-drier. This device made use of a modified conventional freeze-drier. However, it was related to the previous microwave freeze-drier in that it was still a multimode microwave cavity placed inside a vacuum chamber. This arrangement has proven to be even more efficient than the use of microwave energy alone.

Chen et al. (1993) describes the basic microwave freeze-drying system used for

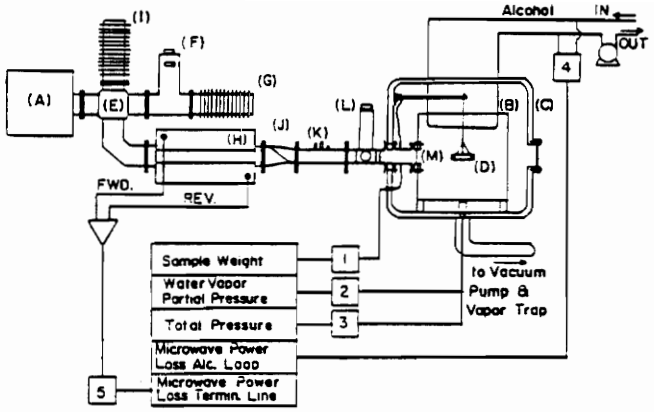

Figure 2.2 Schematic of the experimental setup of Ma and Peltre, 1975b

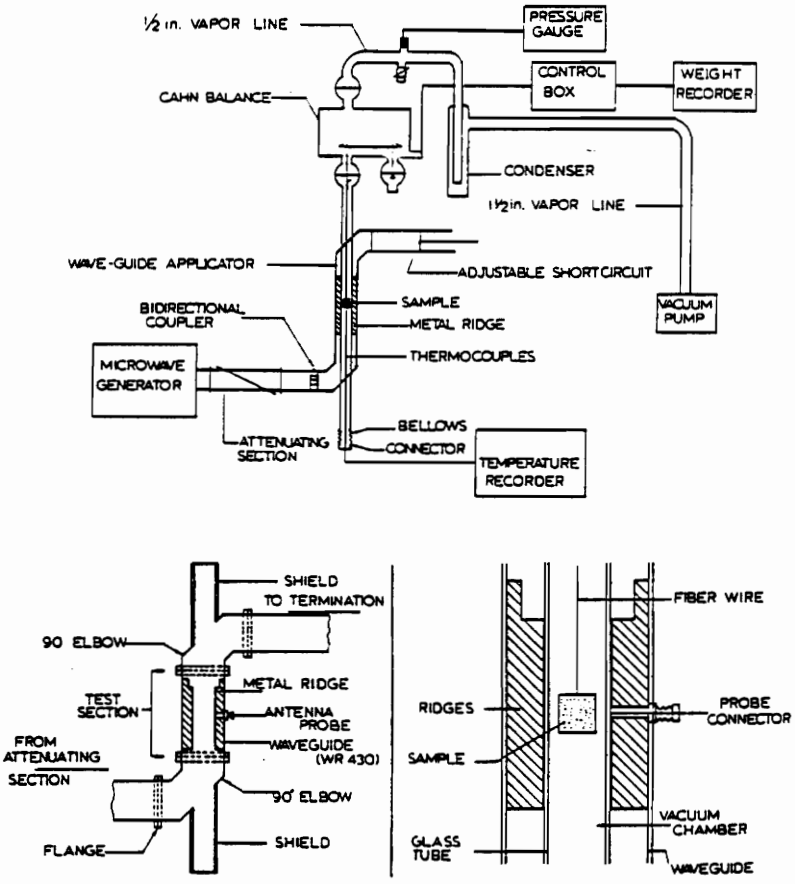

Figure 2.3 Schematic diagrams of microwave freeze-drying apparatus and test section for Ang et al., 1977

the current experimental investigation. Some modifications were made, such as the addition of a scale for measuring the weight of the sample. The resonant mode cavity is described by Asmussen et al. (1987). An experimental demonstration was used to show efficiencies and properties of the cavity for various uses.

Chapter 3

Theoretical Considerations

The freeze-drying process consists of three stages: freezing, primary drying and secondary drying. This chapter discusses theoretical aspects of freeze-drying and the application of microwave heating. The freezing process is an important part of freeze-drying and is discussed in detail in the first section. In the second section, a detailed description of both primary and secondary drying is presented. These two sections comprise the physical aspects of the freeze-drying process. The next two sections cover microwave heating and mass transfer. These sections introduce the physics of microwave heating and an analytical description of mass transfer in vial freeze-drying.

3.1 Freezing Theory

The first step in the freeze-drying process is to freeze the sample and bring the temperature down to a specified value. This temperature will be chosen based on the type of material, the desired drying characteristics and the desired physical characteristics in the dried product. Often, the material or vial of solution is placed on a shelf that is

cooled in order to freeze the product.

The importance of the freezing conditions are often overlooked by researchers and designers of freeze-drying equipment. The freezing rate affects the quality of the product by changing the physical characteristics of the dried material. It has even been suggested that it is possible to design an optimum freezing process that results in desired drying characteristics or favorable attributes in the final product (Kochs et al., 1991). Detailed information on the correlation between freezing conditions and freeze-drying behavior are essential to the optimization of the entire freeze-drying process.

Undercooling is the process of cooling a liquid below its equilibrium freezing point. While a solution is in this undercooled state it is thermodynamically unstable. The system is converted to its stable state by the formation of ice crystals of pure water and a second phase that consists of all other water-soluble components. As a result, substances that might be stable at room temperature may become unstable upon freezing due to a dramatic increase in concentration of a particular component in the mixture. For instance, a mixture to be freeze-dried could consist of an active ingredient, like protein, and other substances, like pH buffers and salts. An increase in the concentration of salts may damage sensitive proteins during freezing and result in product loss (Franks, 1989).

The size of ice crystals has a significant affect on the microstructure of the dried product. Ice crystal size and concentration are dependent on the degree to which the water is cooled below its freezing point. Usually, the slower the freezing rate, the greater the degree of undercooling. It is desirable to achieve as large a degree of undercooling as possible for freeze-drying (Franks, 1989). Ice crystal size is also related to the ice

crystal nucleation rate, which generally increases with decreasing temperature.

The speed at which ice crystals grow is dependent on temperature and viscosity (Franks, 1989). When a solution begins to freeze, the freezing rate is initially fast. As the freezing progresses, water is frozen out of the solution to form ice crystals of pure water. Thus, the remaining concentration of solutes increases, increasing viscosity and decreasing the freezing rate. Also, it has been found that the morphology and size of the ice crystals depend on the cooling rate (Franks, 1989).

The freezing rate is found using a simple method previously used by Thijssen and Rulkens (1969). The freezing rate, S, is defined by

$$S = \frac{T_0 - T_{0.85}}{t_{0.85}} \tag{3.1}$$

where T_0 is sample temperature before cooling, $T_{0.85}$ is eighty-five percent of the difference between T_0 and the temperature of the cooling medium, T^*,

$$T_{0.85} = 0.85(T_0 - T^*) \tag{3.2}$$

and $t_{0.85}$ is the time required to achieve the temperature difference $T_{0.85}$. This method was chosen because it has been used in a study of the effect of the freezing rate on the sublimation rate.

3.2 The Drying Process

This section describes the two drying stages of freeze-drying: primary and secondary drying. Primary drying involves the sublimation of ice crystals while

secondary drying refers to the desorption of bound water that takes place at approximately room temperature after the ice has been sublimated. The effects of chamber pressure and temperature are also discussed.

3.2.1 Primary Drying

The primary drying stage requires that the frozen product is placed in a vacuum at a pressure that is below the triple point of water. At this point it is helpful to look at a pressure-temperature diagram of water in the range that concerns sublimation. Figure 3.1 shows such a diagram. Point 1 is a possible initial state of water in a frozen product at the start of freeze-drying. Point 2 is a possible state of water after sublimation. However, the entire mass of ice does not sublimate over a very short period of time, thus during primary drying, water exists in both the solid and vapor state simultaneously.

Once the frozen product is at the appropriate pressure and temperature, heat is applied. The temperature is increased to a higher value than the equilibrium temperature that corresponds to the chamber pressure. As the temperature reaches the equilibrium solid-vapor temperature, sublimation begins to occur at the surface of the frozen product. Sublimation uses energy that is stored in the product, thus to keep the temperature of the ice core from falling, heat must be continually supplied to the product.

As ice sublimates, two regions develop: a frozen region and a dried region. Sublimation occurs at the boundary between the frozen and dried regions. This boundary is known as the sublimation front or phase front. As the sublimation front moves through the product the dried layer grows in thickness and increase the resistance to mass transfer.

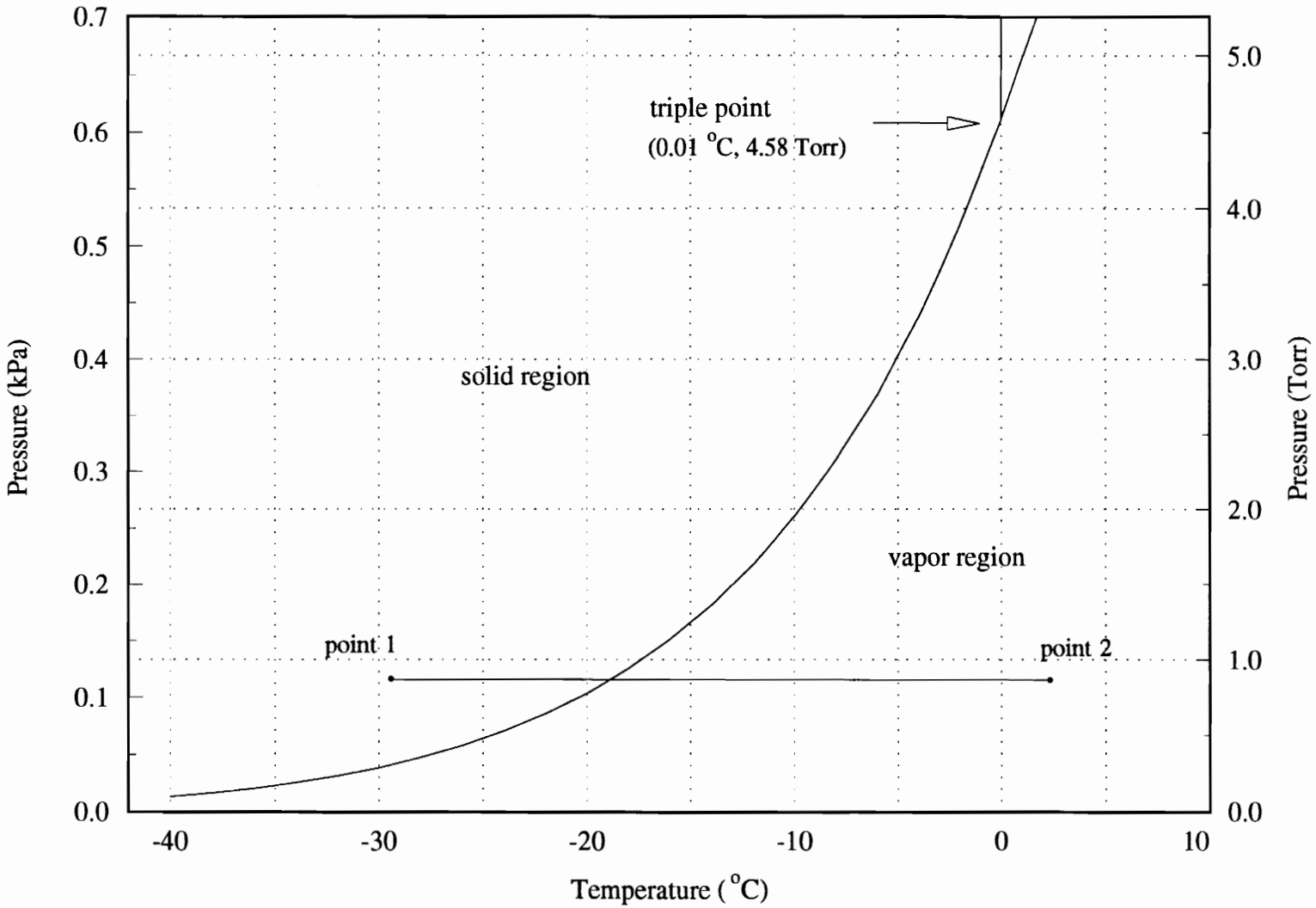

Figure 3.1 Pressure-temperature diagram of water showing sublimation region

Figure 3.2 gives a schematic of one dimensional vial freeze-drying with volumetric heat generation and an open vial. Assuming a one-dimensional model can produce reasonable results until the sublimation front gets about half way into the sample. At this point the sublimation front begins to deviate from a level, constant area phase front and the problem becomes two dimensional. Also at this point, it is expected that radial temperature gradients are too significant to ignore.

The resistance of the dried layer to the flow of vapor causes the pressure at the sublimation front to be higher than the pressure in the chamber. The sublimation front pressure is due only to vapor and corresponds to a point on the solid-vapor equilibrium line. The pressure in the chamber is lower than the pressure at the sublimation front and consists of the partial pressure of vapor and the partial pressure of air. The difference between the vapor pressure at the sublimation front and the vapor pressure in the chamber is the driving force for the vapor flux leaving the product through the dried layer.

The sublimation front is also where heat is dissipated, therefore, it must be that temperature gradients exist in the frozen layer that conduct heat to the sublimation front. The dried layer heat transfer is more complicated since, in addition to conduction, there is also convection due to the escaping vapor.

It has been found that higher pressures increase thermal conductivity in both the dried and the frozen region of a material during freeze-drying (Mellor, 1978), thus increasing the drying rate by increasing the rate of heat transfer. This is one reason for some confusion as to whether or not lower pressures increase the sublimation rate. Since heat and mass transfer are coupled in freeze-drying, it is very difficult to predict the

C moisture concentration

$\dot{G}$ volumetric heat generation

T temperature distribution

X sublimation front position

$\dot{m}$ mass flux

subscripts

D dried layer

F frozen layer

s surface

i interface

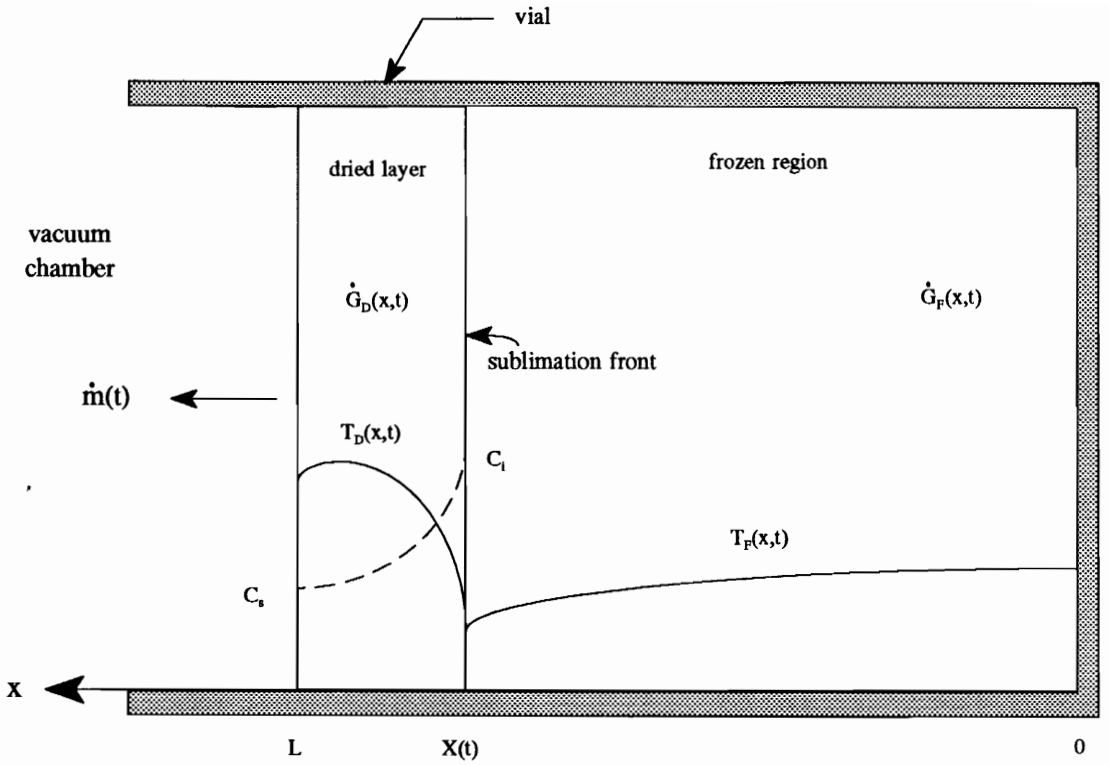

Figure 3.2 Model of a one dimensional vial freeze-drying process with volumetric heating

effects of changing pressure or temperature without experimental data.

3.2.2 Secondary Drying

The secondary drying process involves the desorption of unfrozen water, often called bound water. Bound water is attached to the structure of the dried material either by electrostatic forces or hydrogen bonds (Mellor, 1978). The secondary drying process begins in a region when the ice in that region has been sublimated. However, low levels of residual moisture are not attained until the after primary drying stage has been completed.

Once the primary drying stage has been completed, the usual practice is to reduce the chamber pressure to very low levels and increase the product temperature above room temperature. Pikal et al. (1990) discovered that below 0.2 Torr the drying rate is independent of chamber pressure. It was found that product temperature has a significant effect on the drying rate. It is important to note that these findings are for aqueous solutions and not for food.

3.3 Microwave Heating

The rate limiting process in conventional freeze-drying is usually heat transfer. In vial freeze-drying, one significant barrier to heat transfer is the thermal resistance between the heated shelf and the vial. Since the resistance is not the same for all vials in a batch process, often some vials dry faster than others, making it difficult to determine when the drying process is complete. The most promising technique for improving heat

transfer is by the use of microwave energy. In a microwave field, heat is generated volumetrically in the product and the need to conduct heat from some external heat source and though the dried or frozen layer to the phase front is eliminated. Previous research has shown that with the improved heat transfer, the process becomes one limited by mass transfer resistance and thus drying times are dramatically improved (Arsem and Ma, 1985).

When using microwave energy as a source of heating it is important to understand the interactions of a dielectric with microwave energy. In a dielectric, the time averaged absorbed power density $\langle P \rangle$ at a location, $\boldsymbol{r}$, is given by

$$\langle P \rangle = \frac{1}{2}\omega\varepsilon_0\varepsilon_r'' (\boldsymbol{r}) \, | \boldsymbol{E}_0(\boldsymbol{r}) |^2 \qquad (3.3)$$

where ε_0 is the dielectric constant of free space, ω is the excitation frequency, ε''_r is the loss factor of the material and E_0^2 is the electric field strength in the material (Asmussen et al., 1987). The material loss factor is a very important parameter in microwave heating; it determines how well the material will heat, given a particular frequency and field strength. Usually, the loss factor is also a strong function of temperature and thus, it is important to know how this parameter behaves in the operating temperature range.

During freeze-drying, heat is generated in both the frozen and dried portions of the material, however, ice is usually more lossy than the dried material, so most of the heat generation occurs in the frozen part of the sample. This situation is preferred since thermal conductivity is also typically higher in the frozen layer, permitting good conduction of heat to the phase front.

Table 3.1 *Loss Factors of Materials ([1] from Metaxas and Meredith, 1983)*

Material	**Loss Factor, ε"**	**Temp (°C)**
Pure Ice	0.003 [1]	-12
Mannitol (dry powder)	0.0011	24
Teflon	0.0003 [1]	22
Distilled Water	12.00 [1]	25

Table 1 lists loss factors for the materials involved. Liquid water is also listed for comparison. The loss factor for Mannitol was determined by packing the dry powder into a Nuclear Magnetic Resonance (NMR) tube and using the perturbation technique with a Hewlett Packard Network Analyzer at a frequency of 2.45 GHz. The measurement was made at room temperature.

It is assumed that freeze dried Mannitol will have a lower loss factor due to a larger percentage of air contained in the dried sample. Heat will also be generated in the Teflon that is present, but since the loss factor is so low, 0.0003, and the volume of the material is small, very little heat will be generated in the Teflon compared to that in the frozen layer.

3.4 Mass Transfer

The most significant barrier to mass transfer is the dried layer that forms as the phase front recedes into the product. Due to the small pore size in the dried layer, the

flow of vapor is free molecular flow. As a result, the dried layer can comprise as much as ninety percent of the total mass transfer resistance (Pikal et al., 1983).

In general, the mass flux leaving the frozen portion of the sample and arriving at the condenser is inhibited by certain mass transfer resistances present in the system. Mass transfer resistance is defined as the driving force divided by the mass flow rate. This gives the following equation as the dry layer resistance, R_p:

$$R_P = \frac{P_{eq} - x_v P_{tot}}{\dot{m}} \tag{3.4}$$

where P_{eq} is the equilibrium vapor pressure (Torr), x_v is the mole fraction of water vapor in the chamber, P_{tot} is total pressure in the chamber (Torr) and m is the sublimation rate (g/h).

The driving force in this case is the difference between the partial pressure of water vapor at the sublimation front and in the chamber above the sample. At the sublimation front, the pressure is equal to the equilibrium vapor pressure of water corresponding to the temperature of the phase front. Therefore, the pressure at the phase front is given by the solid-vapor saturation curve for water:

$$P_{eq} = P_{sat}(T_{sat}) \ . \tag{3.5}$$

The partial pressure of water vapor, P_v, in the chamber is given by

$$P_v = x_v P_{tot} = P_{tot} - P_{\min} \tag{3.6}$$

where P_{min} is the minimum pressure in the chamber, recorded after the sample has dried. The sublimation rate is defined as the slope of the curve of the weight of water

$$\dot{m} = \frac{dw(t)}{dt} \tag{3.7}$$

where $w(t)$ is the weight of the amount of water present in the sample as a function of time.

Chapter 4

Experimental Methods

This chapter describes the experimental setup and the experimental procedures used to determine the feasibility of using microwave freeze-drying for drying aqueous solutions and to use the apparatus as a research tool. The experimental apparatus was modeled after the system first developed by Chen et al. (1993).

4.1 Experimental Setup

A schematic of the experimental microwave freeze-drying setup is given in Fig. 4.1. It contains a single-mode microwave applicator, the appropriate microwave circuitry and the vacuum system. However, the experimental setup is currently in the early phases of its development and improvements will be made for future experiments. Some of the planned improvements are: additional pressure measurements, a new single-mode cavity, additional temperature measurements and the ability to reach lower pressures. The following sections give a detailed description of the experimental sample vial, microwave circuit, vacuum apparatus and the data acquisition system.

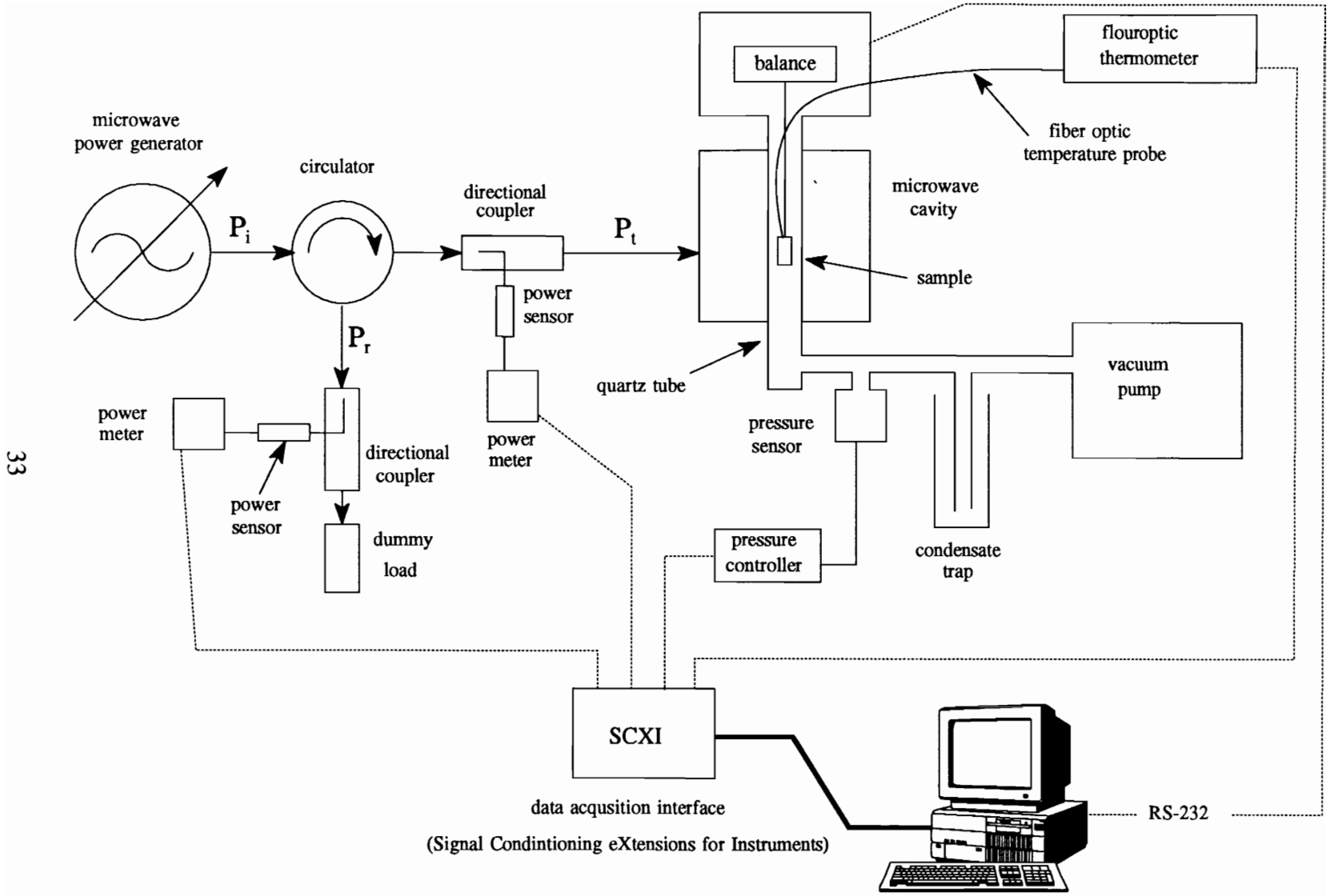

Figure 4.1 Schematic of microwave freeze-drying system

4.1.1 Experimental Sample Vial

In order to ensure that the vial does not significantly affect the results of the experiment, it must have a small volume and a significantly lower loss factor that the frozen solution. The aqueous solution used in the experiments has a low loss factor which is estimated to be approximately the same as pure ice; therefore, a suitable material for the vial would be fused silica glass or Teflon. The fused silica is preferred, because it has a lower loss factor than Teflon. However, fused silica is brittle and would crack during the freezing of the solution. Therefore, Teflon was the material chosen for the vial. Some material dielectric loss factors are given in Table 4.1.

The vial used in all experiments was machined from a 49 mm diameter rod of Teflon and is shown in Fig. 4.2 along with a standard freeze-drying vial. The dimensions of the vial are: i.d., 25.40 mm; o.d., 27.65 mm; height, 31.85 mm; bottom thickness, 1.4 mm. The weight of the vial is 8.13 grams. It is not similar to standard vials used in the pharmaceutical industry, because of the constant diameter and since there is not a stopper used in the experiments. Typically, vials used in the pharmaceutical industry have narrow necks and are partially stoppered. This is done so that the vial can be sealed while it is

Table 4.1 *Loss Factors of Sample Vial Materials (Metaxas and Meredith, 1983)*

Material	Loss Factor, ε"	Temp (°C)
Fused Silica	0.0002	25
Polyethylene	0.0026	23
Teflon	0.0003	22

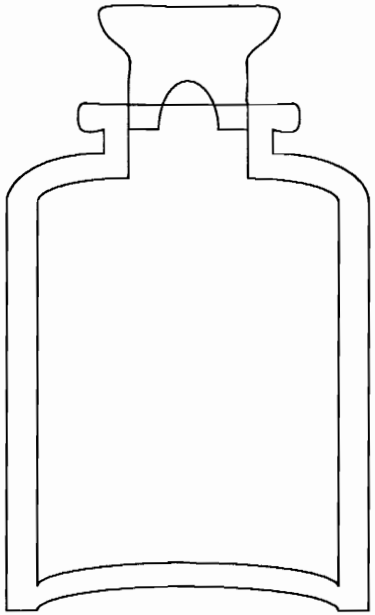

Standard glass freeze-drying vial with rubber stopper in semi-stoppered position

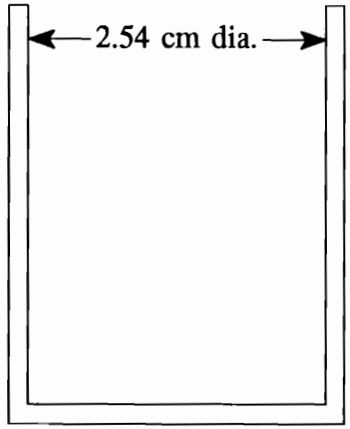

Experimental teflon vial

Figure 4.2 Cross sections of freeze-drying vials

still in the vacuum chamber. Figure 4.2 shows the experimental Teflon vial and a typical glass vial with a stopper.

4.1.2 Microwave Heating Apparatus

The microwave circuit contains coaxial cable, directional couplers, a circulator, dummy load, microwave power generator (2.45 GHz) and the single-mode cavity applicator, shown in Fig. 4.3. A single-mode cavity consists of a metallic enclosure into which a microwave signal is introduced. The particular cavity used for this work was a cylindrical single-mode cavity, pictured in Fig. 4.4. The wave reflections in the cavity set up a standing wave pattern which is well known for simple structures (Metaxas and Meredith, 1983). The benefit of a resonant mode cavity is that, with a known field pattern, the sample can be placed in the position of maximum electric field strength for optimum transfer of the electromagnetic energy.

The apparatus described here differs from many previous microwave freeze-drying systems (Copson, 1957; Hoover et al., 1966; Ma and Peltre, 1975b; Ang et al., 1977) due to the placement of the vacuum chamber inside the cavity and the use of a single-mode microwave cavity applicator. Other systems have used a multimode cavity or a waveguide and placed inside a larger vacuum chamber. In a multimode cavity, multiple modes exist simultaneously. The result is usually more uniform heating for large items and for products with nonuniform dielectric properties. The reason for the use of a single-mode cavity in this work is the optimum transfer of electromagnetic energy that is provided. Also, since the sample is small, a uniform field strength exists throughout

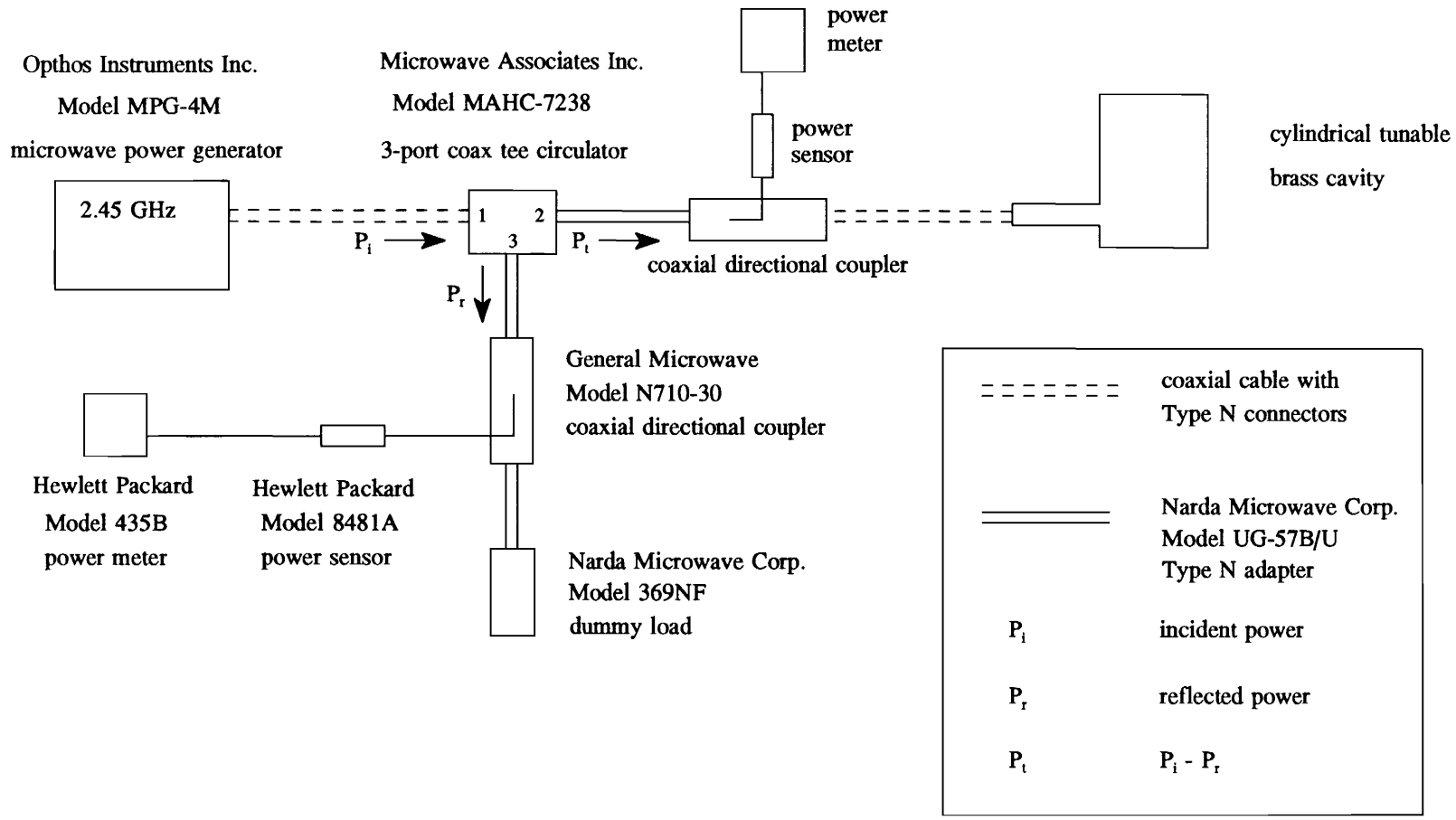

Figure 4.3 Schematic of microwave circuit

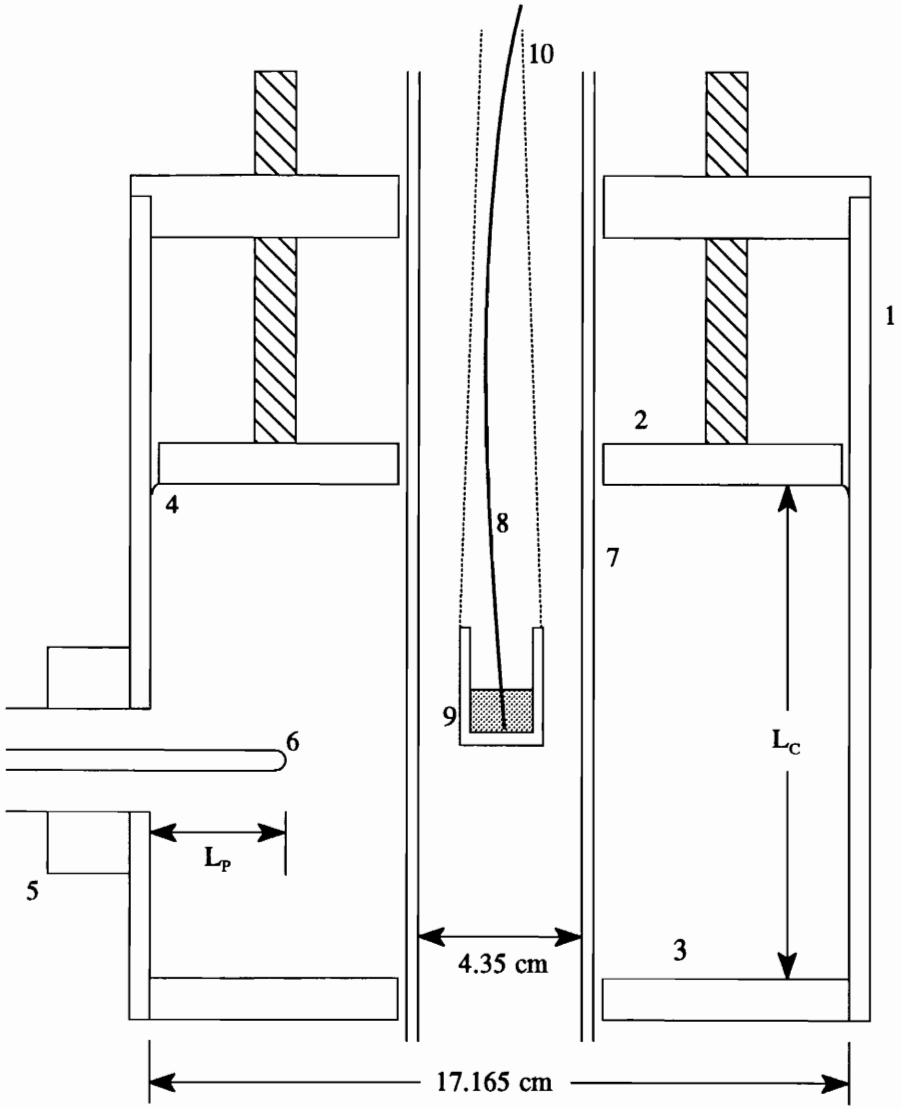

1	conducting cylindrical shell
2	sliding short plate
3	end plate
4	silver finger stock
5	coaxial input port
6	adjustable coupling probe
7	quartz tube
8	Luxtron temperature probe
9	Teflon sample vial
10	cotton thread
L_P	coupling probe depth
L_C	cavity length

Figure 4.4 Close-up view of the single-mode microwave cavity

its volume. To achieve a uniform field strength at the center of the cavity, where the sample is located, the cavity is tuned to excite the TM_{012} mode. The field pattern of the TM_{012} mode is shown in Fig. 4.5.

The power is delivered by a 100 Watt microwave power generator through a coaxial cable to a circulator. In the schematic of the system, Fig. 4.3, P_i is the incident power, which is directed to the circulator from the power generator. The circulator has three ports. The microwave power generator is connected to port one which directs power from the power generator to the cavity. Reflected power, P_r, travelling from the cavity into the circulator at port two is diverted to the dummy load, which is connected to port 3. The dummy load serves to protect the microwave power supply from backward travelling power.

The total power, P_t, is the power dissipated in the microwave cavity. This power is given by

$$P_t = P_i - P_r . \tag{4.1}$$

Power is dissipated by the sample, wall losses and fringing fields. Wall losses result from microwave energy penetrating the surface of the cavity walls. Fringing fields are present when the load in the cavity is small and the incident power is large. These fields extend out of openings in the top and bottom of the cavity.

Two coaxial directional couplers each with a 30 dB attenuator port are used in the system. One is connected to the cavity and one to the dummy load. The directional couplers divert a small percentage of power to the microwave power sensors. The sensors

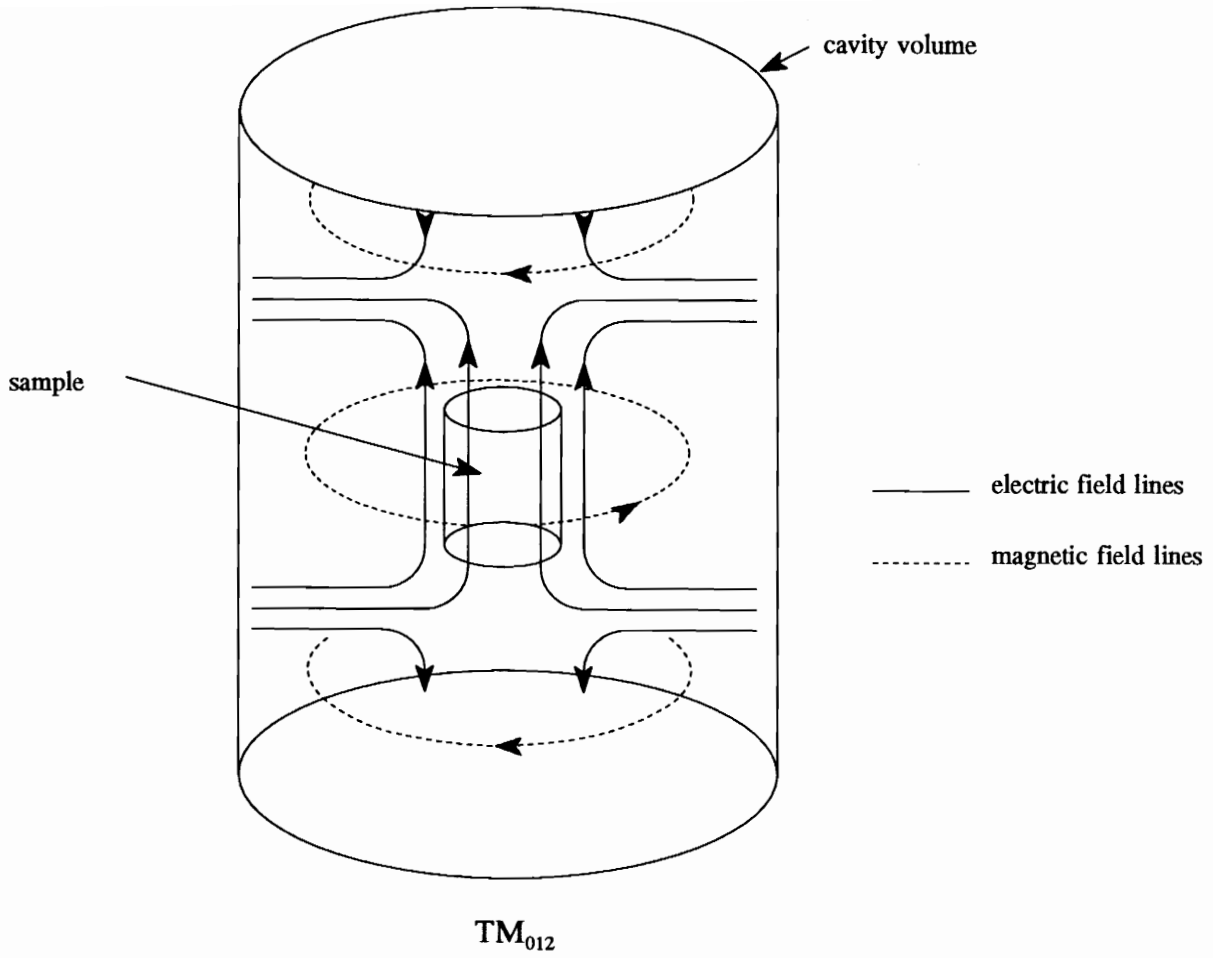

Figure 4.5 Electric and magnetic field patterns for microwave cavity excited in the TM_{012} mode

are then connected to power meters which measure the incident power and the reflected power.

4.1.3 Vacuum Chamber Apparatus

The vacuum system, shown in Fig. 4.6, contains a quartz tube, pressure gauge, condensate trap, vacuum pump and a chamber that holds an electronic balance. The quartz tube is the drying chamber that contains the sample. The sample is frozen in a Teflon vial and suspended from a balance with a thin dry cotton thread. Below the chamber is a pressure sensor and then a liquid nitrogen condensate trap followed by the vacuum pump.

Typical pressures for freeze-drying of aqueous solutions are between 0.03-0.5 Torr (Pikal et al., 1984). The current apparatus can obtain minimum pressures of about 0.6 Torr. However, pressures from 0.1-2.0 Torr have been used in previous microwave freeze-drying experiments (Ma and Peltre, 1975; Ang et al., 1977) and it is believed that the minimum pressures currently obtained are adequate for the present work. Also, the vapor pressure in the chamber can be estimated, but the system has not yet been equipped to accurately measure these data. Presently, the one pressure sensor in the system measures total pressure.

4.1.4 Temperature Measurement

Temperature is measured using a Luxtron fiberoptic thermometry system, model 790. This system is a phosphor decay type which uses probes made of a silica fiber

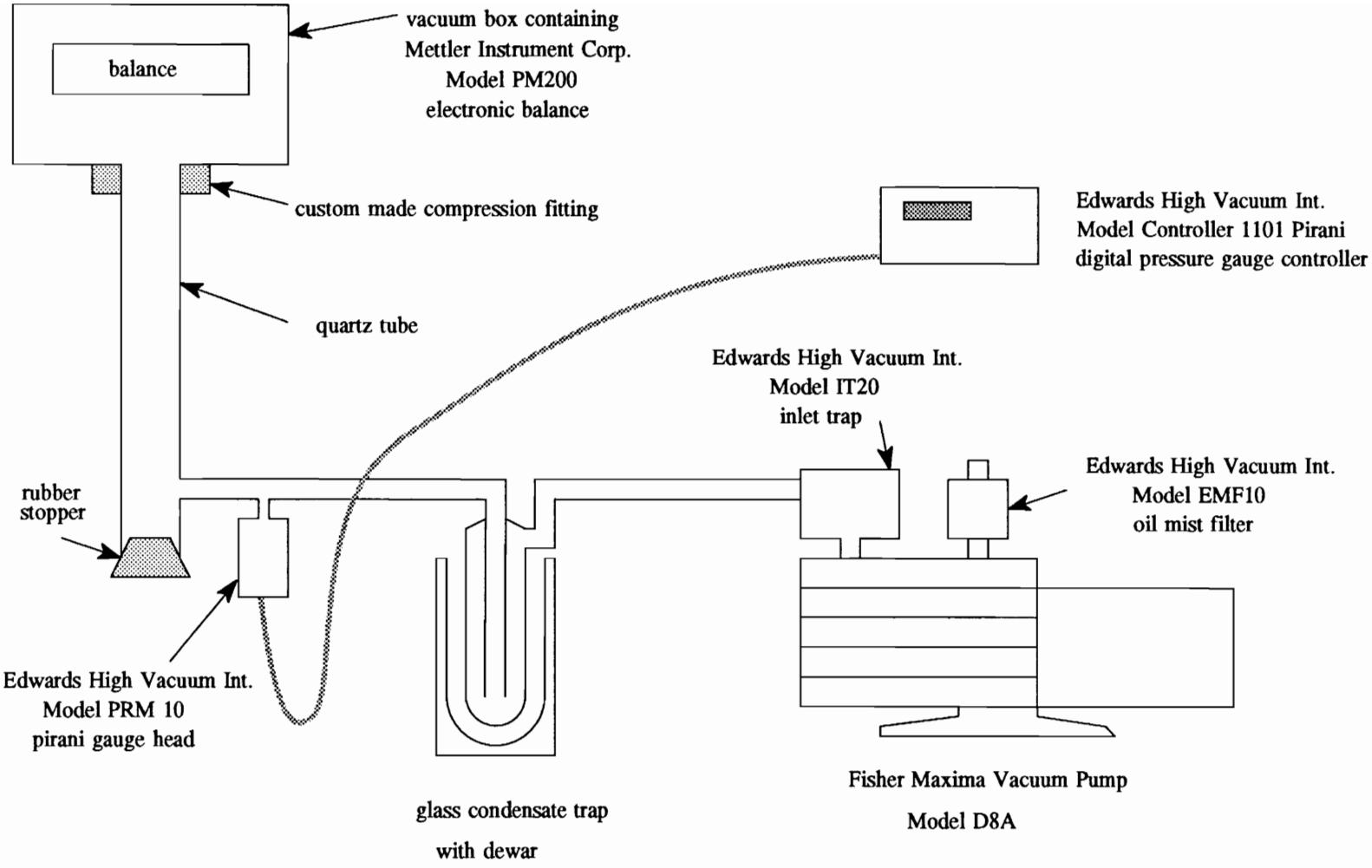

Figure 4.6 Schematic of microwave freeze-drying vacuum system

coated with Teflon. The optical fiber is a nonconducting material and as such will not distort the electric or magnetic fields present in the microwave cavity. A distortion of these fields can cause uneven heating of the sample.

The fiber optic probes are less flexible than thermocouples and have a much larger diameter than the usual thermocouple wire. As a result, it is difficult to place more than one probe in the sample to measure temperature gradients and simultaneously measure the weight loss. However, with only one probe, the influence on the weight is slight, and since only a weight difference is measured, good results can be obtained.

4.1.5 Data Acquisition System

A National Instruments data acquisition system was used. The system consisted of a terminal block connected to a 32-channel SCXI (Signal Conditioning eXtensions for Instruments) multiplexer amplifier, known as the SCXI module. It was connected to a PC plug-in data acquisition board via an SCXI cable. A schematic of the data acquisition system is shown in figure 4.7.

The freeze-drying apparatus contained five devices that output data to the data acquisition system. These devices were: a power meter for incident power, a power meter for reflected power, the pressure controller, the Luxtron Flouroptic Thermometer, and a digital balance. These devices measured: sample temperature, total dissipated power, chamber pressure and weight loss. The output of these devices was recorded every 8 seconds.

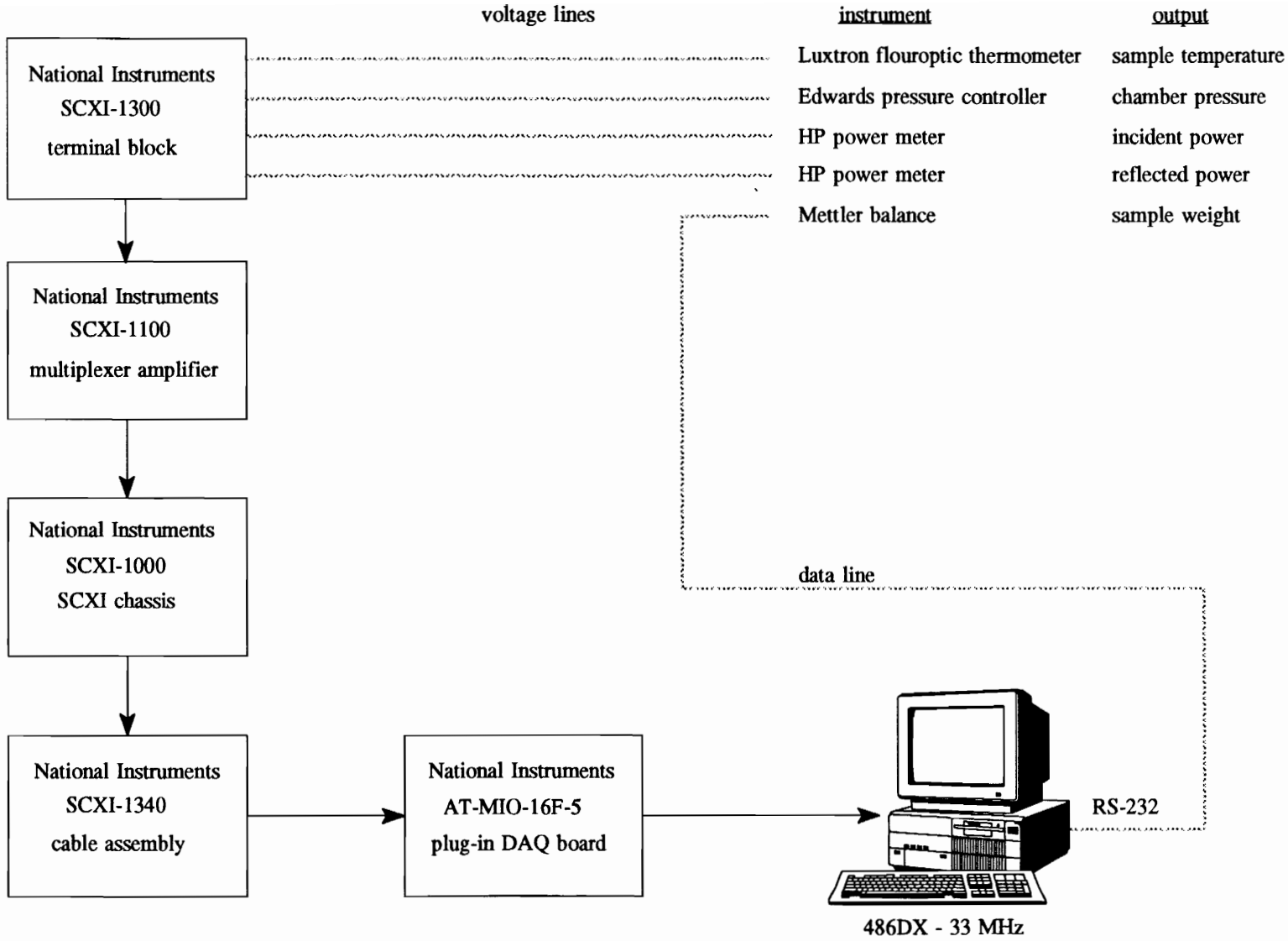

Figure 4.7 Schematic of data acquisition system

The data acquisition program, FRZDRY2.C, is written in C for the National Instrument software, Lab Windows. The program, including comments, is listed in Appendix D with an general description of how the program works.

4.2 Experimental Procedures

This section covers the experimental procedures used during the experiments. They include: sample preparation, description and measurement of the freezing rates, and control of the freeze-drying apparatus.

4.2.1 Sample Preparation

All samples for the experiments conducted for this work are 9 percent by weight aqueous solution of D-Mannitol ($C_6H_{14}O_6$) and water. The Mannitol was purchased from Sigma Chemical Company. The steps for preparing the solution are as follows:

1. Clean a 150 ml beaker.
2. Place the empty beaker on an electronic balance and tare the balance.
3. Put about 20 ml of distilled water in the beaker.
4. Place the beaker of water on the scale and record the weight of the water.
5. Place weighing paper on the balance and tare.
6. Measure an amount of Mannitol equivalent to one tenth the weight of the water.
7. Mix the Mannitol into the water still contained in the beaker.
8. Stir the Mannitol and allow several minutes for the Mannitol to completely

dissolve.

9. Use a funnel and Fisher Scientific P5 qualitative grade filter paper to filter the solution into a second clean 150 ml beaker.
10. Place the vial on the balance and tare.
11. Using an eye dropper, place 5.0 grams of the solution into the vial.

At this point the solution is prepared for freezing. All samples are prepared in this way regardless of freezing conditions or freeze-drying temperatures.

4.2.2 Freezing The Sample

There are three different freezing conditions used in the experiments. Each sample has a fiber optic probe tip placed in the vial for temperature measurement of the freezing rate and for monitoring the sample temperature during freeze-drying. This section will explain the placement of the probes in the sample, the three different freezing conditions and how the samples are frozen.

Placement of the temperature probe is an important aspect of measuring freezing rates of aqueous solutions. To determine the freezing rate, the tip of the temperature probe was placed approximately two thirds the radius in from the outer edge of the vial and about half way between the bottom of the vial and the top of the sample, as illustrated in Fig. 4.8. It is believed that this position gives a temperature reading that is most representative of the sample (Hartmann et al., 1991).

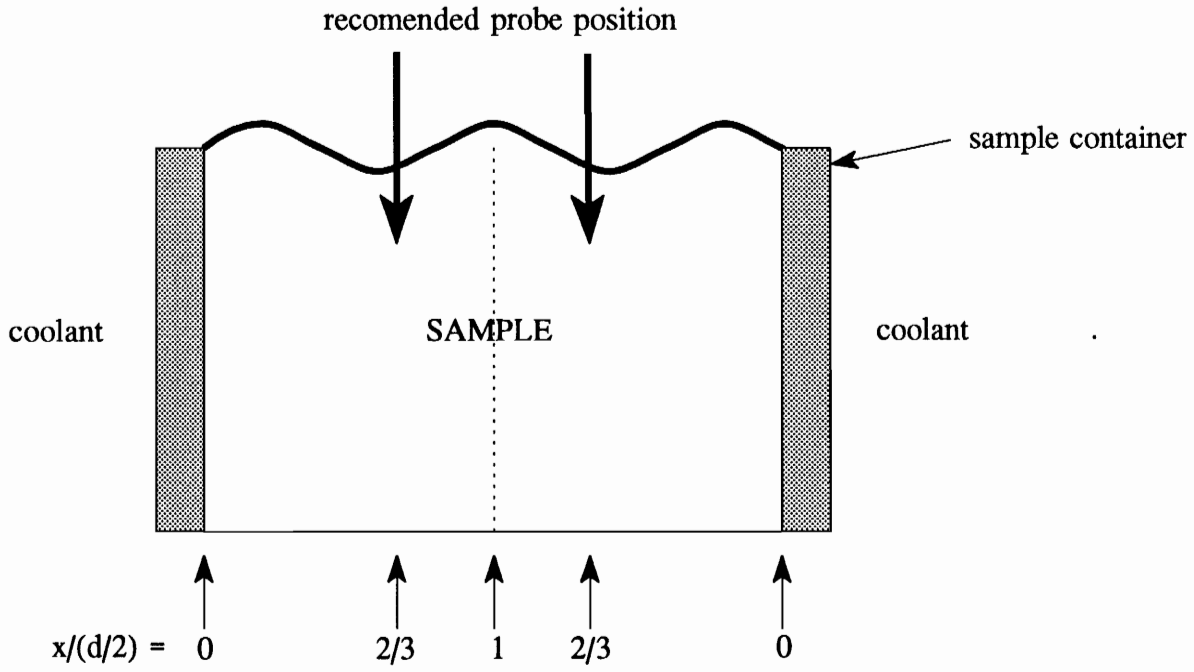

Figure 4.8 Indication of the recomended probe position for monitoring the cooling rate (Hartmann et al., 1991)

4.2.2.1 Fast Freezing Rate

The fast freezing rate was achieved by dipping the vial in liquid nitrogen (-193 °C). The temperature probe was held in position while the vial is slowly lowered into a beaker approximately half full of liquid nitrogen. Using Eq. (1), $T_{0.85}$ can be determined. The variable, $T_{0.85}$, is the temperature that is 85 percent of the difference between initial sample temperature and the temperature of the cooling medium. The time to decrease the temperature by this amount was measured and then the freezing rate was calculated. The procedure used with the fast freezing rate is listed below:

1. Fill a 150 ml beaker about half full with liquid nitrogen.
2. Turn on computer and SCXI and call up appropriate data acquisition program.
3. Start the data acquisition program.
4. Lower vial containing solution slowly into liquid nitrogen until the level of liquid nitrogen is higher than the level of the solution in the vial.
5. Make sure that the probe is not touching the bottom of the vial and that no liquid nitrogen splashes into the vial.
6. Keep vial suspended in liquid nitrogen until the appropriate temperature is reached.

4.2.2.2 Medium Freezing Rate

The medium freezing rate was achieved by placing the vial containing the sample in a freezer. The freezer was maintained at -60 °C and the vial was placed directly on

the floor of the freezer. The temperature probe was held in position by a simple rig made with a foam insulation. This rig is pictured in Fig. 4.9. The temperature probe was slid under a few staples

in the foam to hold the probe against the foam. Once the probe and the rig were in place, the position of the vial could be adjusted so that temperature was measured at the desired point in the solution. The following steps describe the measurement of the medium freezing rate:

1. Set freezer temperature at -60 °C.
2. When the freezer has reached the set temperature, allow some time for the freezer bottom to reach the set temperature.
3. Turn on computer and SCXI chassis and call up appropriate data acquisition program.
4. Run the temperature probe though the access hole in the side of the freezer.
5. Position the probe in the foam rig so that the probe tip is in the correct position in the vial.
6. Start the data acquisition program.
7. Place the vial and the foam rig holding the probe on the floor of the freezer.
8. Close the lid of the freezer and monitor the sample temperature via the computer.

4.2.2.3 Slow Freezing Rate

In this case, the freezing rate was slowed down by maintaining the freezer

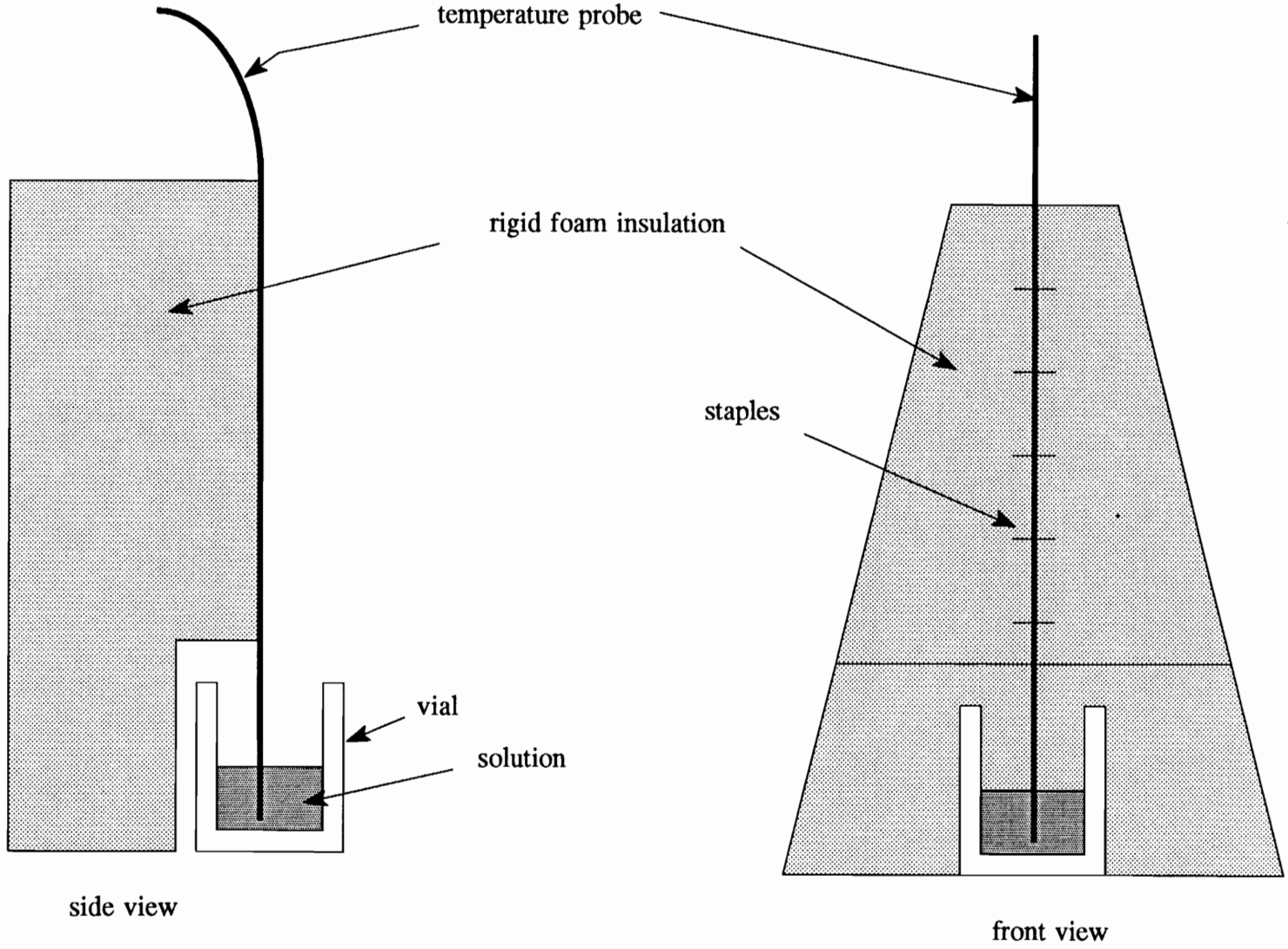

Figure 4.9 Rig for positioning temperature probe during freezing

temperature at -10 °C, and the vial was placed on a thin piece of pipe insulation that was placed on the floor of the freezer. Like the medium freezing rate condition, the temperature probe was held in position by a simple rig made with a foam insulation. The procedure follows:

1. Set freezer temperature at -10 °C.
2. Follow steps 2 through 8 for the medium freezing rate, except that vial is placed on a thin piece of pipe insulation and not directly on the freezer floor.

4.2.2.4 Freezing Samples For Freeze-Drying

When samples were frozen for freeze-drying, the same freezing conditions were used as previously described, however, it was not necessary to measure the freezing rate at this point. Since the freezing conditions did not change, it was assumed that the freezing rates were also unchanged.

The most important aspect of freezing samples for freeze-drying was placement of the probe tip. When the freezing rates were measured, the probe tip was placed in a position that provided a temperature that was most representative of the bulk temperature of the solution. However, the probe tip was placed in the center of the vial and very near the bottom when a sample was frozen for freeze-drying. This was the position that sublimation occurred last. Thus, the probe tip continued to measure the ice core temperature until all the ice had sublimated.

Also, for the slow freezing rate, the temperature was low enough that the sample could begin to melt before the experiment was set up. For the slow freezing rate, it was

suggested that before the sample was removed from the freezer, the freezer temperature was lowered to -20 or -30 °C. Ten to fifteen minutes were allowed to pass and then the sample was removed from the freezer.

4.2.3 Freeze-Drying Procedure

The following is a list of the procedure used to start a freeze-drying experiment once the sample is prepared.

1. Turn on the computer, SCXI chassis, microwave power generator, both microwave power meters, the pressure controller and the Luxtron Fiberoptic Thermometer, and let the equipment warm up for approximately fifteen minutes.
2. Add about 300 ml of liquid nitrogen to the dewar of the vapor trap.
3. Connect the two parts of the vapor trap.
4. Loosen the temperature probe fitting and slide enough of the probe through so that the end stick out of the fitting for the quartz tube.
5. Attach the probe tip to the probe and lower the vial into the quartz tube and hang from the hook that is attached to the balance.
6. Take up the slack in the probe so that it does not push or pull on the sample.
7. Connect the quartz tube and tighten the fitting, also tighten the temperature probe fitting.
8. Turn on the vacuum pump while holding the stopper for the quartz tube in place.

9. Place the dewar of liquid nitrogen over the condensate trap.

10. Once the pressure has stabilized start the data acquisition program.

11. Apply the microwave power.

12. Tune the cavity.

At this point the experiment was started and control of the apparatus depended on the specific objectives of the experiment. There were three possible control strategies used for this work:

A) Maintain the temperature in a specified range.

B) Maintain a constant power.

C) Try to achieve a minimum drying time by applying the maximum power that does not cause overheating.

With the exception of the constant power runs, control was maintained primarily by making adjustments of the power based on the temperature data.

The end of drying was indicated by two outputs. One was the temperature, which usually indicated that drying was complete when it reached 30 or 40 °C. The weight indicated that drying was complete when it remained unchange for one or two minutes. If the weight began to increase rather than decrease, the sample was probably dry and the sample was beginning to loose its ability to grip the temperature probe.

4.2.4 Experiment Shut Down

Once it had been determined that the sample was dry, the data acquisition program was terminated and the following list was executed:

1. Turn off the pump.
2. Open the vacuum system.
3. Place the remaining liquid nitrogen back into large dewar.
4. Remove the lower half of the condensate trap.
5. Turn off all equipment and remove the sample for inspection.

At this point the data was evaluated and the apparatus was prepared for another sample.

Chapter 5

Results and Discussion

The objectives of this research are to develop an experimental microwave freeze-drying apparatus, test the feasibility of using the apparatus to freeze-drying aqueous solutions and, finally, study the effects of freezing rate on the freeze-drying samples. The development of the apparatus and freeze-drying procedures were integrated with the feasibility study. Once the apparatus was working properly, drying rate experiments were conducted in order to study the effects of freezing rate on the drying characteristics. In this chapter, the development of the experimental apparatus and procedures are discussed and results of experiments are presented.

The experiments were conducted with a nine percent by weight solution of Mannitol and water. The solution of Mannitol and water was chosen because it is a simple sugar solution and there are some freeze-drying data presented in the literature (Pikal et al., 1985) based on experiments with Mannitol and water. Also, Mannitol is a crystalline solute which is expected to be more sensitive to freezing rates than an amorphous solute. For a more complicated solution, it is important to know the collapse temperature, which corresponds to the glass transition temperature.

5.1 Freezing Rates

Before the experiments were conducted for a particular freezing rate case, the freezing curve for that case was measured. This was done once for each different freezing condition. The freezing rate was determined according to Eq. (1). Results for the slow, medium and fast freezing rate cases are shown in Fig. 5.1. The results of the three freezing rate calculations based on the curves shown in Fig. 5.1 are given in Table 5.1.

The slow freezing rate curve has a sharp discontinuity caused by undercooling. In this case, the freezing of the sample occurs slowly so that the temperature distribution throughout the sample is uniform. Under these conditions it is possible that the nucleation of ice crystals will not occur until the solution reaches a certain level of undercooling which corresponds to thermodynamic instability. Once the nucleation begins, ice crystals form at rapid rate until all the water is frozen. The rapid formation of ice crystals causes the sharp increase in temperature at the discontinuity shown in Fig. 5.1a.

Under the other two freezing conditions, freezing of the water happens too rapidly

Table 5.1 *Freezing Temperatures and Calculated Freezing Rates*

	Freezing Temp (°C)	Freezing Rate (°C/min)
Slow Freezing Rate	-10	0.21
Medium Freezing	-60	3.1
Fast Freezing Rate	-196	43

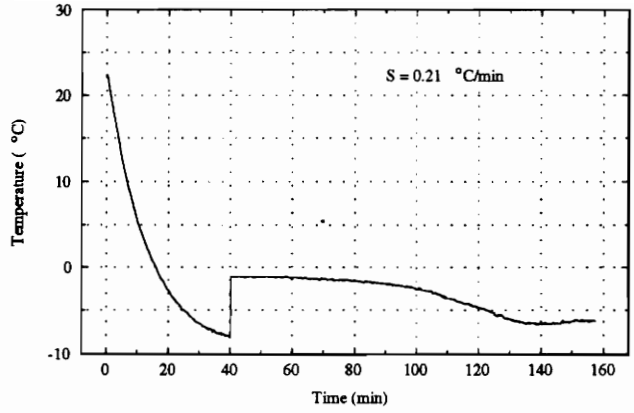

a) Slow freezing rate, S

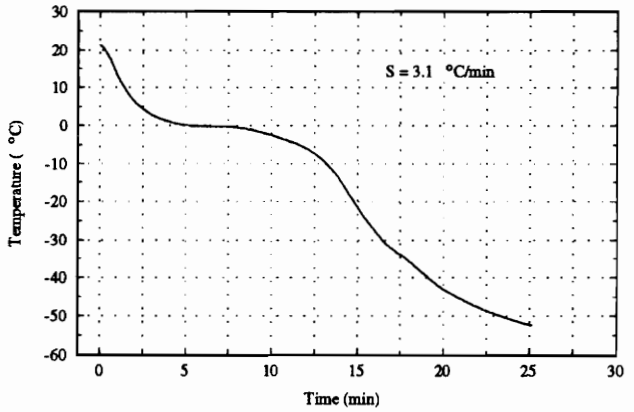

b) Medium freezing rate, S

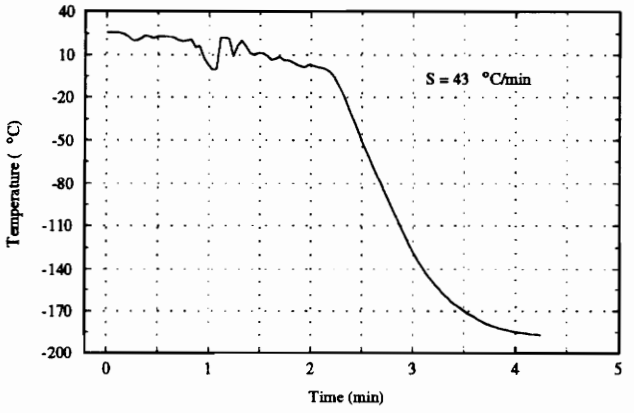

c) Fast freezing rate, S

Figure 5.1 Freezing curves, S = freezing rate

for undercooling to occur. Ice actually begins to form at the outer surfaces of the sample. The ice front then travels inward towards the temperature probe preventing the temperature of the liquid water from falling below the freezing point. Also, the fast freezing rate conditions are very different from the other two. When the sample vial is lowered into the liquid nitrogen, the turbulence generated by the boiling of the liquid nitrogen prevents the sample from freezing in a steady manner which adds to the difficulty of measuring this freezing rate.

When comparing the three freezing rates it is obvious that there is a significant difference in the numerical results. The medium freezing rate, 3.1 °C/min, is approximately fourteen times the slow freezing rate, 0.21 °C/min, and the fast freezing rate, 43 °C/min, is approximately fourteen times the medium freezing rate. It was expected that the significant difference in freezing rates would produce noticeable differences in the results of the freeze-drying experiments.

5.2 Microwave Freeze-Drying Results

Microwave freeze-drying experiments were conducted in two phases: apparatus testing/feasibility experiments and freezing rate study experiments. Initial experiments were conducted to test the performance of the apparatus. Once the initial problems with the apparatus were corrected and the feasibility of microwave freeze-drying of aqueous solutions had been established, experiments were conducted to determine the effects of the freezing rate on drying characteristics of the aqueous solution.

This section covers the development and the results of the microwave freeze-

drying experiments. Data is presented and explained and the data analysis program is also discussed. Also, drying rates, dried layer mass transfer resistance and physical characteristics are discussed in detail.

5.2.1 Experimental Development

The initial tests of the apparatus exposed several problems. The first problem encountered concerned the chamber pressure. Microwave freeze-drying pressures of less than 1 Torr were desired for the drying rate experiments that were to be conducted. But, the system was not able to reach pressures this low. With the use of a vacuum bag sealant and the addition of a larger vacuum pump, appropriate pressures for microwave freeze-drying were reached.

Once the system pressure could be maintained less than 1 Torr, freeze-drying experiments were conducted. The first step was to freeze a sample in a glass sample vial. However, it was found that upon freezing the glass vial would crack at low temperatures. Polyethylene sample vials were tried next. These vials also crack in the freezer. The next attempt was with polypropylene sample vials. These vials did not crack during freezing of the sample. However, during the first attempt at microwave freeze-drying, the top rim of the polyethylene vial had melted. It was apparent that the sample vial had to be made of a material that would not crack during freezing and has a very low dielectric loss factor.

The best material available for the sample was Teflon. Two vials were machined from a two inch rod of Teflon. These vials had a 24.5 mm inner diameter and were 41.8

mm in height with a 35 mm wall thickness. These vials performed better than any previous sample vial. However, it was found that the vials would heat during the secondary drying stage. It seems that the loss factor of the dried material was lower than that of the Teflon and under the high field strength present during secondary drying, the Teflon could be heated to temperatures as high as 40 °C. To solve this problem a new vial was machined with a much smaller wall thickness. The dimensions of this vial are given in Chapter 4.

Once these problems were overcome, experiments were conducted to test the feasibility of microwave freeze-drying. It was immediately apparent that the apparatus was capable to freeze-drying the aqueous solution. However, it was difficult to control the process such that a particular temperature profile or drying curve could be achieved. Particularly with the fast freezing rate case, the power had to be continuously adjusted when tying to maintain a certain temperature range. The data obtain from the experiments are presented in the following subsections.

5.2.2 Experimental Results

During the experiments, four types of data were taken: total power, chamber pressure, sample temperature and sample weight. These data are recorded by the data acquisition and then plotted. All four curves are shown together on a single data plot for easy comparison.

The plots of experimental data are presented in Appendix A. An example of a data plot from experiment No. 0309 is given in Fig. 5.2. This plot shows data from a

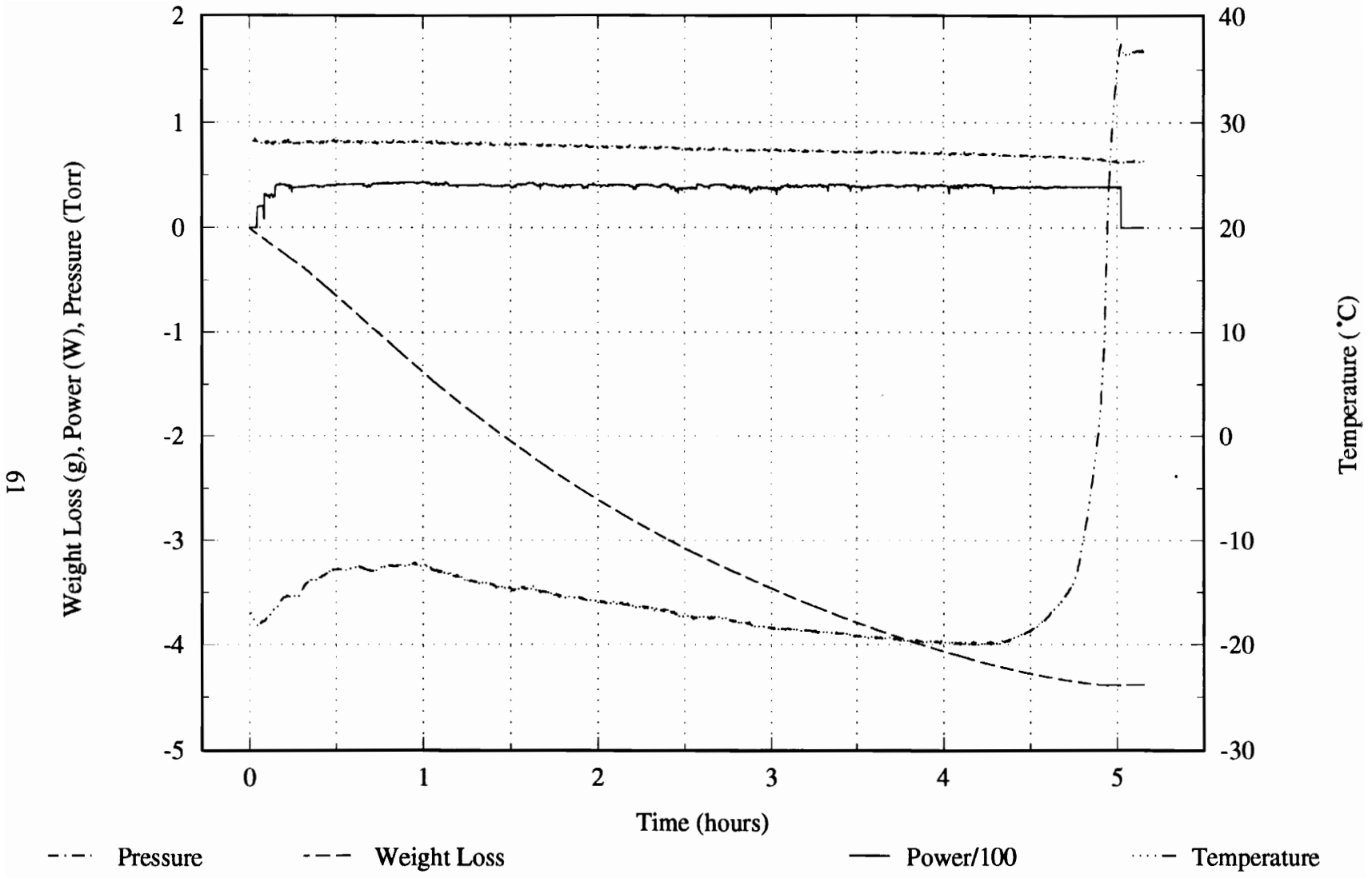

Figure 5.2 Data plot from experiment No. 0309

slow freezing rate case. Notice that there is an initial increase of the measured temperature and then a gradual decrease. This phenomenon is probably due to the fact that the sublimation front is the lowest temperature in the sample and as the sublimation front gets closer to the temperature probe, the measured temperature decreases. Several of the slow freezing rate data sets exhibit this type of temperature behavior.

A list of the experiments for which data plots are included in Appendix A is given in Table 5.2 along with some basic information on each experiment. There are twenty-four data sets listed in this table: eight for the slow freezing rate, seven for the medium rate and nine for the fast rate. Under the column labeled "Control Str", the uppercase letters, A, B and C represent the three control strategies described in Chapter 4. Drying times are listed in hours, and the "Freeze Rate" column denotes whether the sample was frozen under slow, medium or fast freezing rate conditions. The experiment number corresponds to the date when the experiment was conducted.

The primary difference between data sets is due to the difference in freezing conditions. The three different control strategies were attempted for each freezing rate. However, not all control strategies could be applied to each of the different freezing rate cases. The medium and fast freezing rate cases show a lot of variability in the data due to difficulties in controlling the drying rate. In fact, the difference in freezing rates seems to have made so much difference in the behavior of the sample while drying that it was very difficult if not impossible to maintain similar control strategies among different types of samples. It was also difficult to achieve consistent results among identical samples. This was primarily due to difficulties in achieving identical start-up conditions for the

Table 5.2 *Results of Microwave Freeze-Drying Experiments*

Exp. number	Freezing Rate	Drying Time (hours)	Control Strategy	Comments
0523	slow	6.0	B 40W / A	-14C / results OK
0524	slow	5.75	B 40W	-10 to -20C / missing data
0525	slow	6.0	B 40W / A	-14C / good results
0526	slow	5.25	B 40W	no temp / foaming
0314	slow	5.5	B 40W / A	-12C/temp bad, drying curve good
0311A	slow	5.75	B 40W	-12 to -15C/ rough drying curve
0309	slow	5.0	B 40W	-12 to -20C/ good results
0301	slow	5.75	variable power	increasing temp/ OK drying curve
0509	med	9.5	A -13C	increasing power/ thick surface skin
0510	med	9.0	A -12C	very low power / radiant heating
0511	med	3.25	no control	erratic temp and weight/ foaming
0512	med	6.75	no control	spurious results / missing data
0527	med	8.25	A -10C	very low power/ radiant heating
0528	med	7.75	increasing power	no temp / good drying curve
0601	med	6.5	increasing power	no temp/ correlation of power+mdot
0513	fast	9.0	no power	increasing temp / cracked / miss data
0517	fast	8.0	B 20W/slight inc	no temperature data
0516	fast	-	C / stopped	removed for inspection
0518	fast	7.0	increasing power	increasing temp / good results
0519	fast	7.5	variable power	attempted control A / not good results
0203	fast	6.5	C/increasing pow	sharp drop in temp then slow increase
0207	fast	6.5	C	large vial / foaming
0131	fast	6.0	C	large vial / foaming
0128	fast	5.5	C	large vial / foaming

experiments.

5.2.2.1 Data Analysis

In determining how the freezing rate affects the drying characteristics, two comparisons are made: one is a comparison of the mass transfer resistance as a function of dry layer thickness and the other is a comparison of drying curves. Equation (3.3) is used to find the mass transfer resistance as a function of time. Ideally, the variable P_{eq} would be found directly from Eq. (3.4). However, this equation requires knowledge of the temperature at the sublimation front as it moves through the sample. Also, this logic assumes that either the sublimation front is of a uniform temperature or an average sublimation front temperature is known. Measuring this temperature, as the sublimation front moves through the sample, is very difficult. So, the temperature is measured at the bottom of the sample, and it is assumed that

$$T_{sat} = T_{measured} \tag{5.1}$$

where T_{sat} is the saturation temperature. This assumption is based on the fact that the sample is small and the temperature gradient between the bottom of the sample and the sublimation front is expected to be negligible.

To further process the data, FRZDRY2.HST, a history file program, written for AXUM technical graphics and data analysis software from TriMetrix, Inc., was run on the raw data. This program is listed in Appendix C along with MAKEPLOT.HST, another AXUM history file program that produced plots of the measured and calculated

data, such as those shown in Fig. 5.3. This figure contains three individual plots which are of: mass flux verses time, mass transfer resistance verses dried layer thickness and the energy required dissipated by sublimation.

The data shown in Fig. 5.3a-c are also for experiment No. 0309. The mass flow rate is found by calculating the slope of the drying curve at each data point. This rate is assumed to be equivalent to the sublimation rate. The mass flow rate curve, shown in Fig. 5.3a, shows the expected behavior: an initial warming up period, then a constant rate period and, finally, a deceasing rate period. This behavior is consistent with other types of drying. With the mass flow rate known, Eq. (3.3) can be used to compute the dried layer mass transfer resistance, which is shown in Fig. 5.3b.

Figure 5.3c gives the energy required to drive the sublimation at a rate corresponding to the mass flux curve. Considering only the sublimation front, the energy (W), E, required to sublimate the ice is given by

$$\dot{E} = \frac{\dot{m} h_{ig}(T_{sat})}{3600} \tag{5.2}$$

where m is the sublimation rate (g/h), h_{ig} is the enthalpy of sublimation (kJ/kg) and T_{sat} is the saturation temperature (°C). It is expected that the sample will absorb more energy than what is shown in Fig. 5.3c. However, this curve gives a general idea of how much energy is dissipated in the sample. Notice that, in this case, about 40 Watts of total power is being dissipated in the cavity, but according to Fig. 5.3c the sample requires only about 4.5 Watts at the peak mass flow rate. This indicates that a significant portion of the microwave energy is dissipated by wall losses and fringing fields.

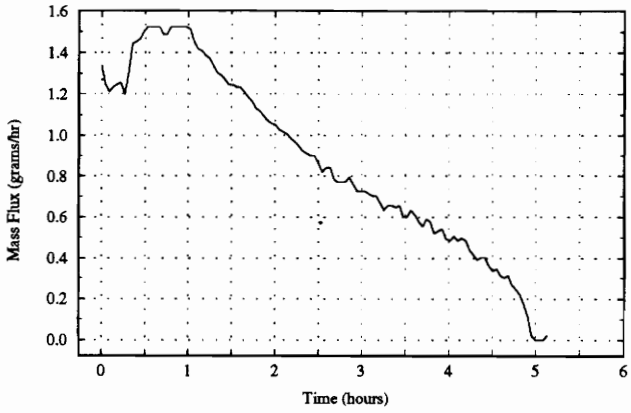

a) Water vapor mass flux

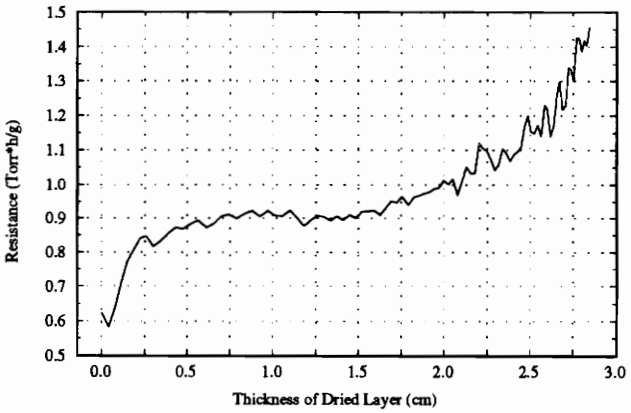

b) Mass transfer resistance of the dried layer

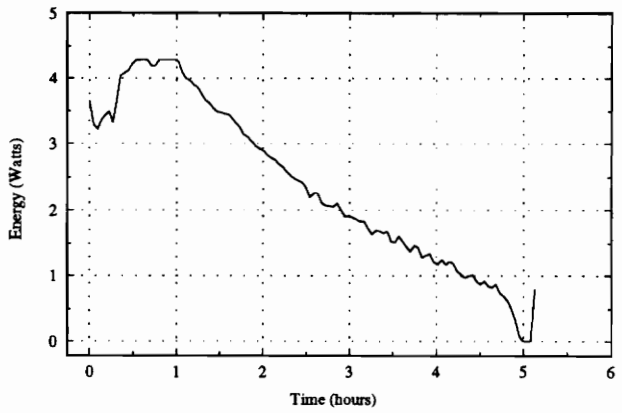

c) Energy required at sublimation front

Figure 5.3 Results of experiment No. 0309

5.2.2.2 Drying Rates

The most basic method of comparing freeze-drying results is to compare the drying curves and associated drying times. For this work, a comparison of drying curves is appropriate because the samples are identical in size, shape and material. It is expected that if only the freezing conditions differ between samples then that difference will show up in the resulting drying curve. However, this assumes that the operating conditions of the microwave freeze-drying apparatus are also similar between experiments.

Figure 5.4 shows a comparison of averaged drying rates for the three different freezing conditions. Each curve is determined by averaging the curves for individual cases. The slow freezing rate result is based on the average of six out of eight drying curves. The medium freezing rate result is based on the average of five out of seven drying curves and the fast freezing rate results is based on seven out of nine drying curves. Some of the curves were left out when calculating the averages due to either missing data in part of the curve or it was very different from the majority of the curves for that freezing rate case. Appendix B contains composite plots of the drying curves for each freezing rate case and information on which curves were used to calculate the average.

The drying times for the slow, medium and fast freezing rate conditions are 5.5 hours, 8.5 hours and 7.0 hours, respectively. The fastest drying time is achieved by the sample with the slowest freezing rate. This is the expected result, because the slower freezing rate allows the growth of larger ice crystals which create larger pore diameters and lower mass transfer resistance caused by the dried layer.

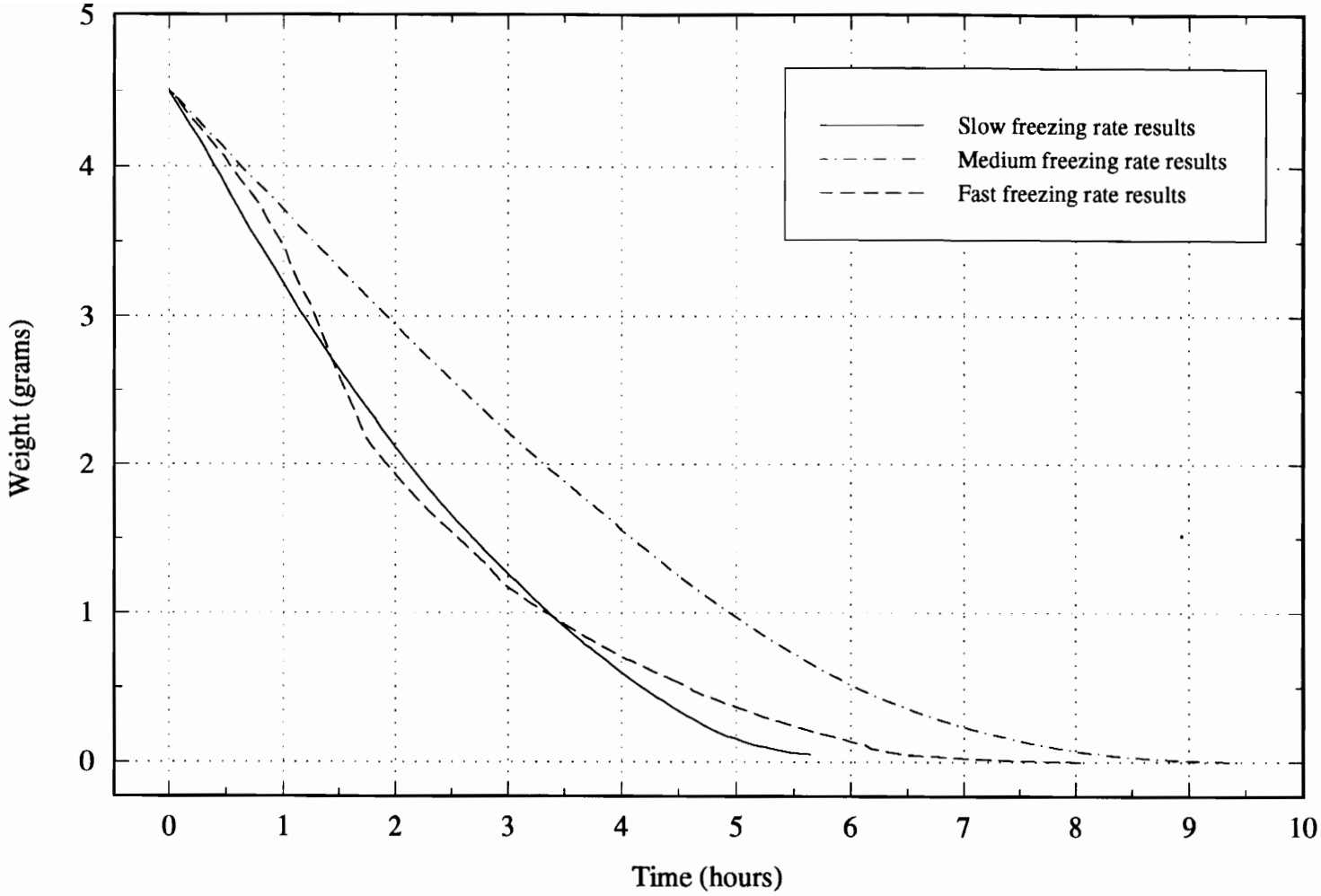

Figure 5.4 Comparison of averaged drying curves

The fast freezing rate case shows an unexpected result. It has an initial drying period where the rate is slow which extends into the second hour, then a rapid drying rate for approximately thirty minutes and, finally, a third period of slow drying. This phenomenon is common among the fast freezing rate cases were the temperature is initially high, around -5 to -3°C. It is believed, after viewing the dried samples, that this phenomenon is caused by cracks in the frozen material that open up after the phase front has receded into the sample. These cracks allow a temporary lowering of mass transfer resistance. In some of the samples, the Mannitol seems to have bubbled up from the surface. This occurrence is referred to as foaming. It is possible to dry a sample with a fast freezing rate without causing foaming. However, it requires the use of a very low power which greatly extends the drying time. In experiment No. 0513, given in Fig. 5.5, a fast freezing rate case, there was little or no power used to heat the sample. The results show no foaming, but the drying time was very long, 9 hours, compared to most other runs which are around in the range of 5.5 to 7.0 hours.

As a comparison to conventional freeze-drying, Pikal (1985) records the drying time for a semi-stoppered vial containing 8 ml of a five percent by weight solution of Mannitol as 14.0 hours. There are significant differences in the conditions under which this time was measured. Pikal held chamber pressure constant at 0.2 Torr, where the microwave freeze-drying case was conducted with chamber pressures of 0.6 to 0.9 Torr. Also, the processing temperature for the slow freezing rate case of the microwave freeze-dried samples was lower than the temperature cited by Pikal. Another difference is that the vial used by Pikal is semi-stoppered, which adds to the total mass transfer resistance

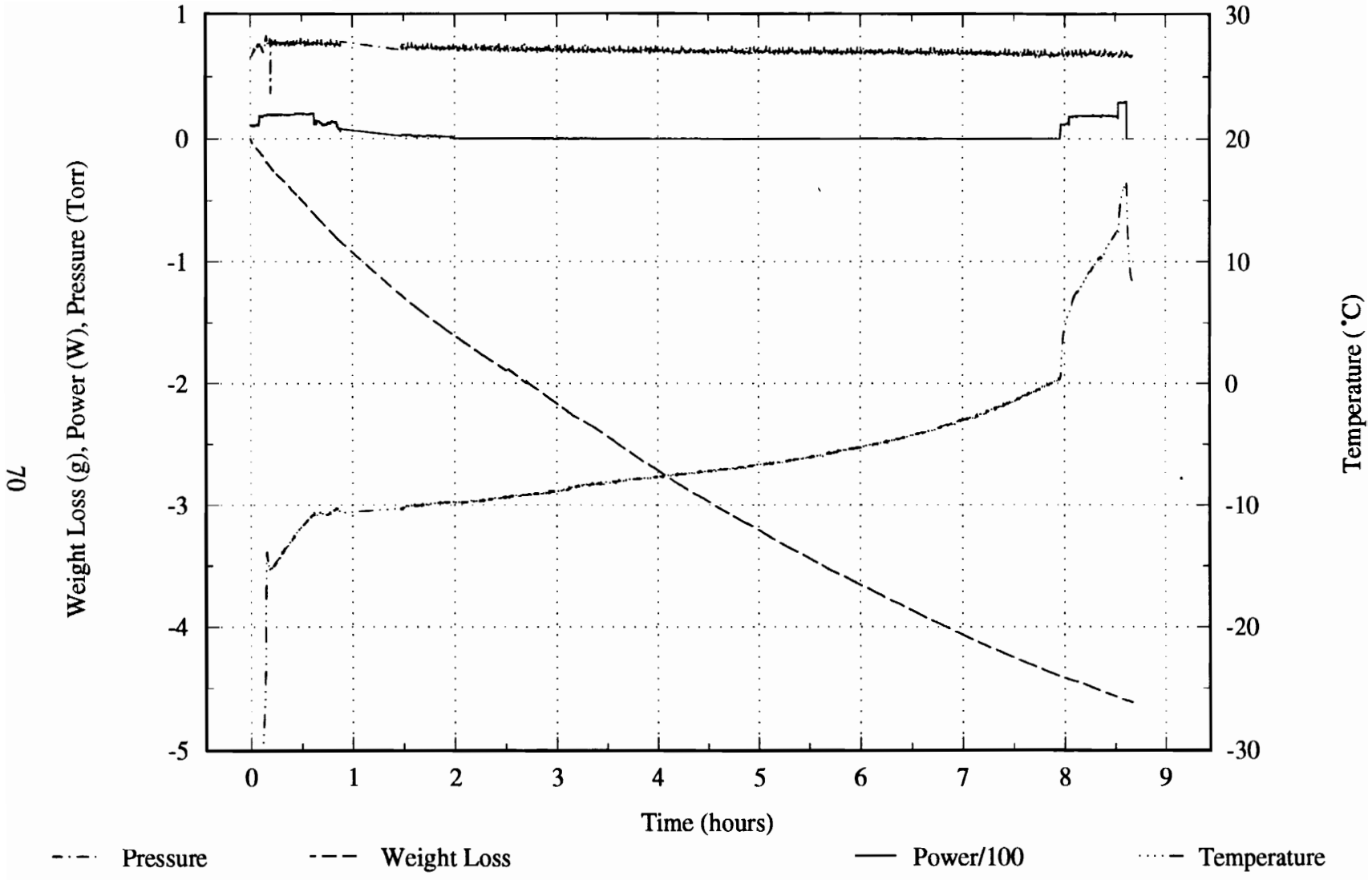

Figure 5.5 Data plot from experiment No. 0513

of the system. Even so, a rough comparison can be made, which shows that microwave freeze-drying can greatly reduce drying times.

5.2.2.3 Dried Layer Resistance

The usual theoretical model of dried layer mass transfer resistance suggests that resistance is both directly proportional to thickness and independent of temperature (Pikal et al., 1983). Pikal et al. (1983) found that the mass transfer resistance with respect to the material thickness for a sample which has a constant area sublimation front, and thus can be considered a one dimensional problem, has two basic types of curves. One is a leveling off of the resistance and the other is a continuous linear increase with material thickness. These results were also found to be temperature dependent. Figure 2.1 shows two variations of each basic type of curve found by Pikal et al. (1983).

The comparison of the dried layer resistances as a function of thickness is shown in Fig. 5.6. This figure shows the expected results: for slower freezing rates the mass transfer resistance of the dried layer is lower. The mass transfer data for the slow freezing rate case, shown in Fig. 5.7, fits well to the model suggested by Pikal et al. (1983) while the sublimation front is moving through the first half of the sample. When the dried layer reaches a thickness of 1.6 cm it begins to deviate from the expected trend and curve upward. This is caused by the phase front increasing in area as it moves through the material. Thus, it becomes a two dimensional problem.

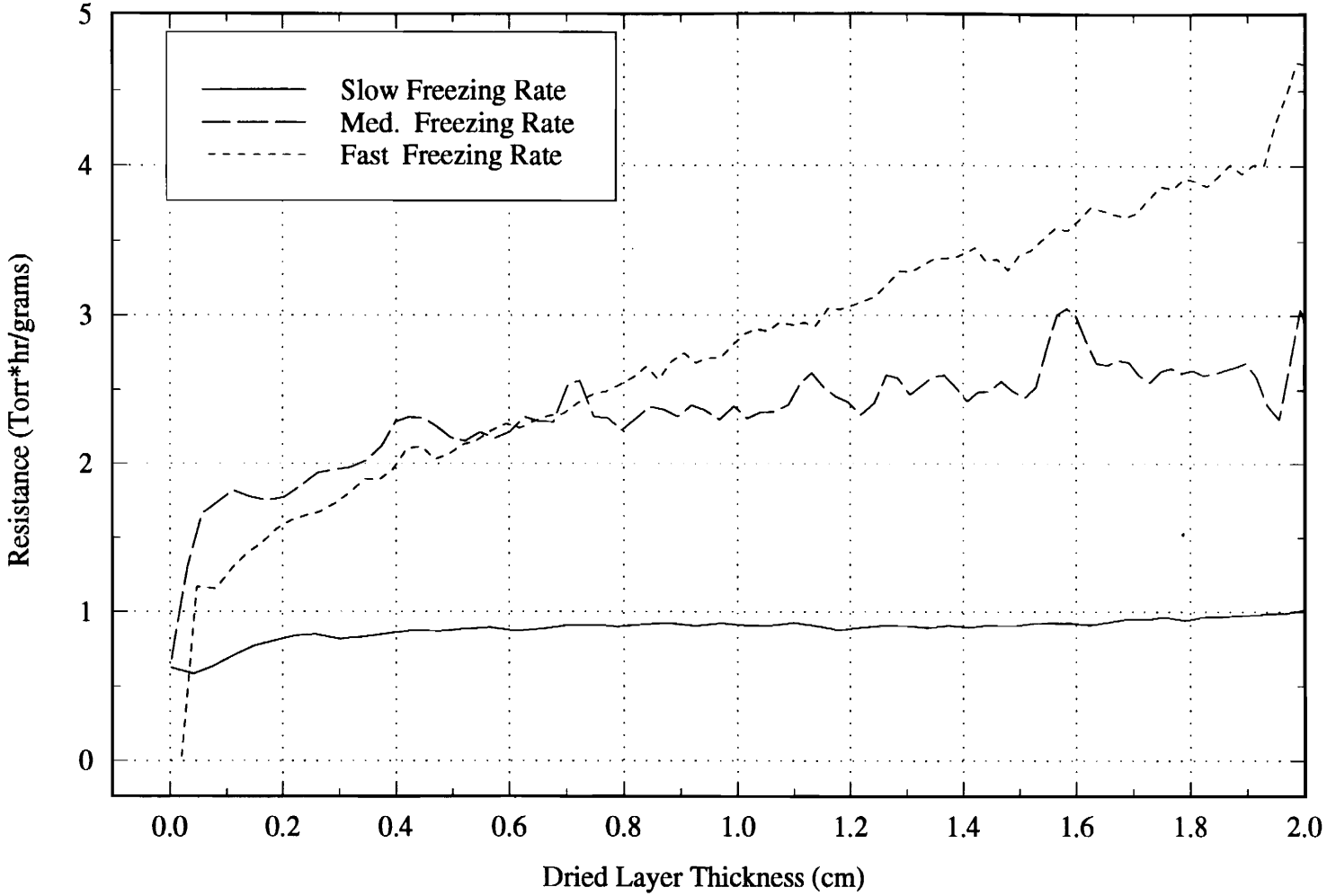

Figure 5.6 Comparison of dried layer mass transfer resistance

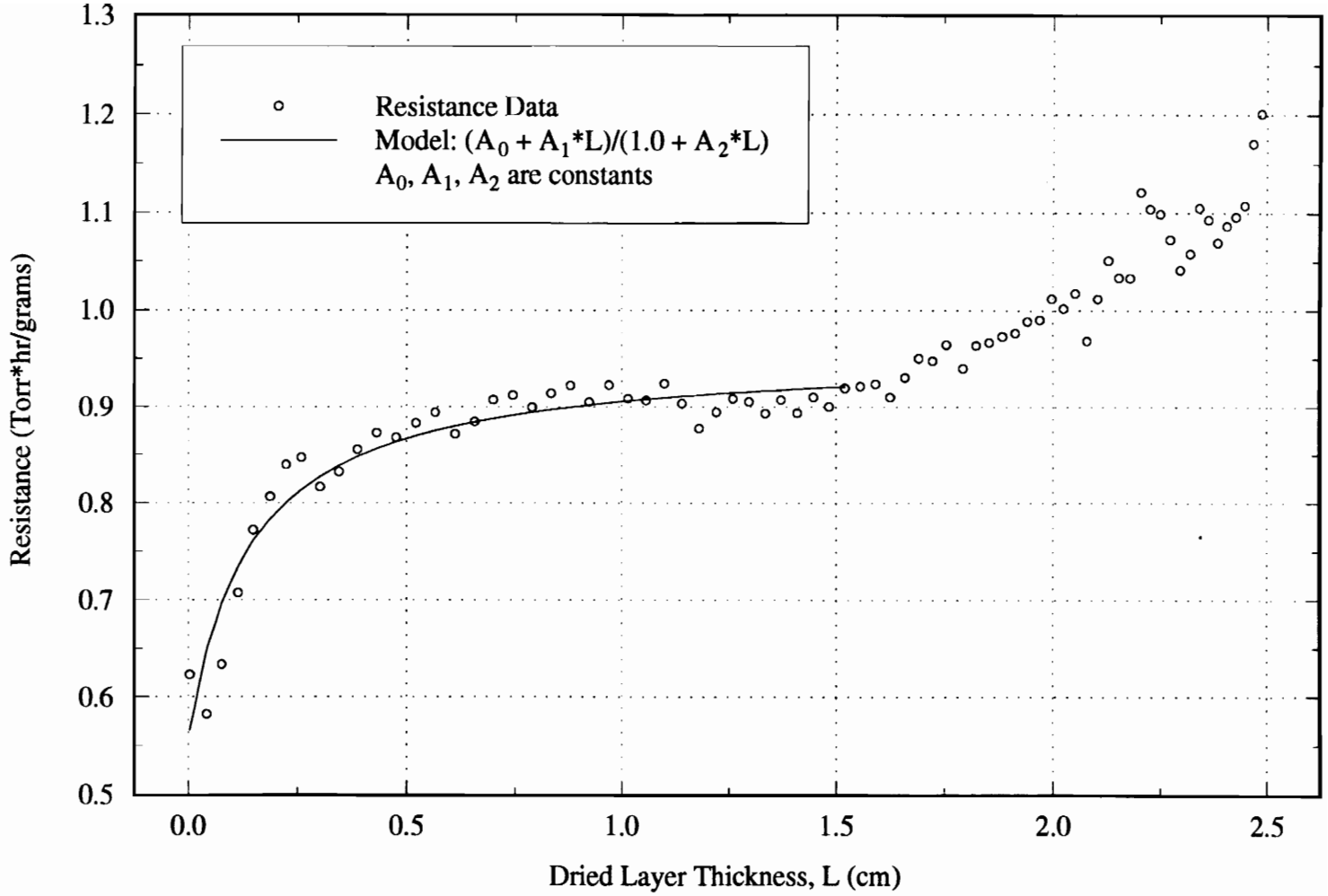

Figure 5.7 Dried layer resistance from experiment No. 0309

5.2.2.4 Physical Characteristics

In addition to the difference in drying characteristics, there are noticeable physical differences in the dried samples. The different physical characteristics can be seen in the scanning electron microscope pictures presented in figure 5.8a-h. Figure 5.8a shows the top crust of the dried product for a slow freezing rate case. This picture, taken at 0.050 kx magnification, shows the formation of large crystals and large holes in the crust that allowed the vapor to escape. As a comparison, pictures were taken at the same magnification of a dried medium freezing rate sample and a dried fast freezing rate sample.

The medium freezing rate sample develops a thick surface skin, shown in Fig. 5.8b. In comparing this picture to Fig. 5.8a, it is apparent that the surface of this sample has a smoother appearance and much smaller holes. Figure 5.8c shows the same surface at 0.200 kx magnification. Here the holes in the surface can be seen clearly. Since the medium freezing rate sample has this thick surface skin and an almost linear drying curve, it is believed that the mass transfer rate is controlled by the surface skin.

The samples dipped in liquid nitrogen do not have a thick skin on top, but often the sample cracks. Figure 5.8d shows a 0.050 kx magnification of the surface of a fast freezing rate sample. In this picture, vertical bands which contain very small holes and alternating with bands which do not have any visible holes can be seen. Figure 5.8e is a 0.400 kx magnification of the same surface. On the left hand side of the picture, small holes and a crack are visible. On the right hand side of the picture there are no holes in the surface. Also, in Fig. 5.8e, there appears to be a very fine crystal structure that is

very different from what is seen on the surface of the slow freezing rate sample in Fig. 5.8a.

Figures 5.8f-h show the structure of the material underneath the surface skin. The slow freezing rate sample is shown in Fig. 5.8f and the medium in Fig. 5.8g. Both of these pictures were taken at 0.100 kx magnification. There is a difference in the structure of the dried material. However, both appear to have about the same degree of porosity. Thus, it would seem that the difference in the surface crusts of these two samples is more of a mass flow rate controlling factor. Figure 5.8h shows the interior of the fast freezing rate sample at 0.200 kx magnification. In this case, it is apparent that this sample has a less open structure compared to the other two samples.

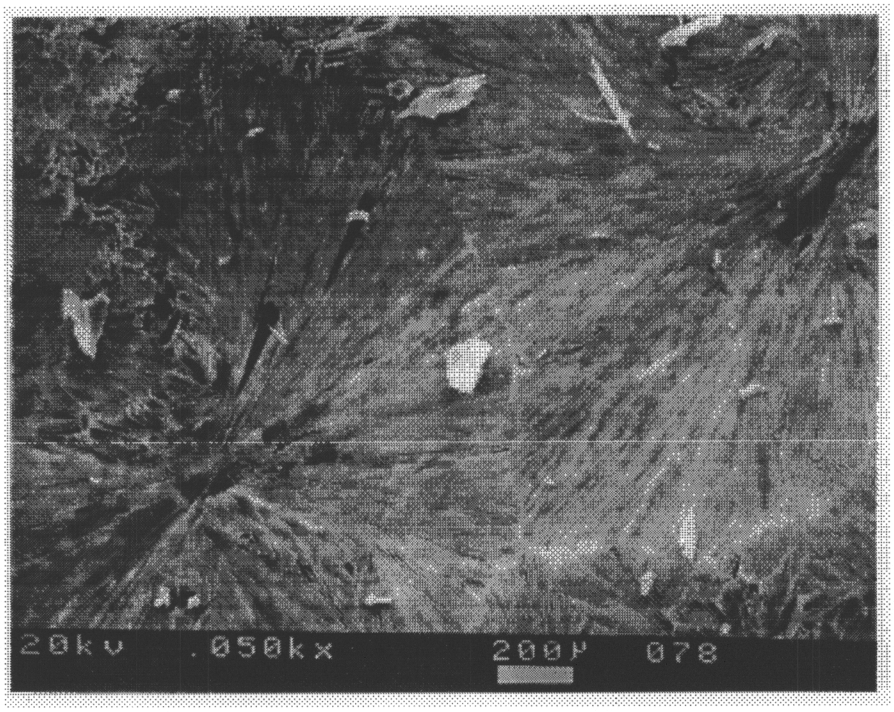

Figure 5.8a Top crust of slow freezing rate case

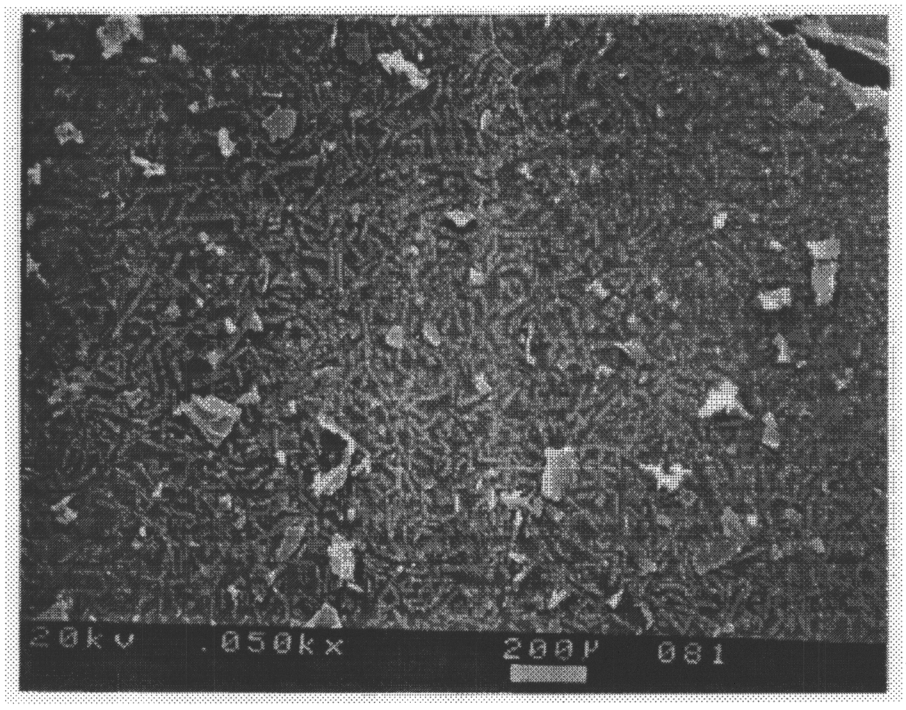

Figure 5.8b Top crust of medium freezing rate case

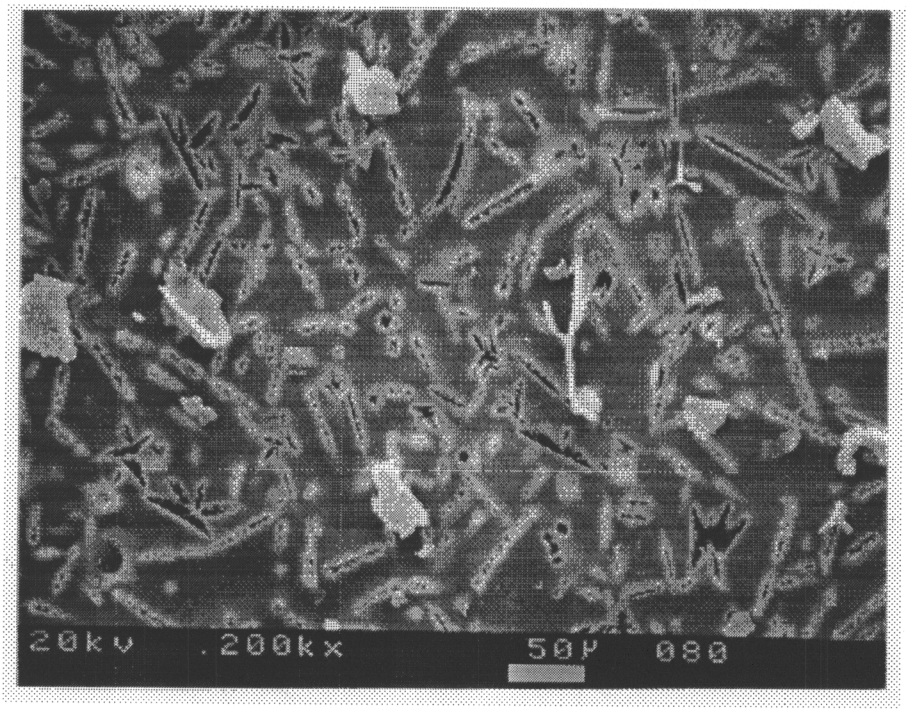

Figure 5.8c Top crust of medium freezing rate case

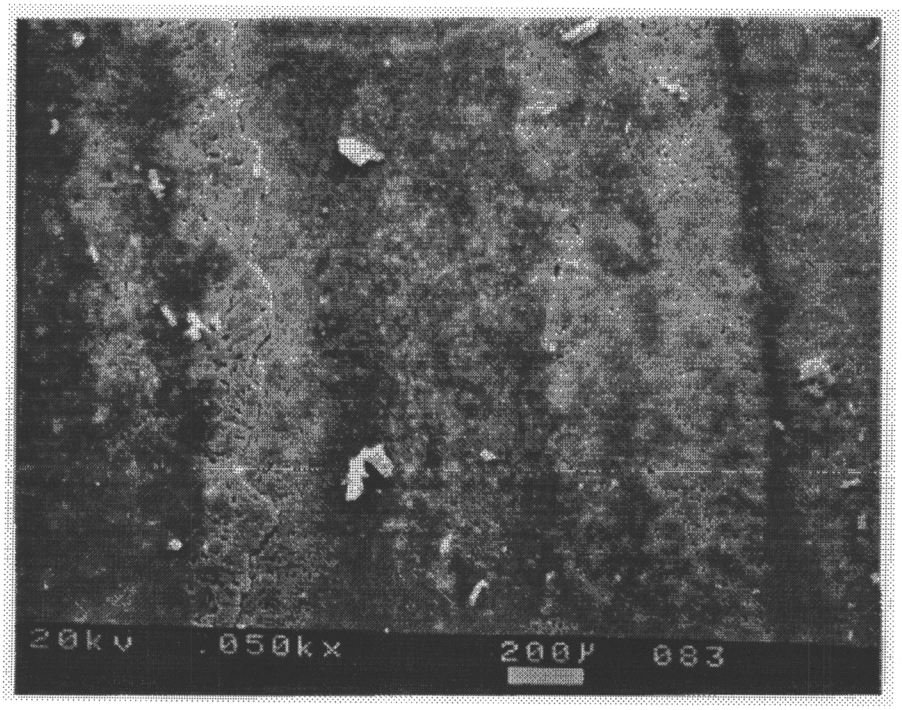

Figure 5.8d Top crust of fast freezing rate case

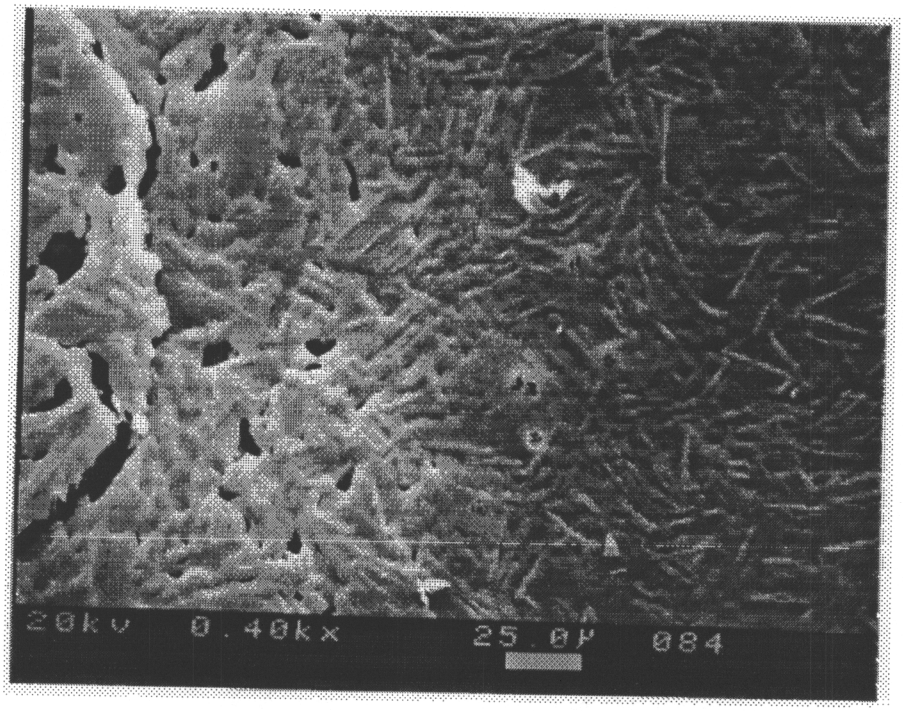

Figure 5.8e Top crust of fast freezing rate case

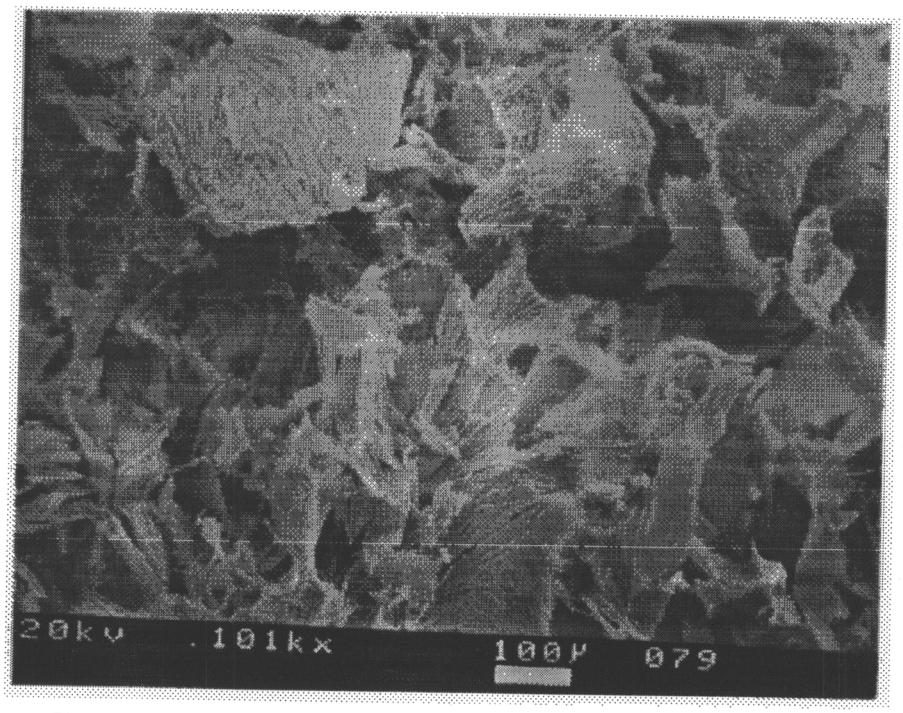

Figure 5.8f Material structure below the surface (slow)

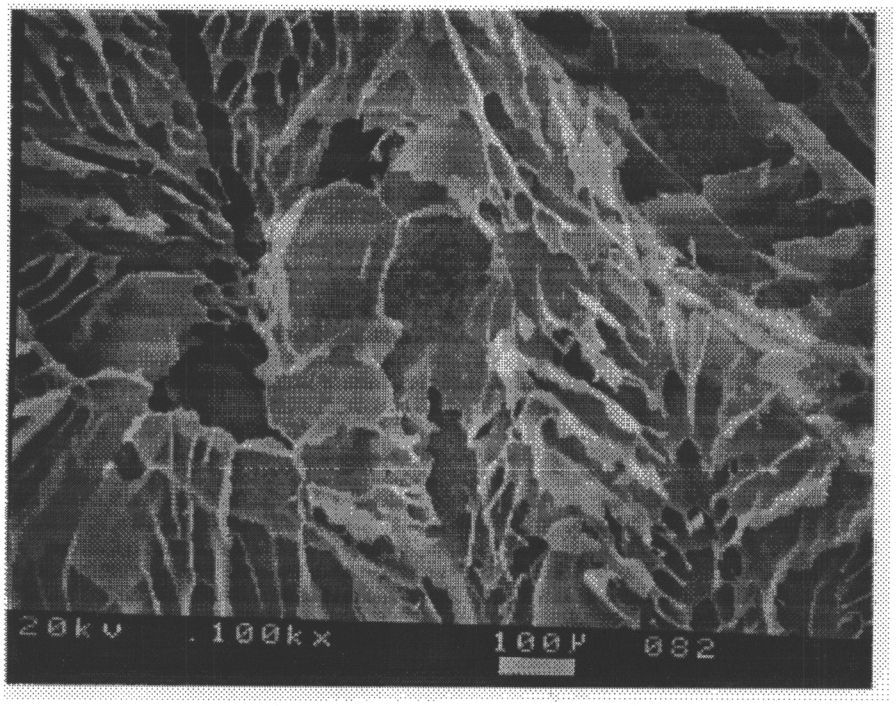

Figure 5.8g Material structure below the surface (medium)

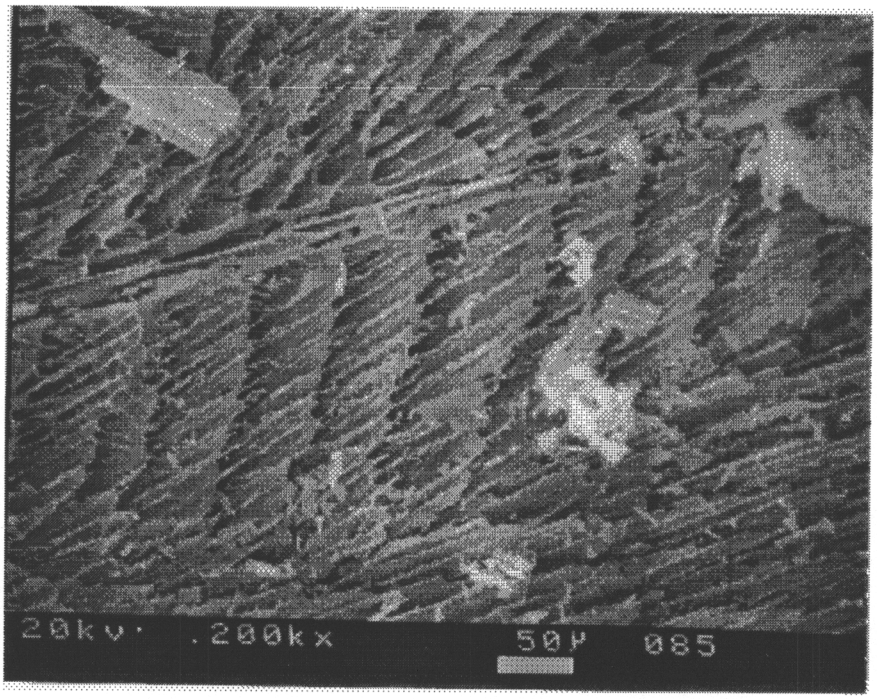

Figure 5.8h Material structure below the surface (fast)

Chapter 6

Conclusions

The results demonstrate the feasibility of freeze-drying aqueous solutions with the aid of microwave energy. The apparatus has been used to show that freezing conditions affect the drying characteristics of the aqueous solution as well as the microstructure of the dried product. As expected, the sample frozen at the slowest freezing rate has the shortest overall drying time and produced the dried product with the lowest mass transfer resistance.

The three different freezing rates produced not only different drying characteristics but also different difficulties with control of the experiment. It appears that the freezing rate significantly affects the freeze-drying process. The effects shown in the results of the experiments demonstrate the need for further study of freezing rates and microwave freeze-drying of aqueous solutions.

Through experimentation, information can be produced that can increase the level of understanding of the heat and mass transfer that takes place during freeze-drying. In addition, the use of microwave energy in freeze-drying can significantly reduce the time required to dehydrate a material. The successful development and utilization of the apparatus presented in this work is part of a continuing effort to improve the freeze-

drying process.

Future work on this subject will entail an expansion of the capabilities of the experimental apparatus. Some of the planned improvements are: pressures comparable to the range of conventional freeze-drying pressures, the ability to obtain data on the temperature gradient that exists in the frozen portion of the sample, and a more detailed investigation into the microstructure of the dried product, which will include more scanning electron microscope pictures. There will also be an attempt to make a more direct comparison between a conventional freeze-drying process and the microwave freeze-drying process.

BIBLIOGRAPHY

Ang, T. K., Ford, J. D., and Pei, D. C. T., 1977, "Microwave Freeze Drying of Food: A Theoretical Investigation," *International Journal of Heat and Mass Transfer*, Vol. 20, pp. 517-526.

Ang, T. K., Ford, J. D., and Pei, D. C. T., 1977, "Microwave Freeze Drying of Food: An Experimental Investigation," *Chemical Engineering Science*, Vol. 32, pp. 1477-1489.

Ang, T. K., Ford, J. D., and Pei, D. C. T., 1978, "Optimal Modes of Operation for Microwave Freeze Drying of Food," *Journal of Food Science*, Vol. 43, pp. 648-649.

Arsem, H. B., and Ma, Y. H., 1980, "Microwave Freeze Drying: A Brief Review," *Drying '80*, A.S. Mujumdar, ed., Hemisphere Publishing Corp., pp. 258-264.

Arsem, H. B., and Ma, Y. H., 1985, "Aerosol Formation During the Microwave Freeze Dehydration of Beef," *Biotech. Prog.*, Vol. 1, No. 2, pp. 104-110.

Arsem, H. B., and Ma, Y. H., 1990, "Simulation of a Combined Microwave and Radiant Freeze Dryer," *Drying Technology*, Vol. 8, No. 5, pp. 993-1016.

Asmussen, J., Lin, H. H., Manring, B., and Fritz, R., 1987, "Single-Mode or Controlled Multimode Microwave Cavity Applicators for Precision Materials Processing," *Rev. Sci. Instrum.*, Vol. 58, No. 8, pp. 1477-1486.

Chang, T. N., and Ma, Y. H., 1985, "Application of Optimal Control Strategy to Hybrid Microwave and Radiant Heat Freeze Drying System," *Drying '85*, T. Ryozo and A.S. Mujumdar, ed., Hemisphere Publishing Corp., pp. 249-253.

Chen, S. -D., Ofoli, R. Y., Scott, E. P., and Asmussen, J., 1993, "Volatile Retention in Microwave Freeze-Dried Model Foods," *J. Food Sci.*, Vol. 58, No. 5, pp. 1157-1161.

Copson, D. A., and Decareau, R. V., 1957, "Microwave Energy in Freeze Drying Procedures," *Food Research*, Vol. 22, pp. 402-403.

Copson, D. A., 1958, "Microwave Sublimation of Foods," *Food Technology*, Vol. 12, pp. 270-272.

Franks, F., 1989, "Improved Freeze-Drying: An Analysis of the Basic Scientific Principles," *Process Biochem.*, Vol. 24, pp. III-VII.

Gould, J. W., and Kenyon, E. M., 1971, "Gas Discharge and Electric Field Strength in Microwave Freeze Drying," *J. Microwave Power*, Vol. 6, No. 2, pp. 151-167.

Hoover, M. W., Markantonatos, A., and Parker, W. N., 1966, "UHF Dielectric Heating in Experimental Acceleration of Freeze Drying of Foods," *Food Technology*, Vol. 20, pp. 103-107.

Hoover, M. W., Markantonatos, A., and Parker, W. N., 1966, "Engineering Aspects of Using UHF Dielectric Heating to Accelerate the Freeze Drying of Foods," *Food Technology*, Vol. 20, pp. 107-110.

Kochs, M., Korber, C. H., Nunner, B., and Heschel, I., 1991, "The Influence of the Freezing Process on Vapor Transport during Sublimation in Vacuum-Freeze-Drying," *Int. J. Heat Mass Transfer.*, Vol. 34, No. 9, pp. 2395-2408.

Livesey, R. G., and Rowe, T. W. G., 1987, "A Discussion of the Effect of Chamber Pressure on Heat and Mass Transfer in Freeze-Drying," *J. Parent. Sci. Technol.*, Vol. 41, No. 5, pp. 169-171.

Ma, Y. H., and Peltre, P. R., 1973, "Mathematical Simulation of a Freeze Drying Process Using Microwave Energy," *AIChE Symposium Series*, Vol. 69, No. 132, pp. 47-.

Ma, Y. H., and Peltre, P. R., 1975a, "Application of Computer Simulation in the Study of Microwave Freeze Drying," *Proceedings, 10th Annual Microwave Power Symposium*, pp. 70-71.

Ma, Y. H., and Peltre, P. R., 1975b, "Freeze Dehydration by Microwave Energy: Part 1. Theoretical Investigation," *AIChE Journal*, Vol. 21, pp. 335-344.

Ma, Y. H., and Peltre, P. R., 1975c, "Freeze Dehydration by Microwave Energy: Part 2. Experimental Study," *AIChE Journal*, Vol. 21, pp. 344-350.

Ma, Y. H., and Arsem, H. B., 1982, "Low Pressure Sublimation in Combined Radiant and Microwave Freeze Drying," *Drying '82*, A.S. Mujumdar, ed., Hemisphere Publishing Corp., pp. 196-200.

Mellor, J. D., 1978, *Fundamentals of Freeze-Drying*, Academic, New York.

Metaxas, A. C., and Meredith, R. J., 1983, *Industrial Microwave Heating*, Peter Peregrinus Ltd., London.

Owusu-Ansah, Y. J., 1991, "Advances in Microwave Drying of Foods and Food Ingredients," *Can. Inst. Food Sci. Technol. J.*, Vol. 24, No. 3/4, pp. 102-107.

Peltre, P. R., Arsem, H. B., and Ma, Y. H., 1977, "Applications of Microwave Freeze Drying: Perspective," *AIChE Symposium Series*, Vol. 73, No. 163, pp. 131-133.

Pikal, M. J., 1985, "Use of Laboratory Data in Freeze-Drying Process Design: Heat and Mass Transfer Coefficients and the Computer Simulation of Freeze-Drying," *J. Parent. Sci. Technol.*, Vol. 39, No. 3, pp. 115-138.

Pikal, M. J., Roy, M. L., and Shah, S., 1984, "Mass and Heat Transfer in Vial Freeze-Drying of Pharmaceuticals: Role of the Vial," *J. Pharm. Sci.*, Vol. 73, No. 9, pp. 1224-1237.

Pikal, M. J., Shah, S., Senior, D., and Lang, J. E., 1983, "Physical Chemistry of Freeze-Drying: Measurement of Sublimation Rates for Frozen Aqueous Solutions by a Microbalance Technique," *J. Pharm. Sci.*, Vol. 72, No. 6, pp. 635-650.

Roy, M. L., and Pikal, M. J., 1989, "Process Control in Freeze-Drying: Determination of the End Point of Sublimation Drying by an Electronic Moisture Sensor," *J. Parent. Sci. Technol.*, Vol. 43, No. 2, pp 60-66.

Scott, E. P., 1994, "An Analytical Solution and Sensitivity Study of Sublimation-Dehydration within a Porous Medium with Volumetric Heating," *J. Heat Transfer.*, Vol. 116, No. 3, pp. 686-693.

Sunderland, J. E., 1982a, "Microwave Freeze Drying," *J. Food Processing Engineering*, Vol. 4, No. 4, pp. 195-212.

Sunderland, J. E., 1982b, "An Economic Study of Microwave Freeze Drying," *Food Technology*, Vol. 36, No. 2, pp. 50-52,54-56.

Thijssen, H. A. C., and Rulkens, W. H., 1969, "Effect of Freezing Rate on Rate of Sublimation and Flavour Retention in Freeze-Drying," *International Institute of Refrigeration.*, Vol. 1, pp. 99-113.

APPENDICES

APPENDIX A

FREEZE-DRYING RESULTS

This section includes the data plots from the experiments listed in Table 5.2.

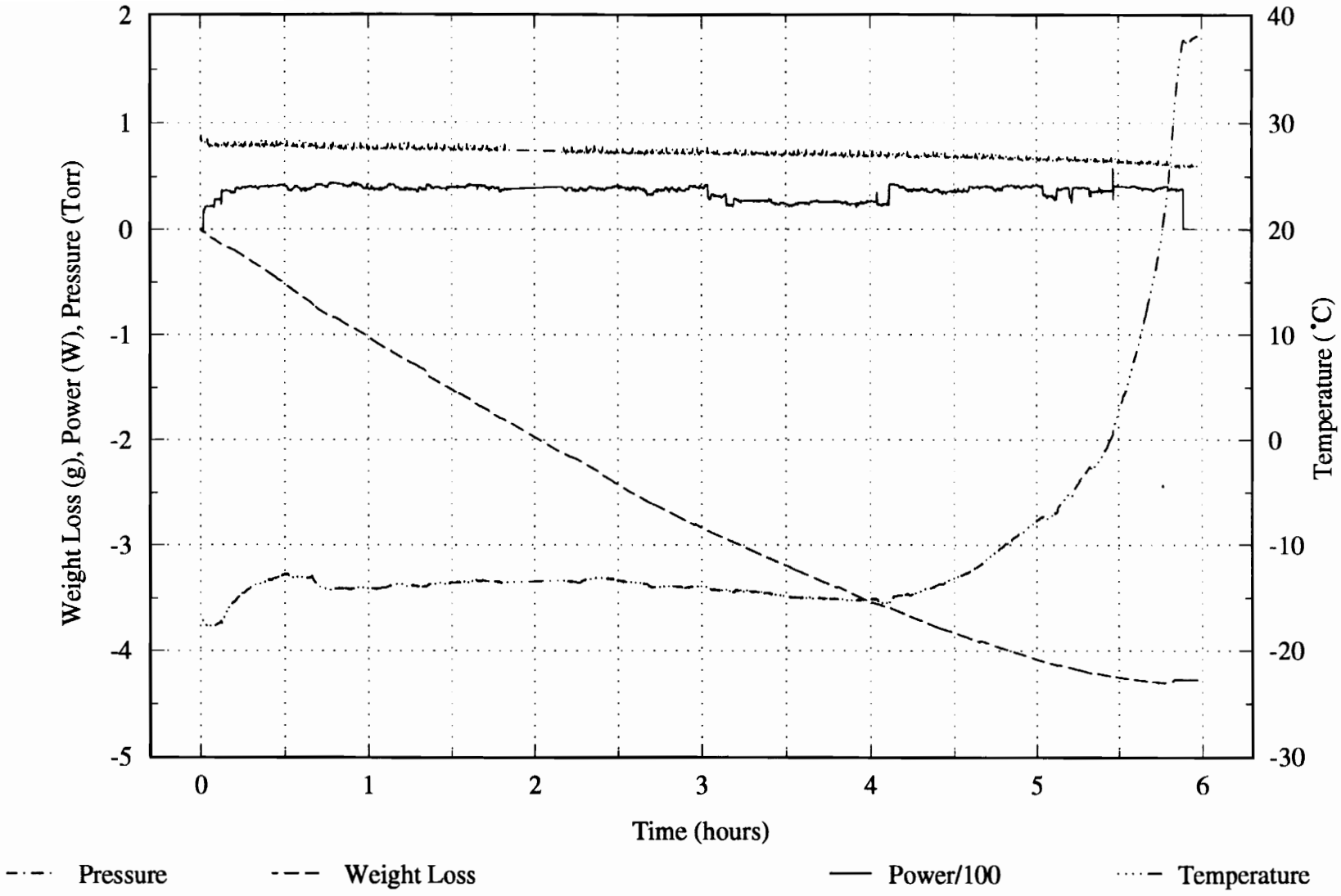

Figure A.1 Data plot from experiment No. 0523

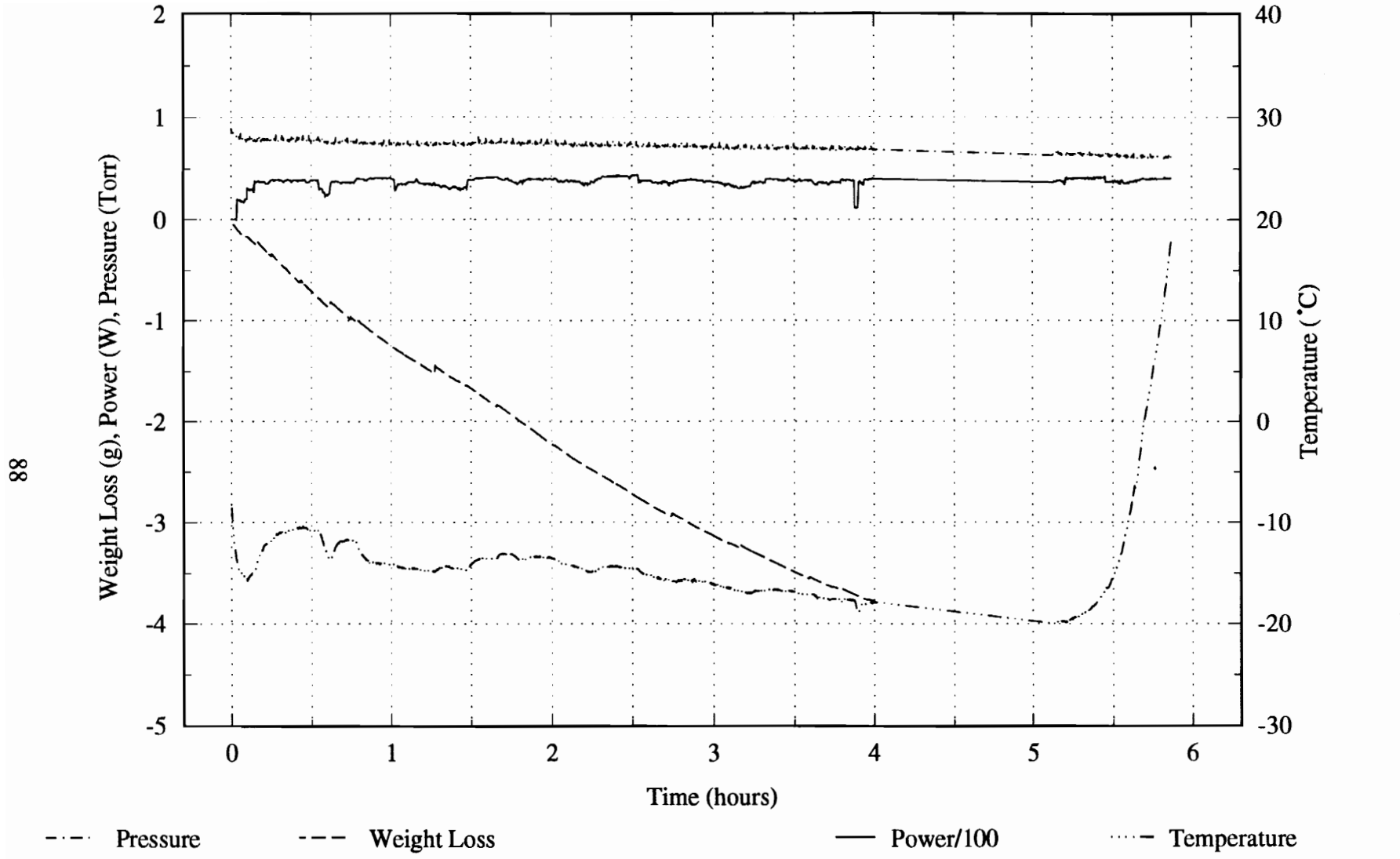

Figure A.2 Data plot from experiment No. 0524

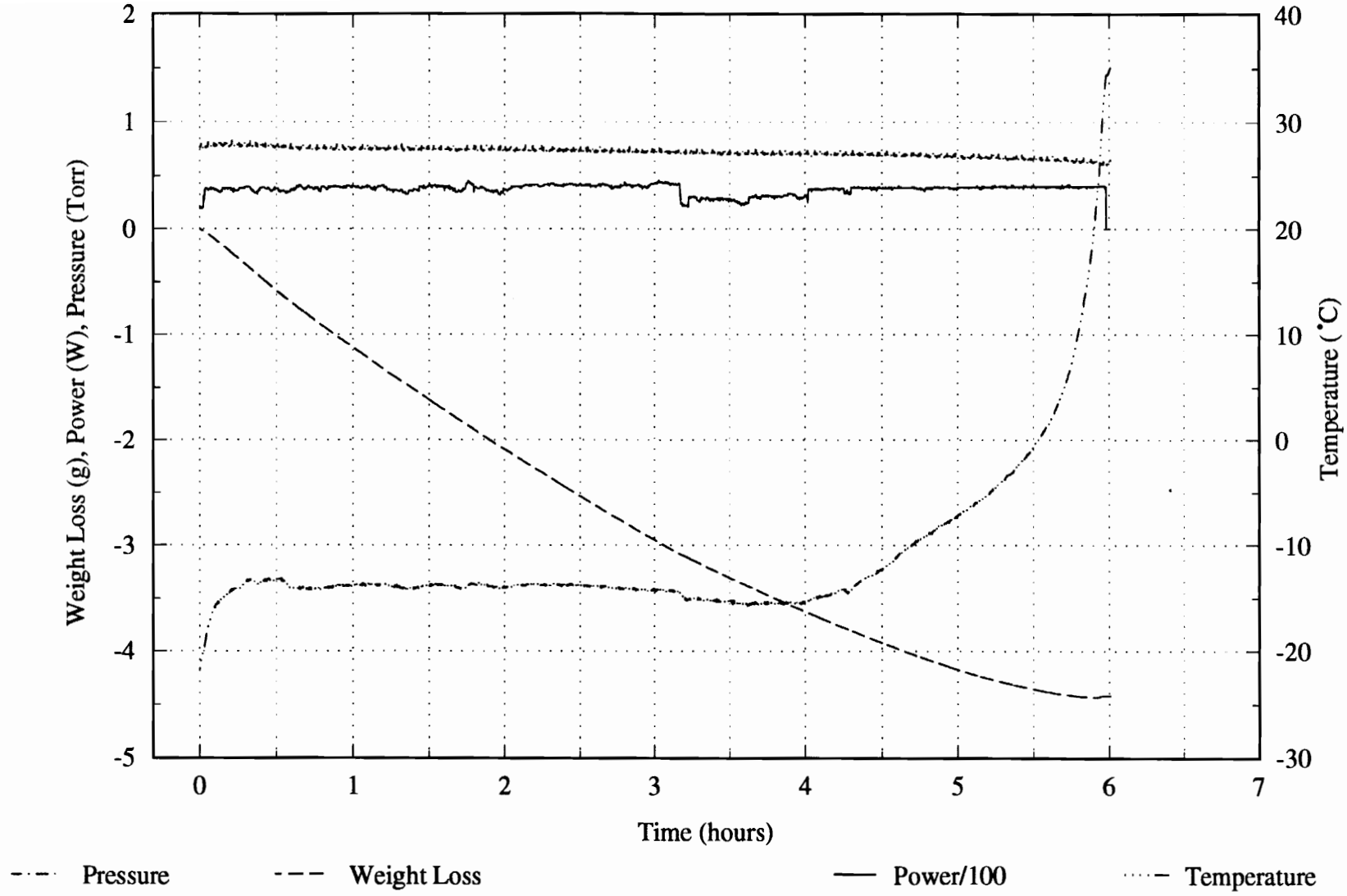

Figure A.3 Data plot from experiment No. 0525

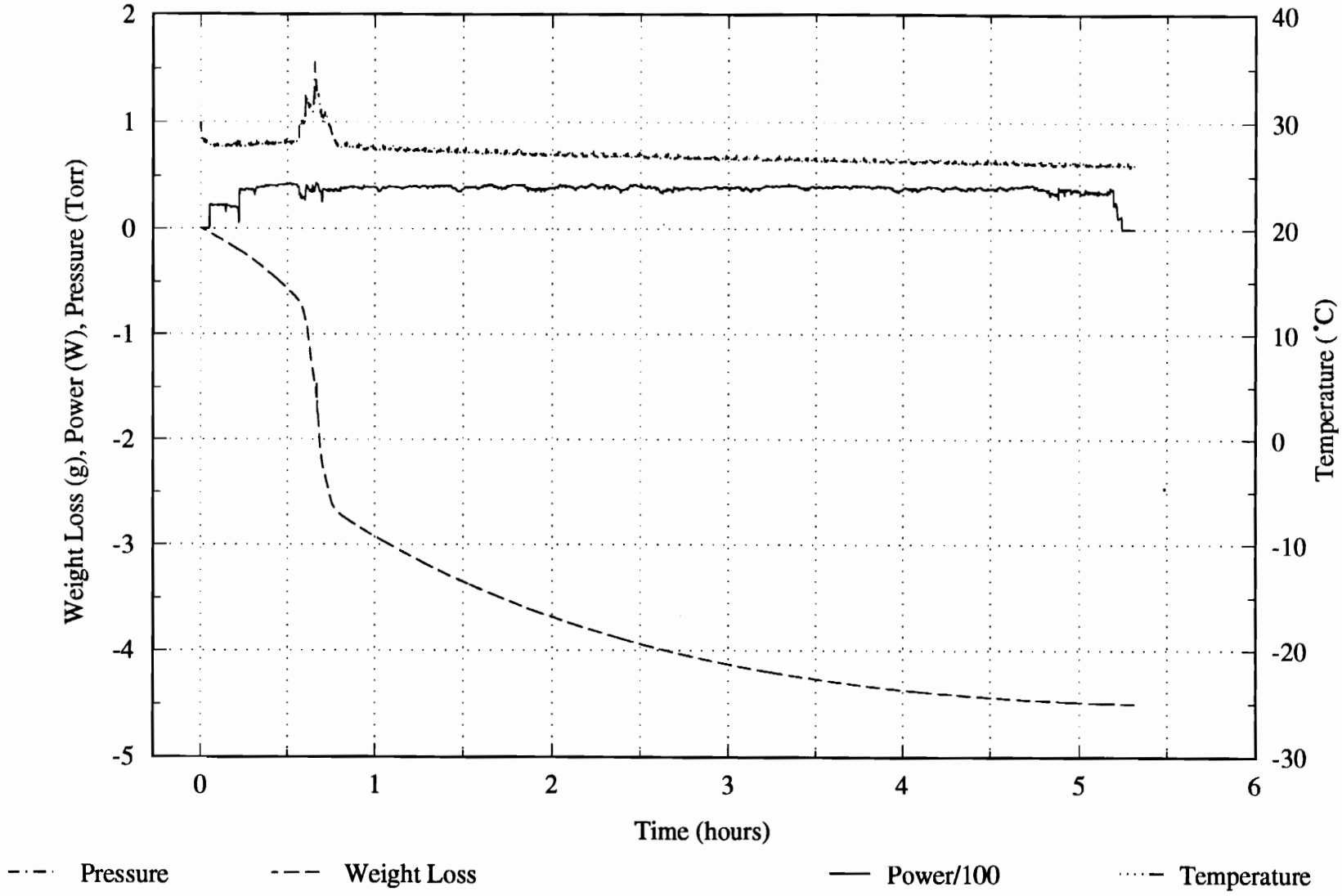

Figure A.4 Data plot from experiment No. 0526

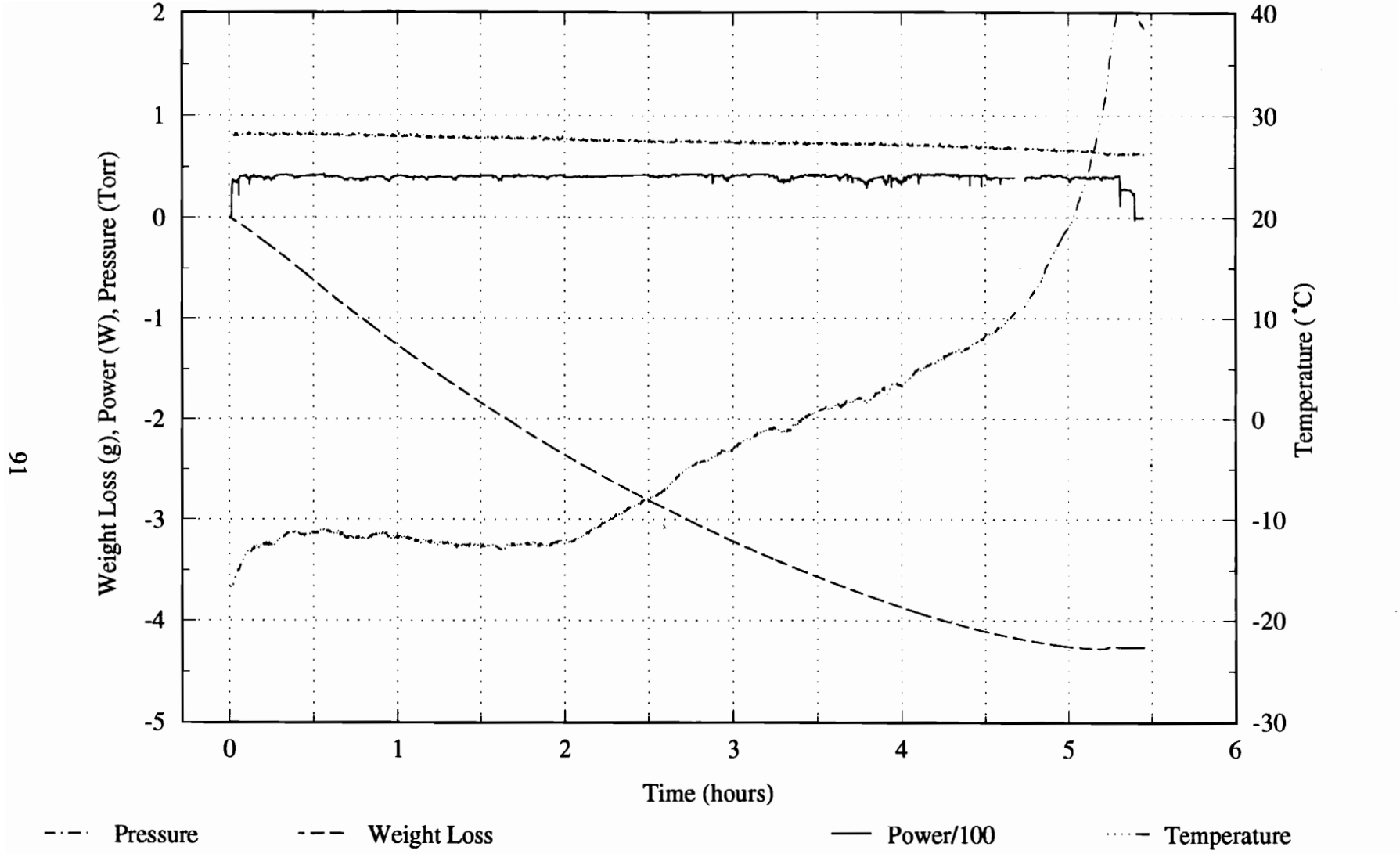

Figure A.5 Data plot from experiment No. 0314

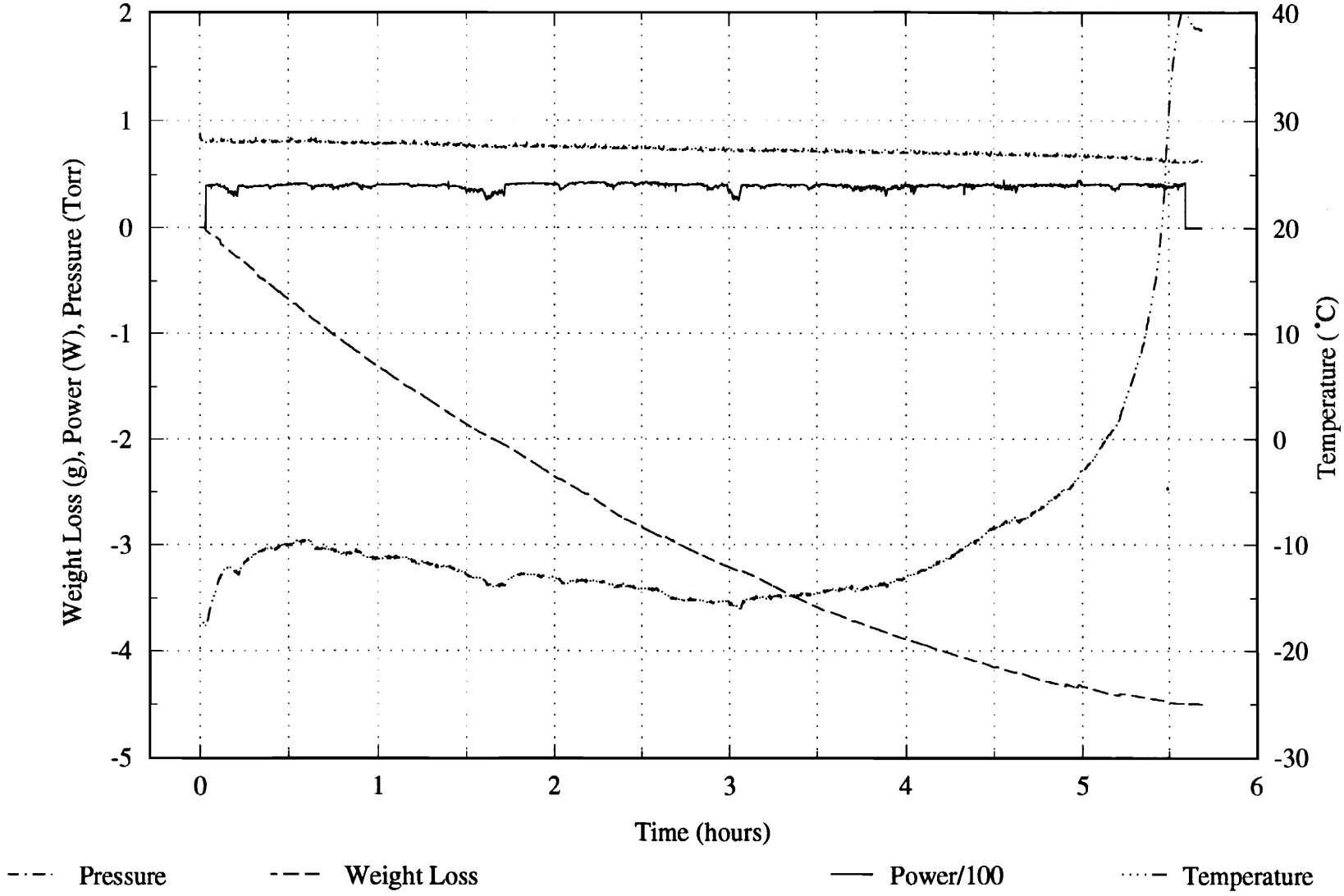

Figure A.6 Data plot from experiment No. 0311A

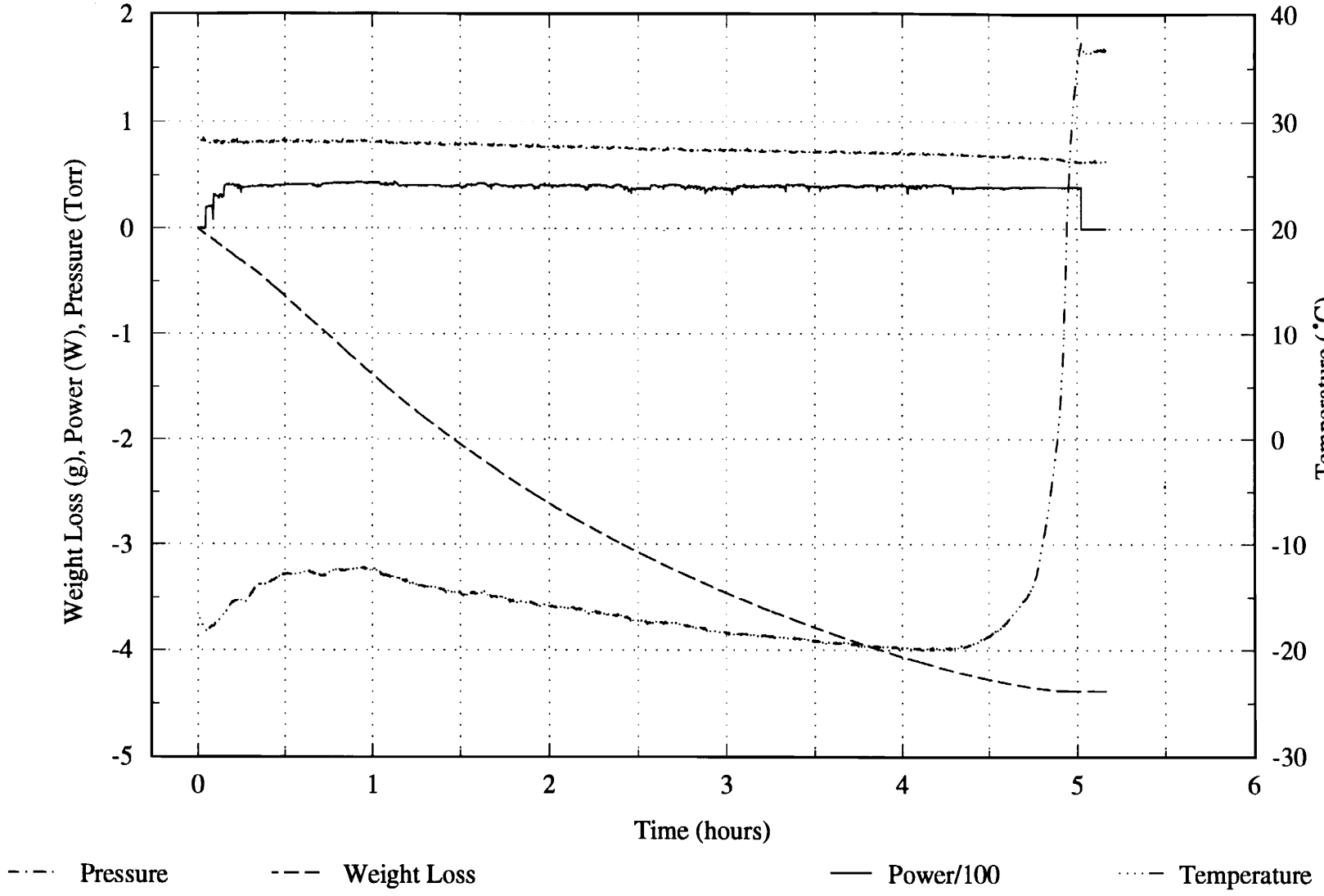

Figure A.7 Data plot from experiment No. 0309

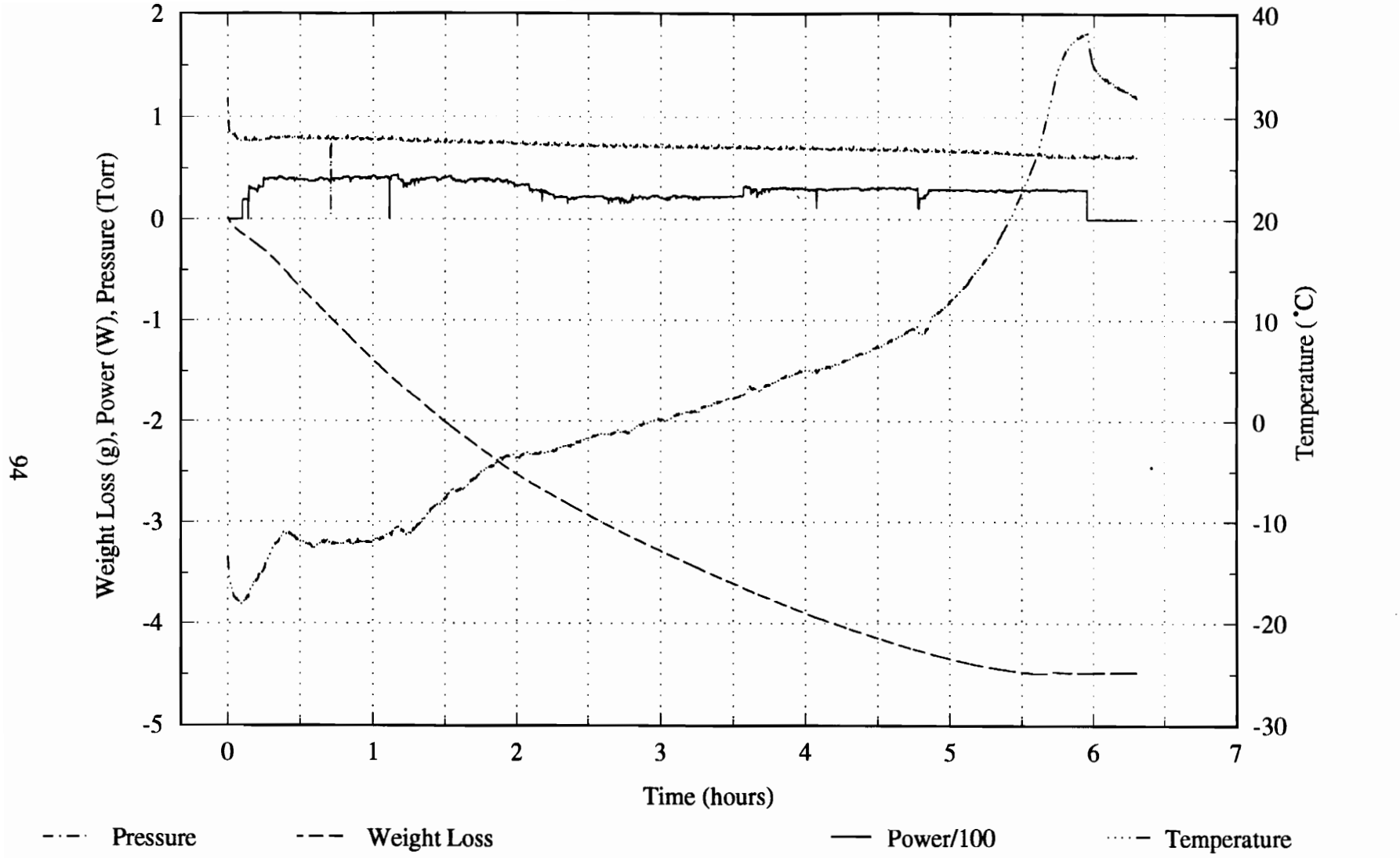

Figure A.8 Data plot from experiment No. 0301

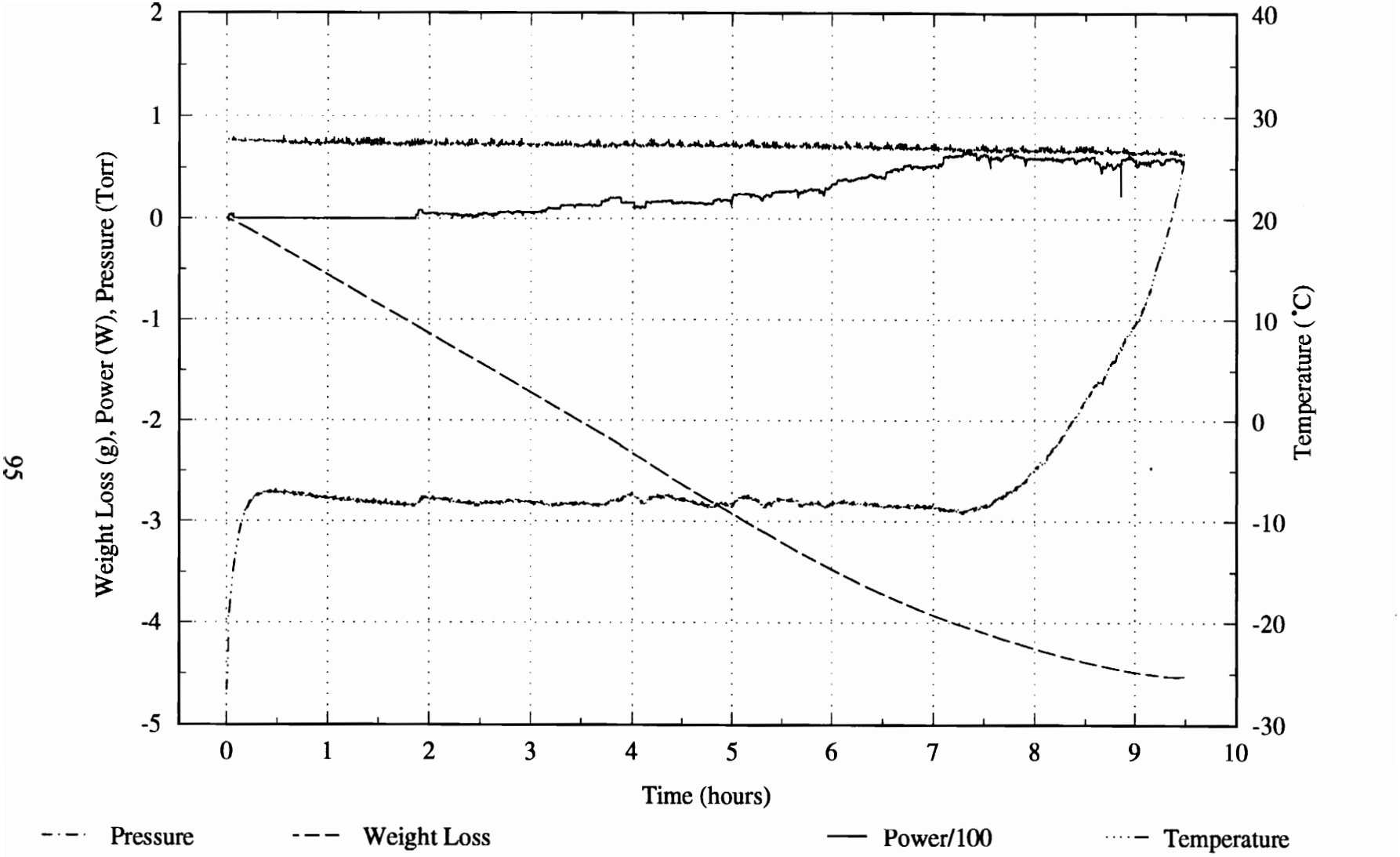

Figure A.9 Data plot from experiment No. 0509

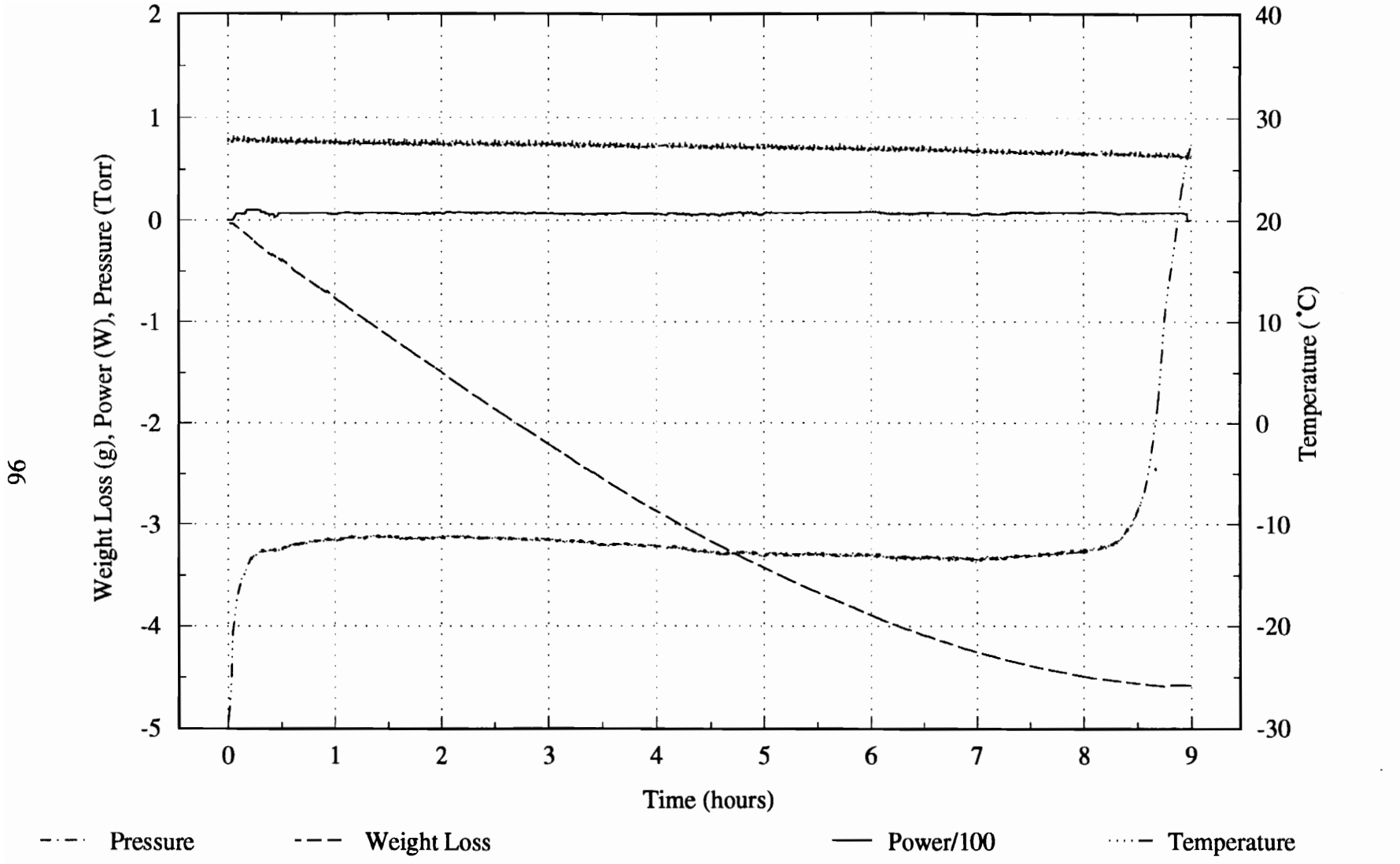

Figure A.10 Data plot from experiment No. 0510

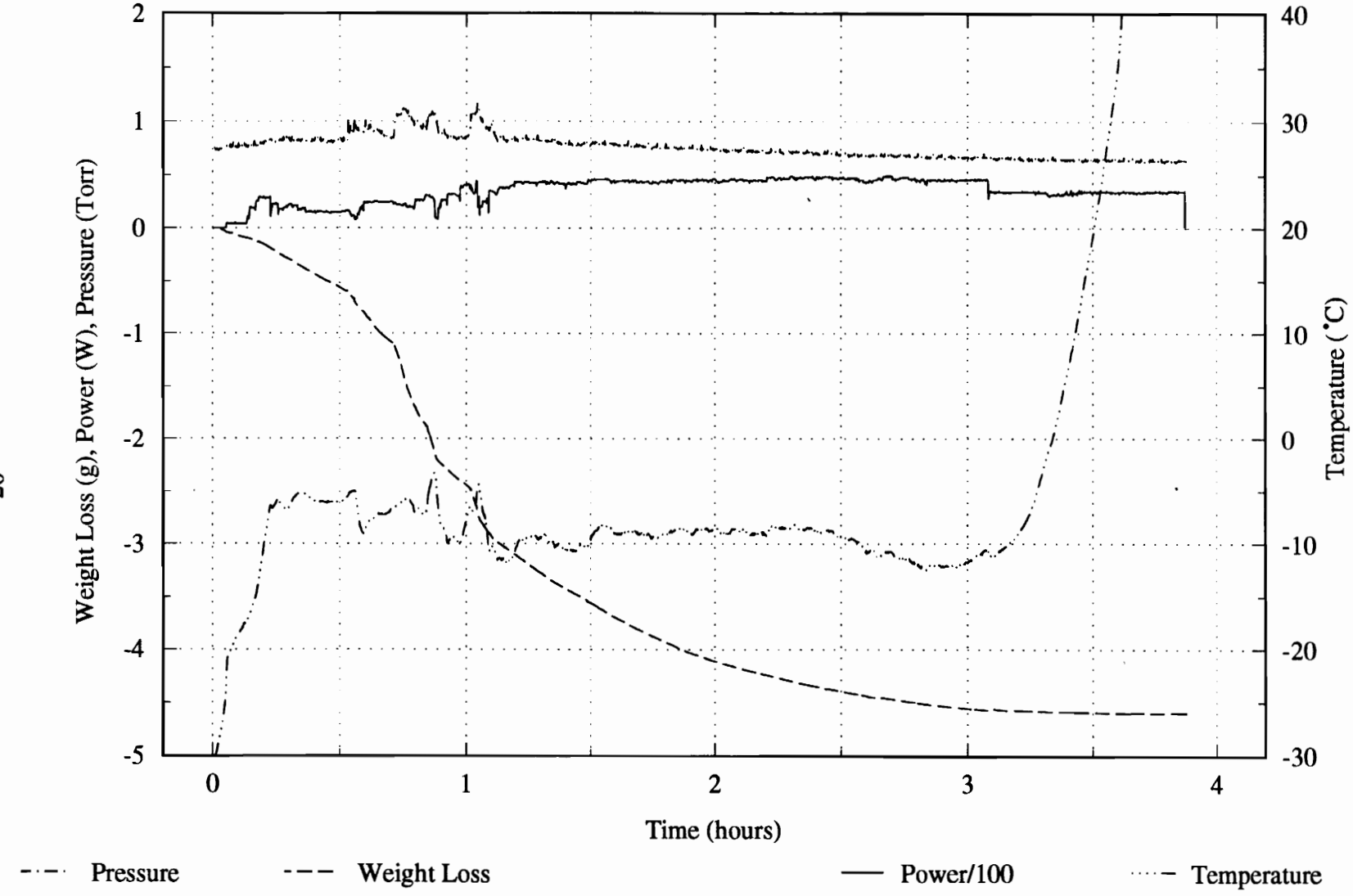

Figure A.11 Data plot from experiment No. 0511

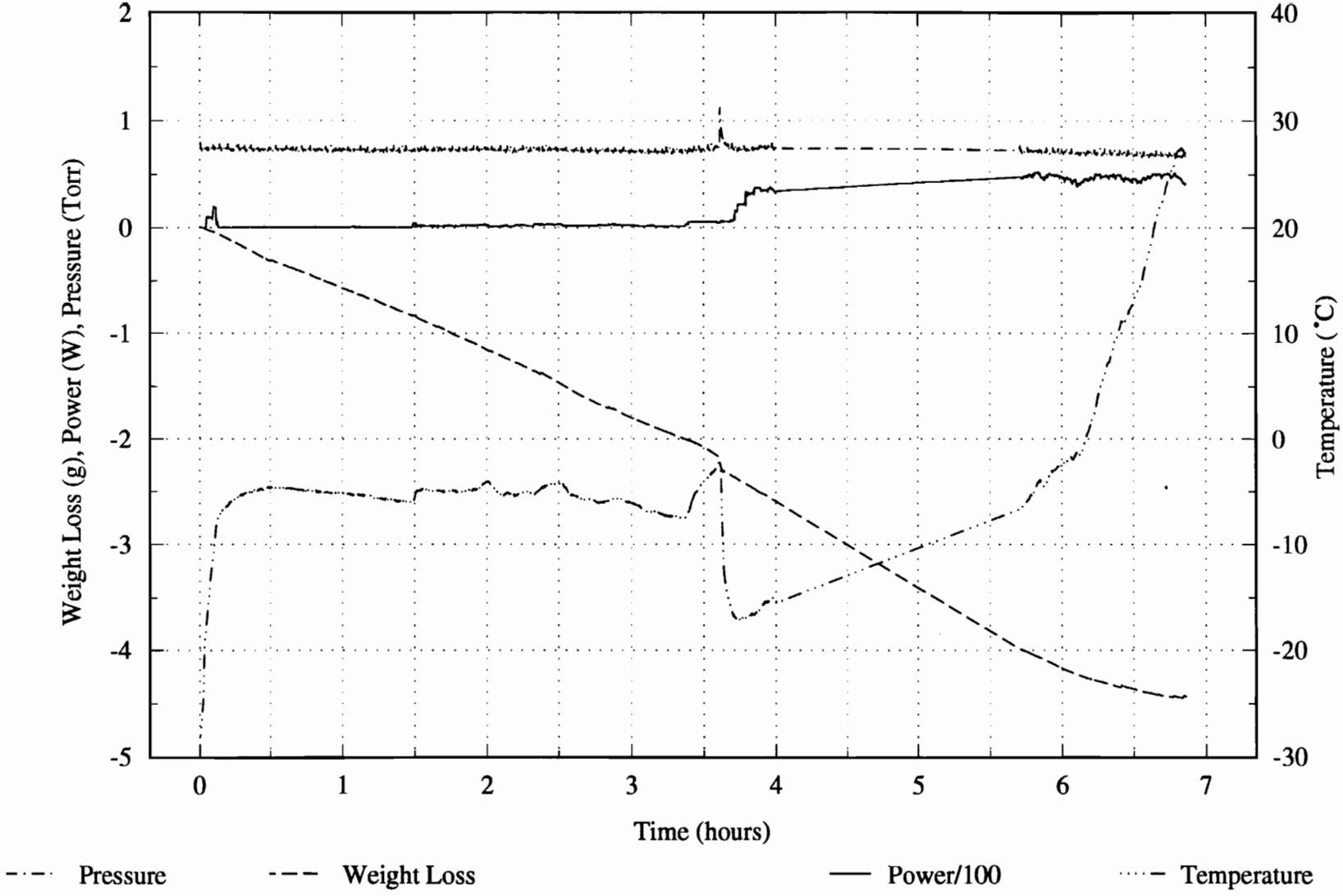

Figure A.12 Data plot from experiment No. 0512

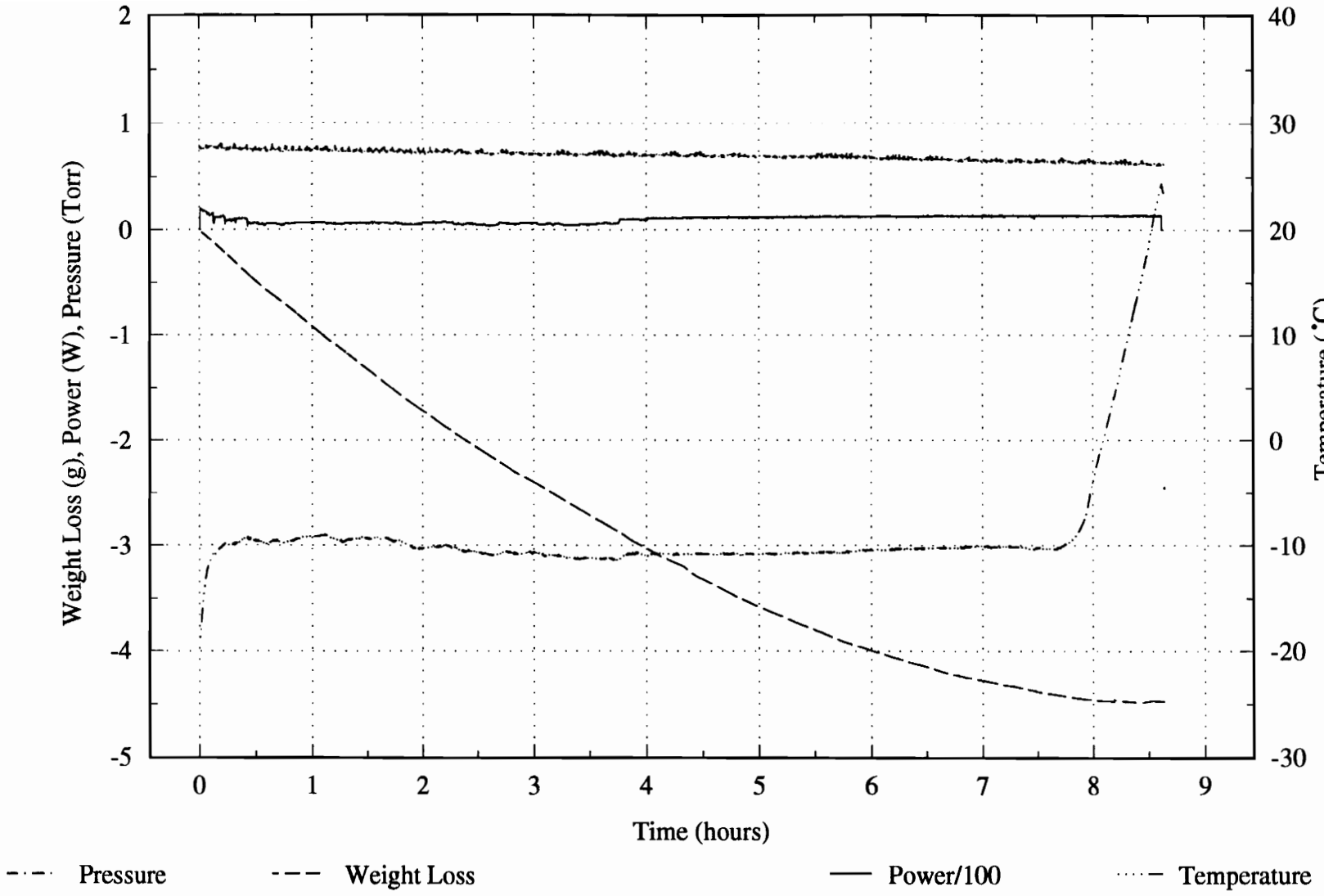

Figure A.13 Data plot from experiment No. 0527

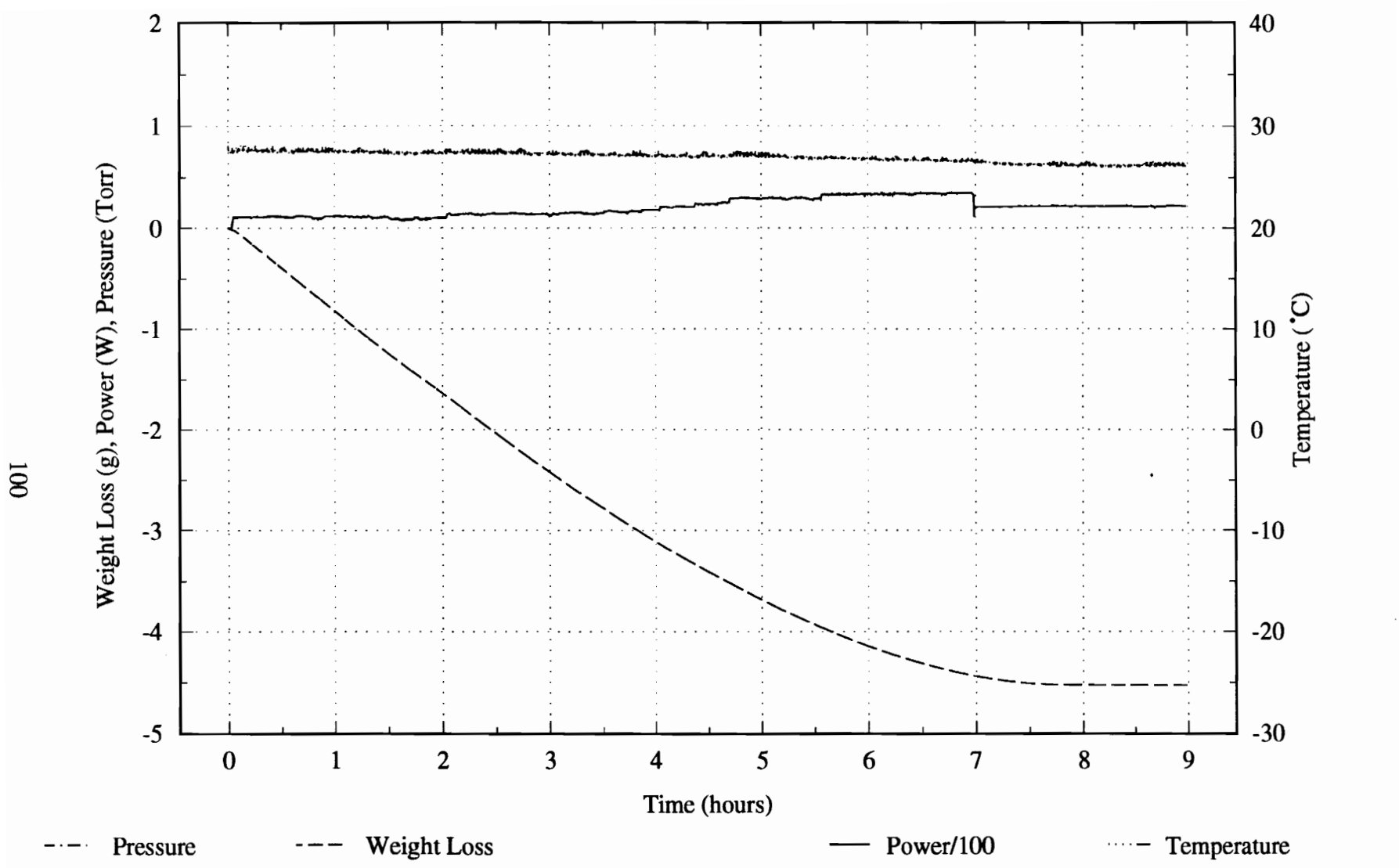

Figure A.14 Data plot from experiment No. 0528

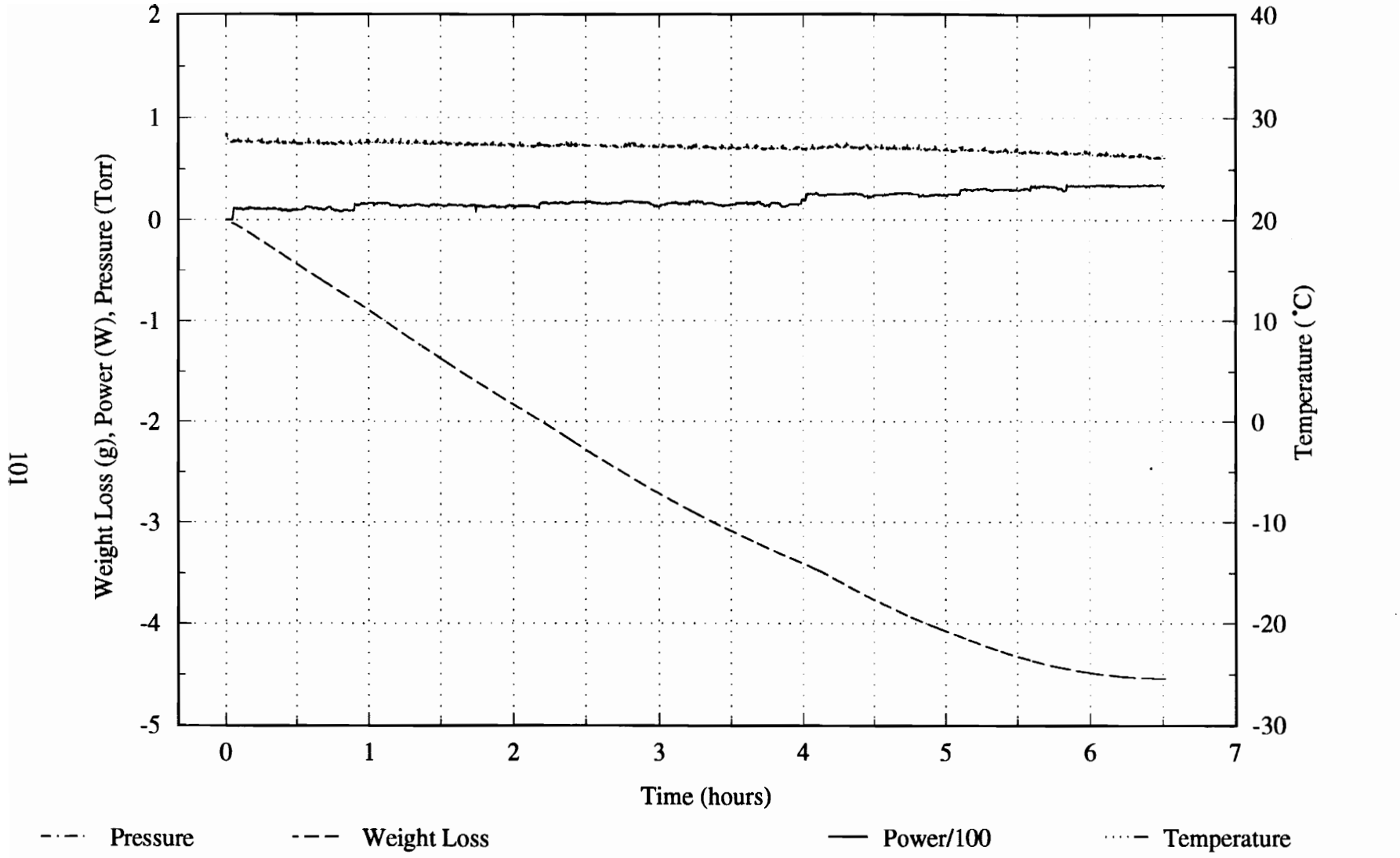

Figure A.15 Data plot from experiment No. 0601

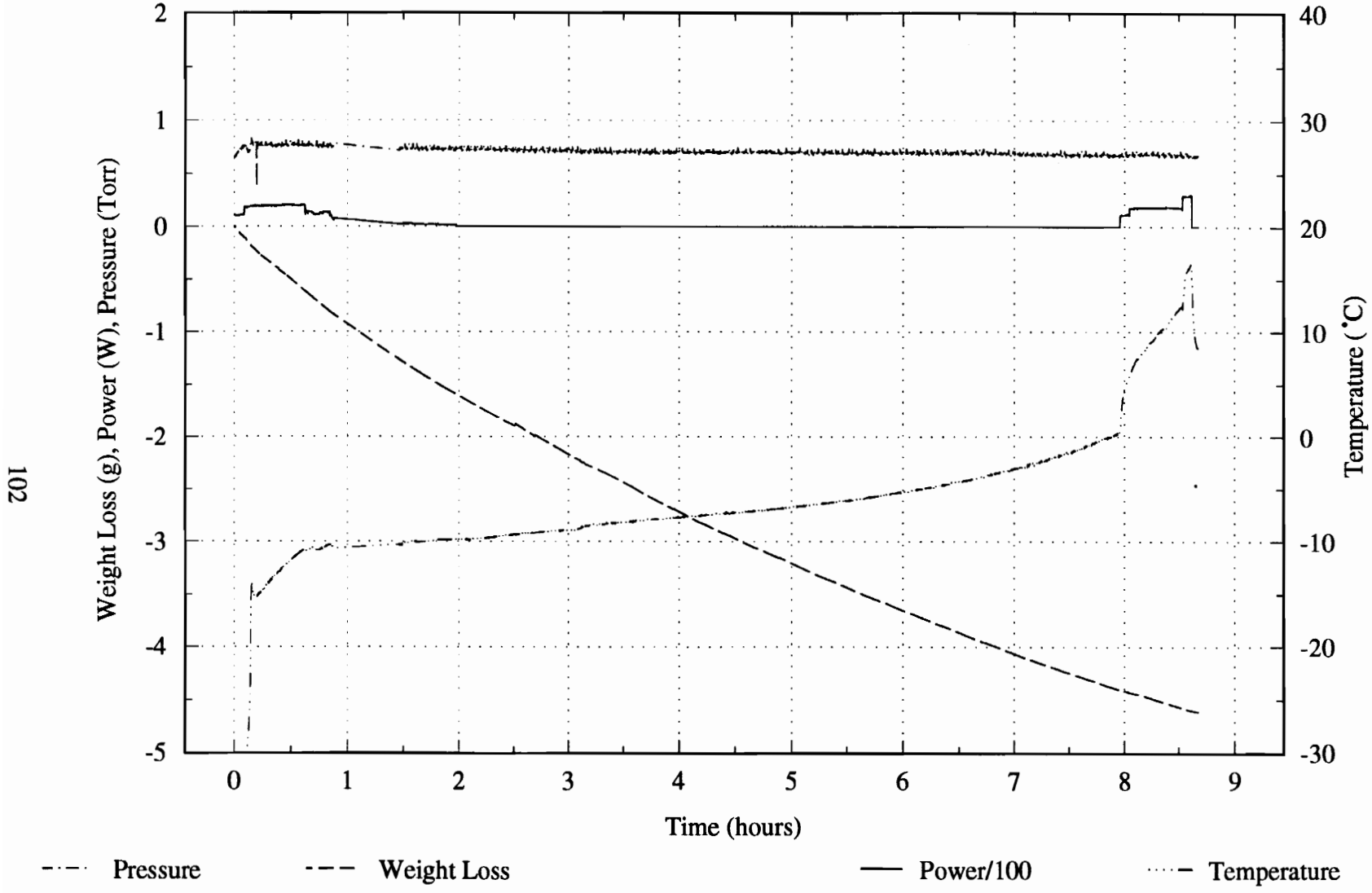

Figure A.16 Data plot from experiment No. 0513

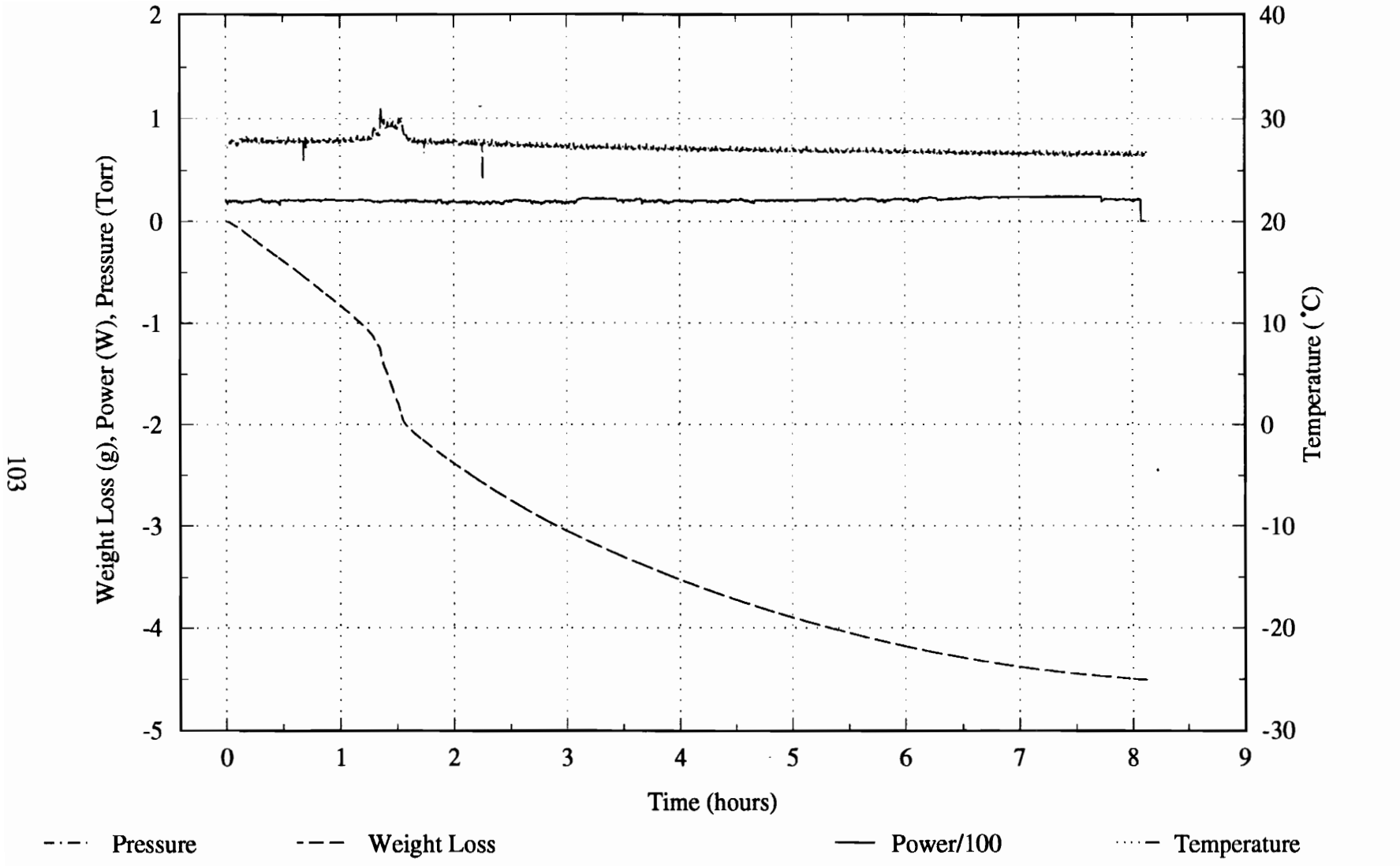

Figure A.17 Data plot from experiment No. 0517

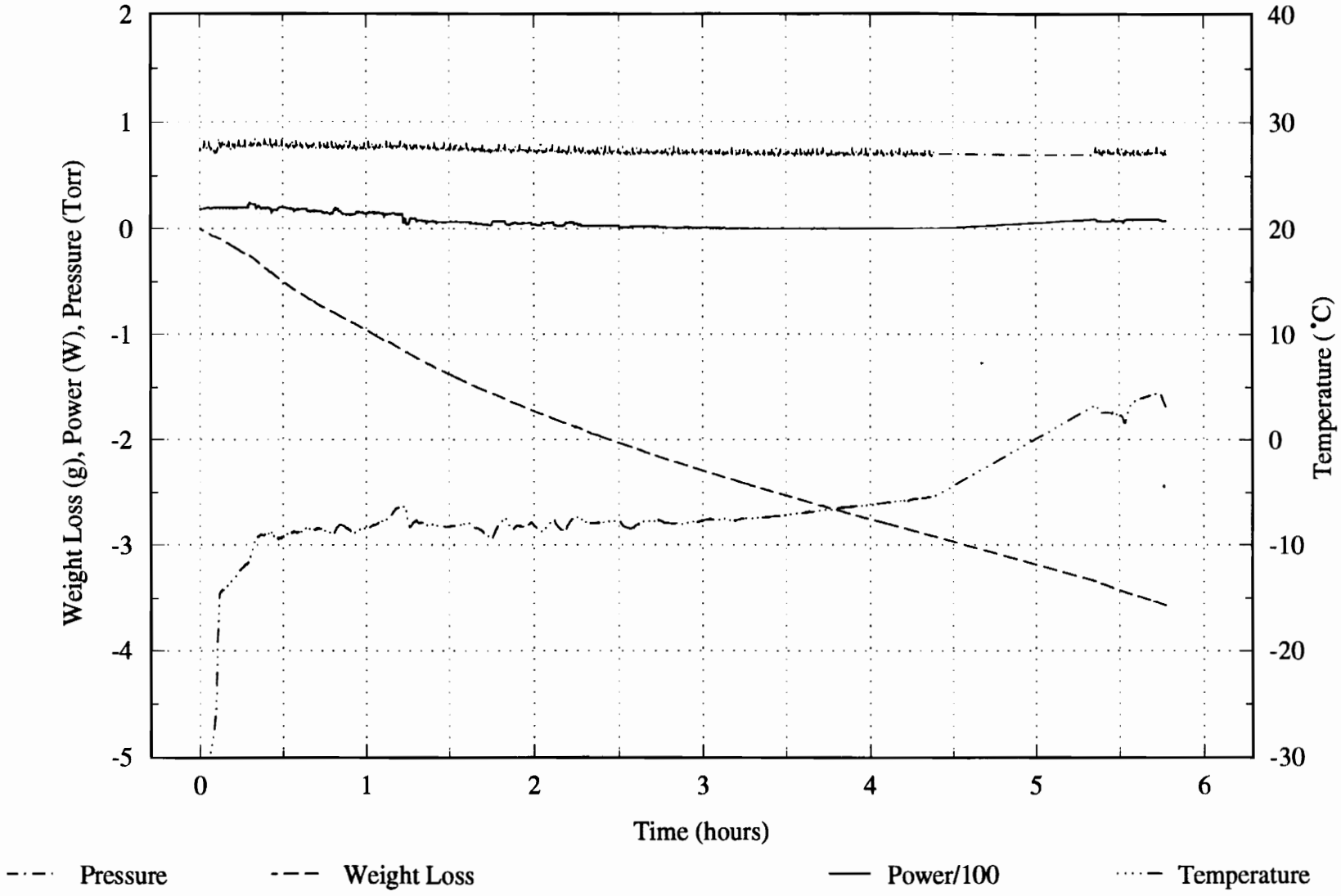

Figure A.18 Data plot from experiment No. 0516

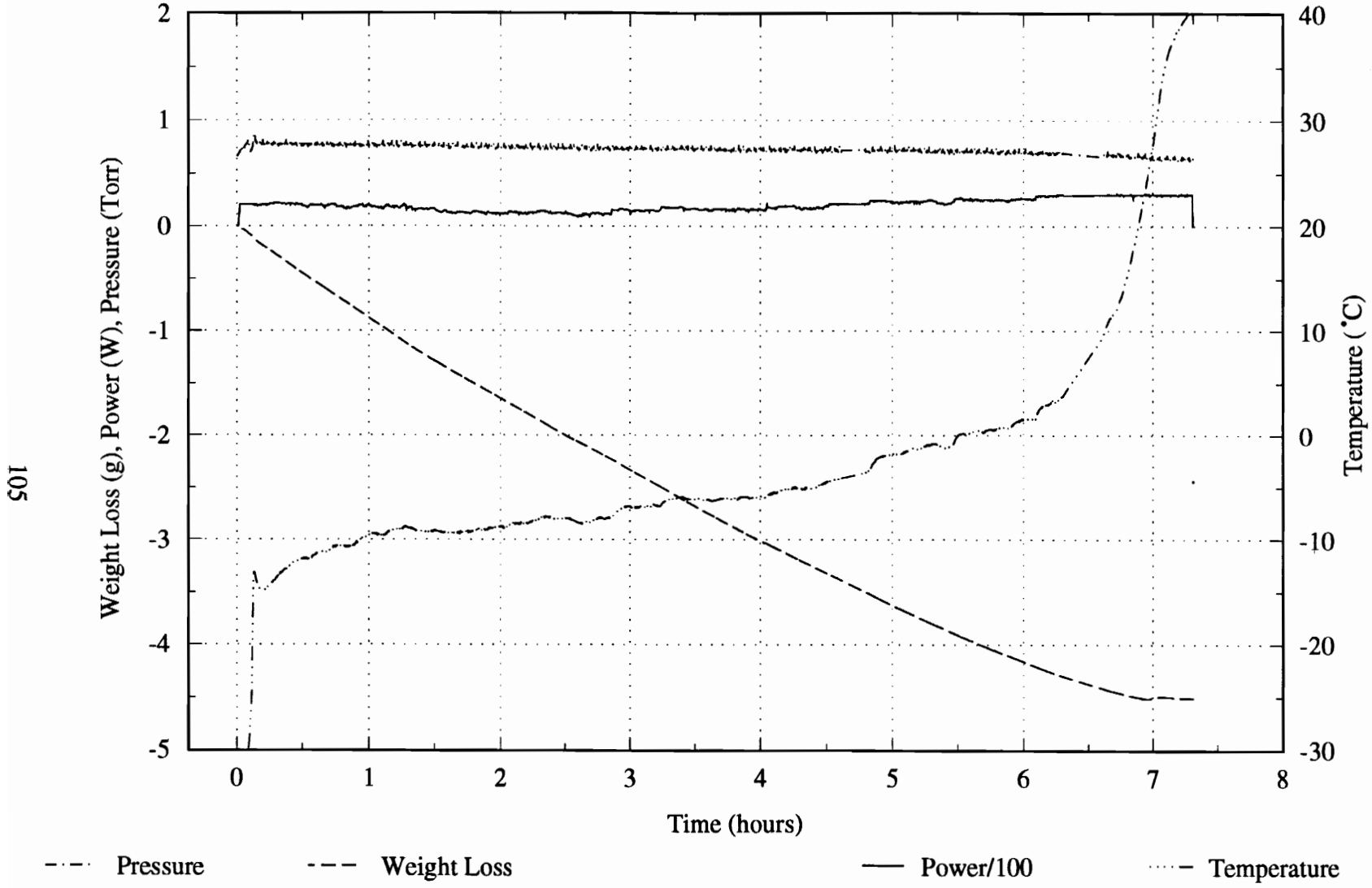

Figure A.19 Data plot from experiment No. 0518

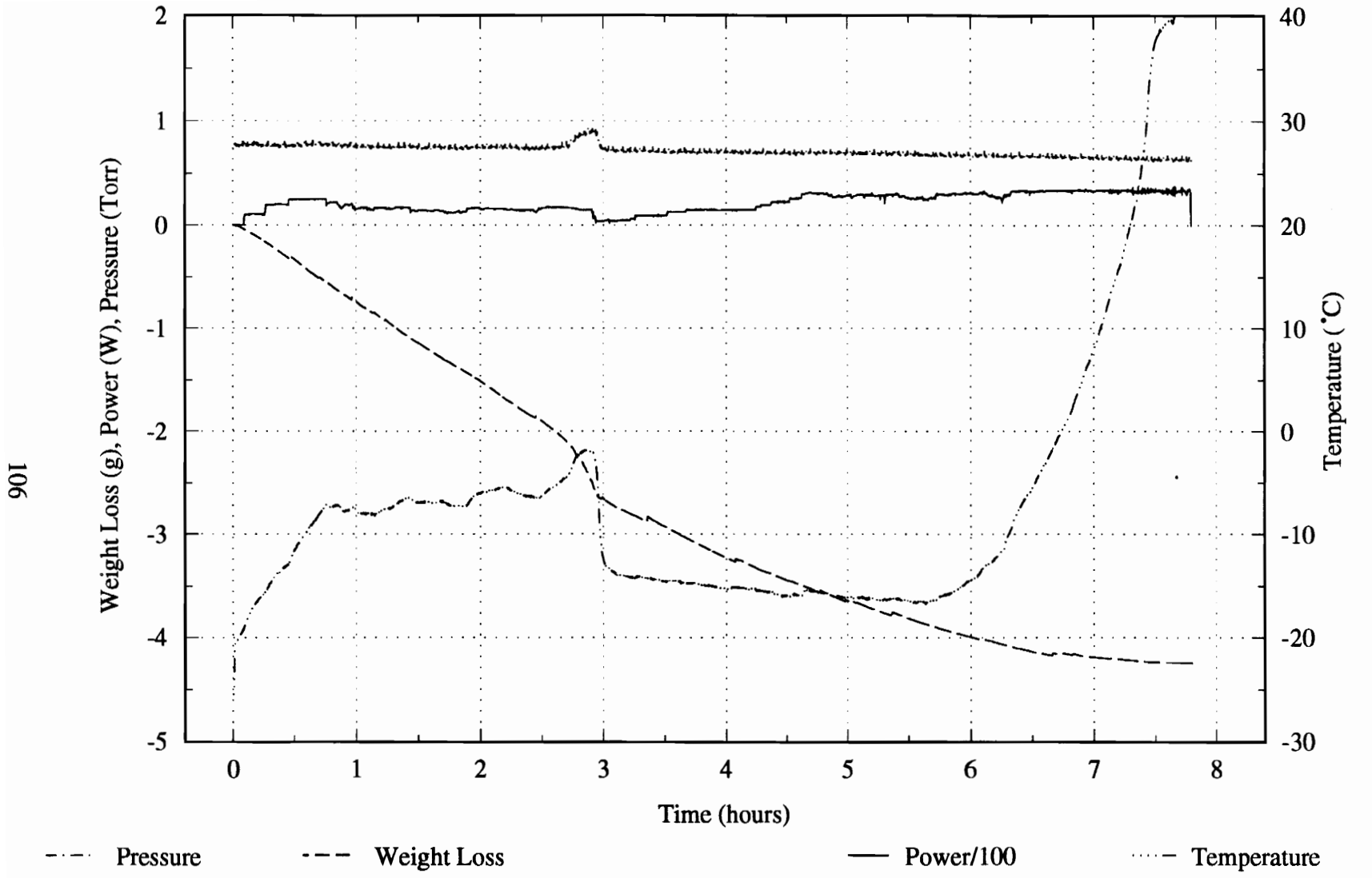

Figure A.20 Data plot from experiment No. 0519

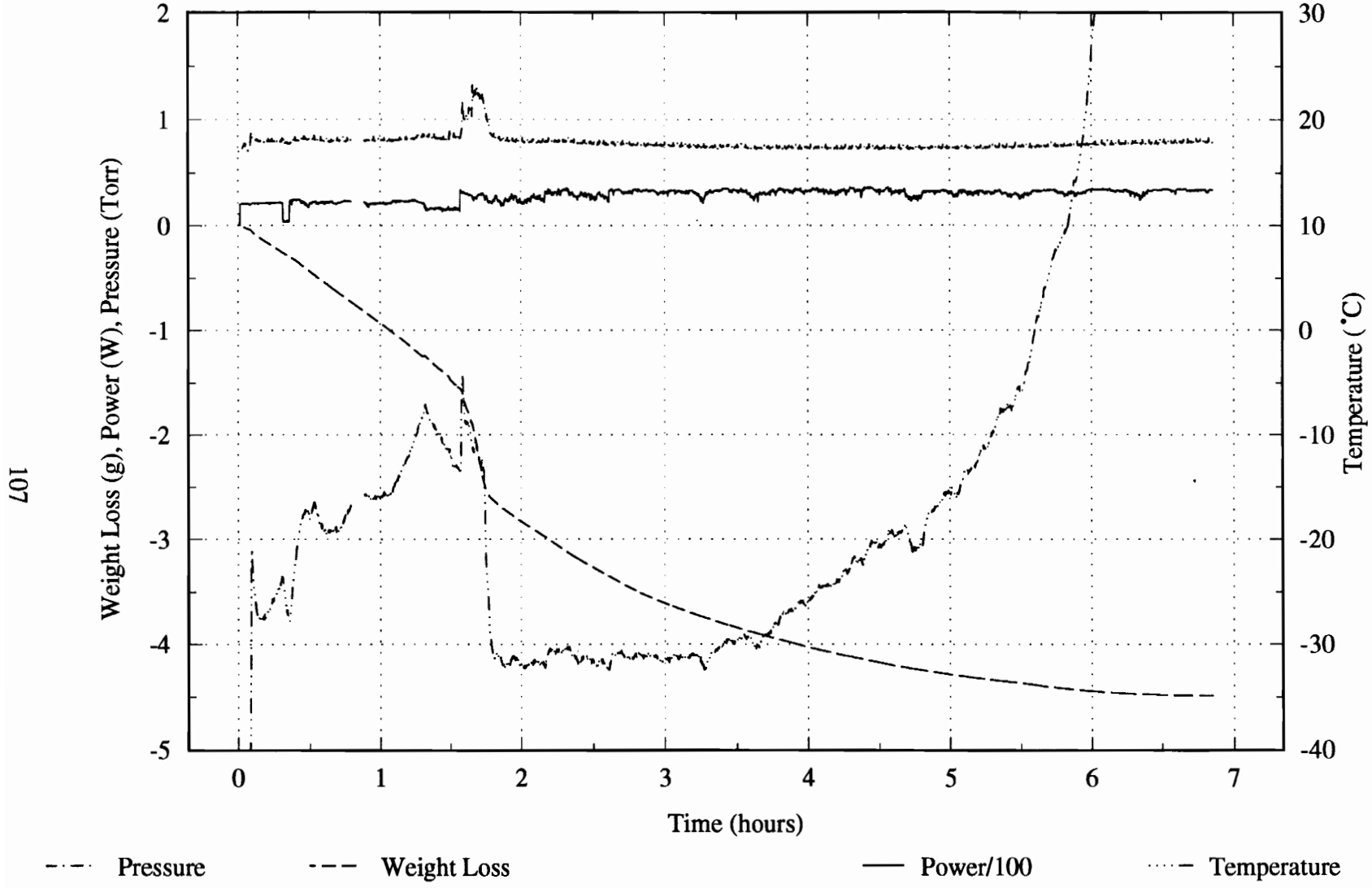

Figure A.21 Data plot from experiment No. 0203

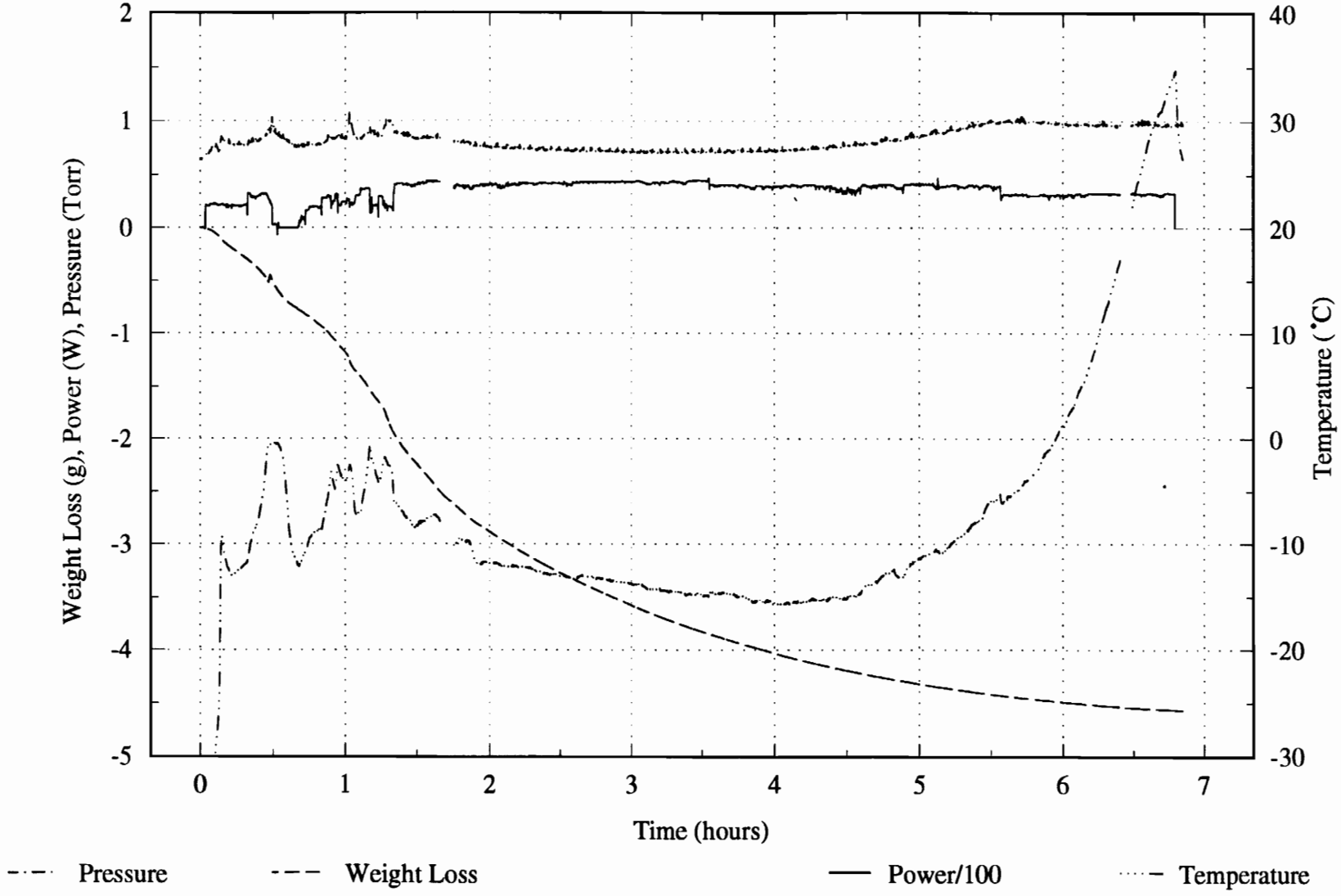

Figure A.22 Data plot from experiment No. 0207

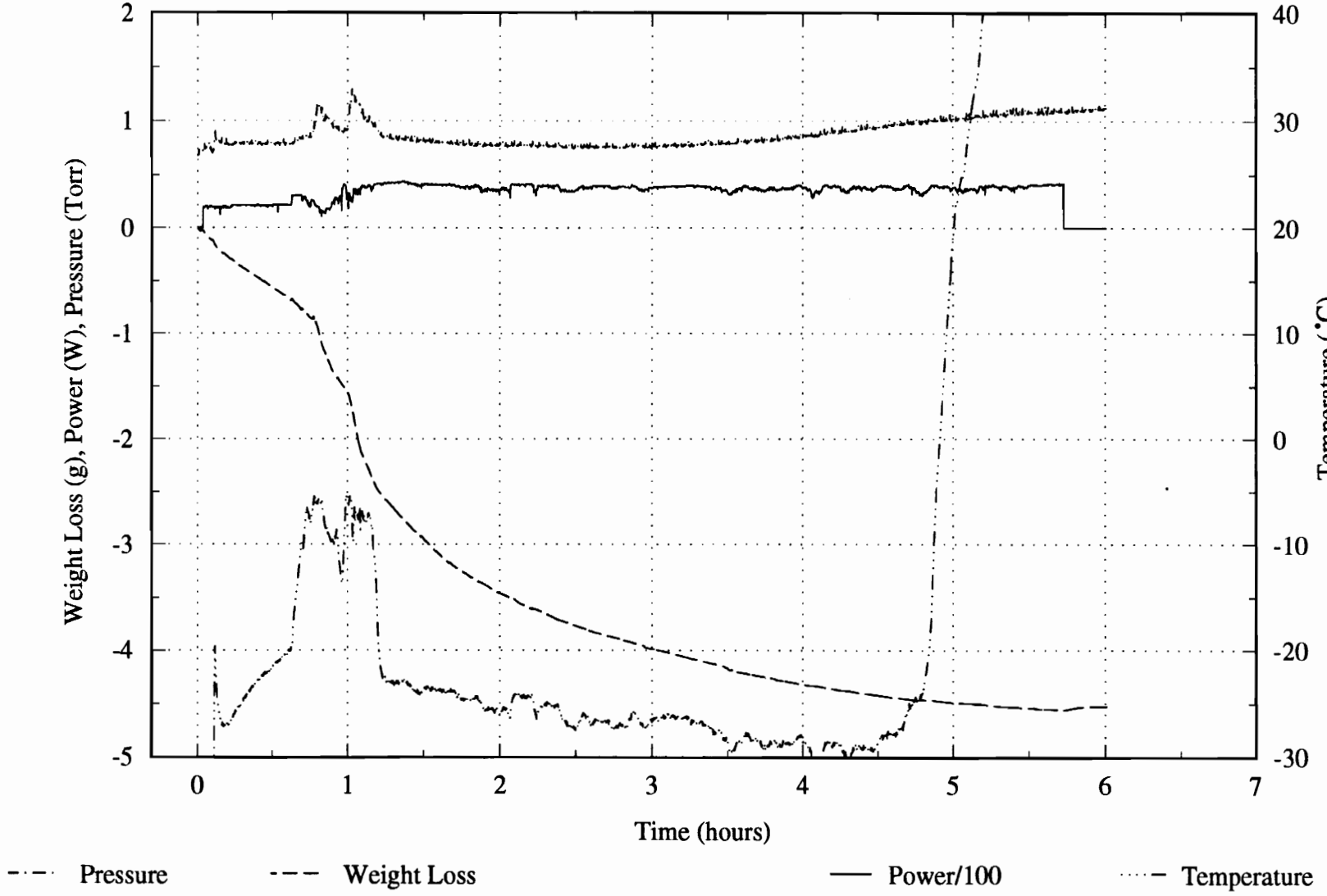

Figure A.23 Data plot from experiment No. 0131

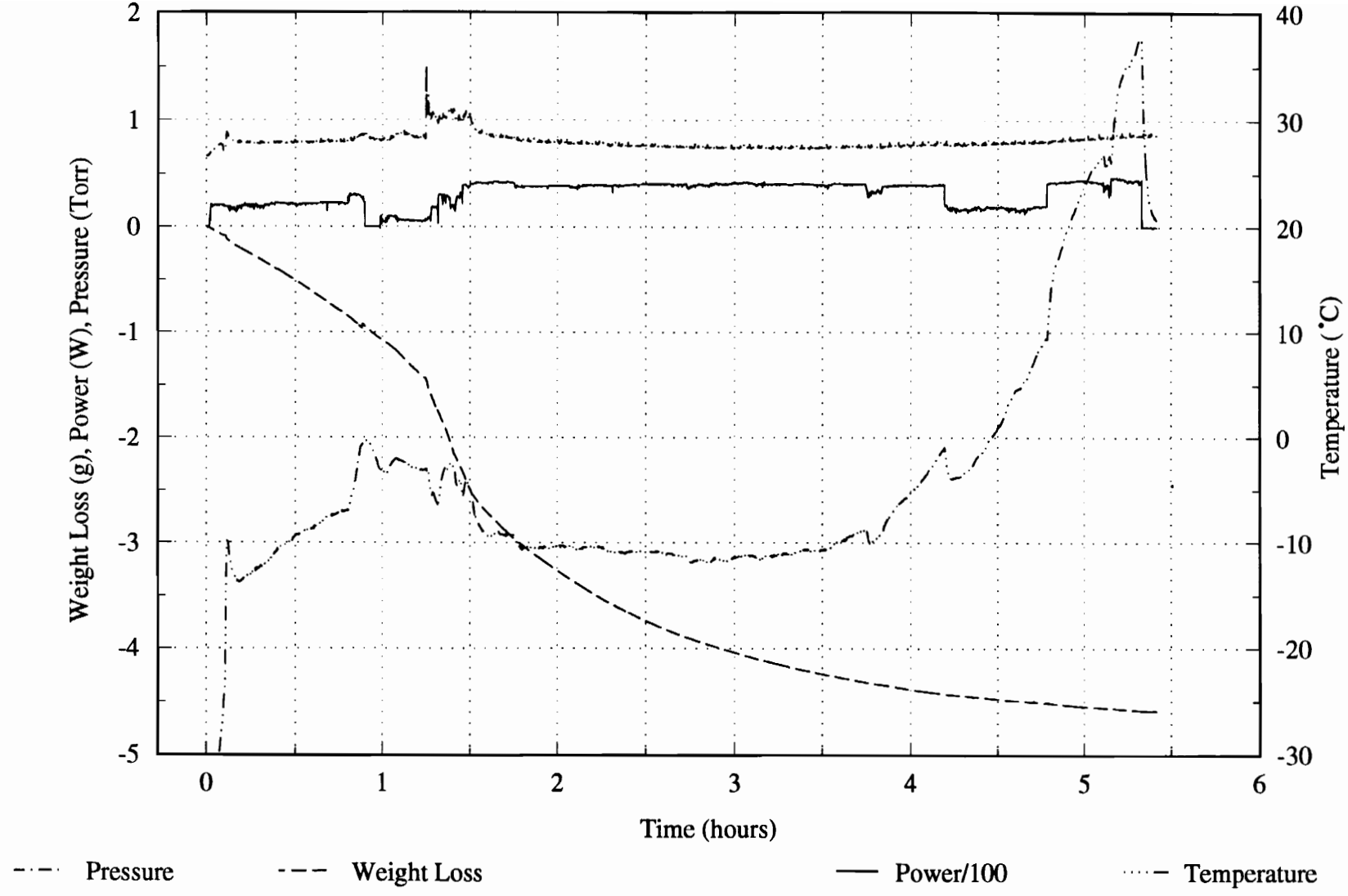

Figure A.24 Data plot from experiment No. 0128

APPENDIX B

AVERAGED DRYING CURVES

The appendix contains three plots of drying curves. Figure B.1 shows the drying curves of six of the eight slow freezing rate data sets listed in Table 5.2 and the average of these curves. Figure B.2 shows the drying curves of five out of the seven medium freezing rate data sets listed in Table 5.2. Figure B.3 shows the drying curves of seven out of the nine data sets listed in Table 5.2. These figures do not show the drying curve from each data set listed in Table 5.2. Some of the drying curves were left out because they were either very different from the rest of the data or that curve was missing data.

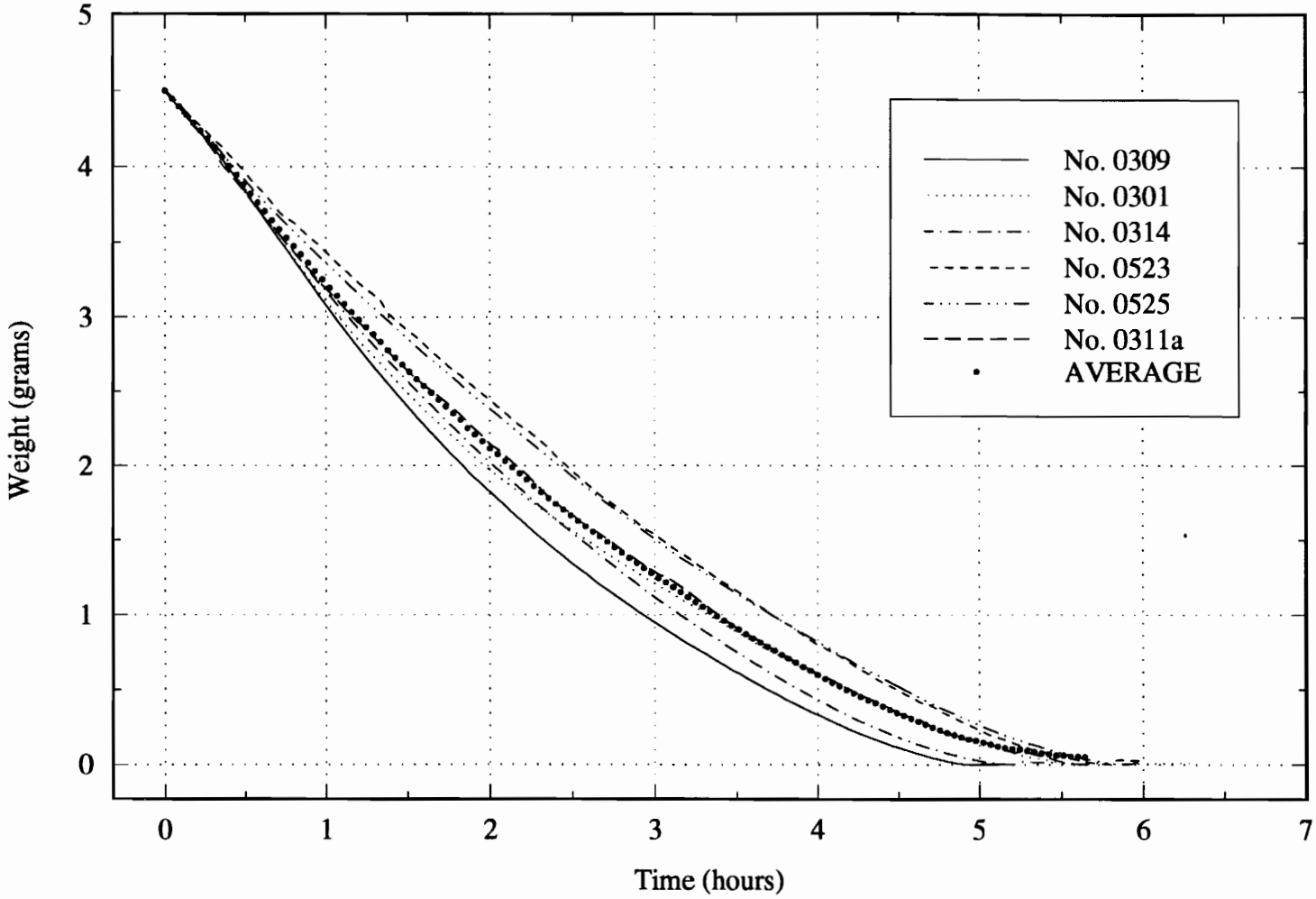

Figure B.1 Slow freezing rate average drying curve

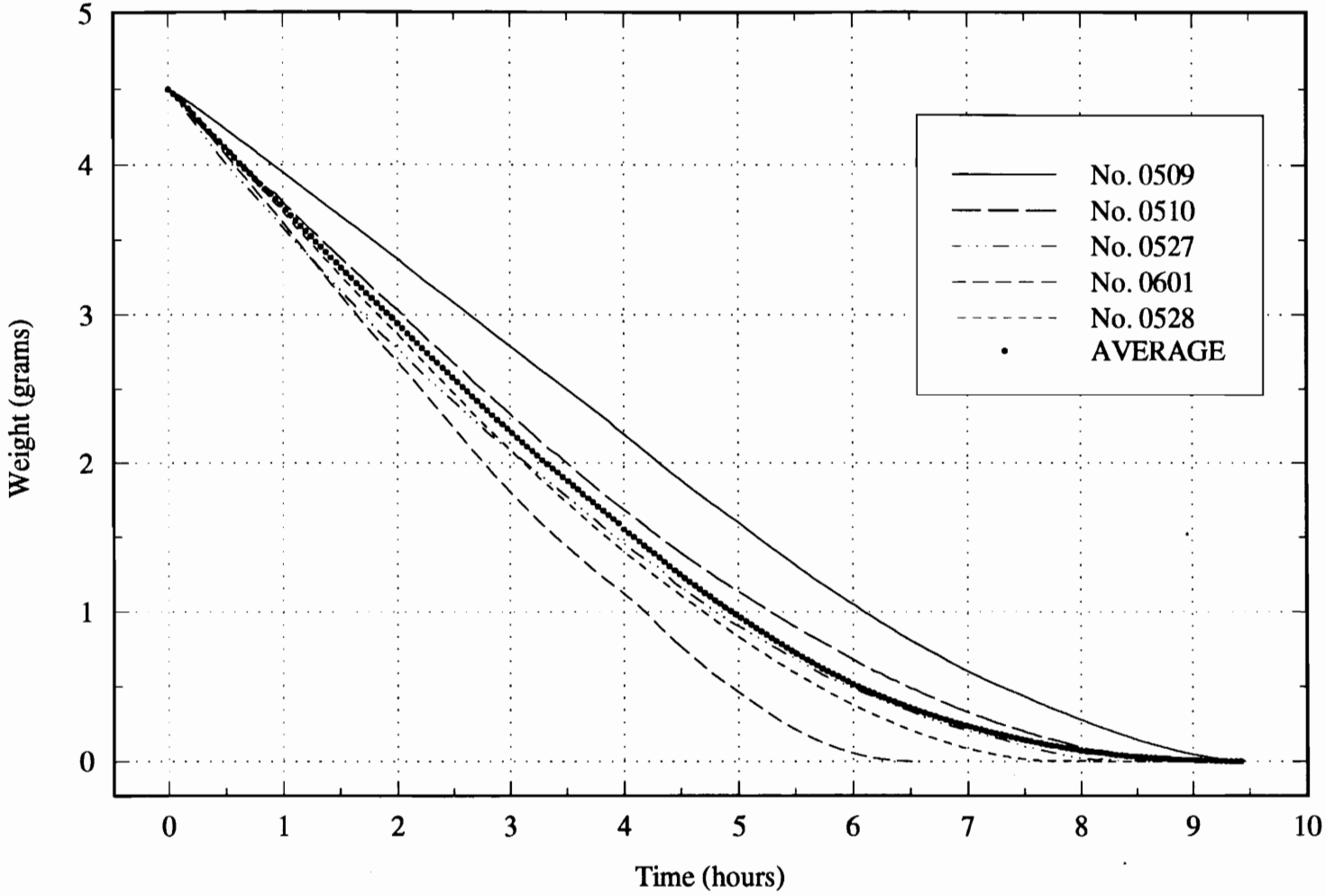

Figure B.2 Medium freezing rate average drying curve

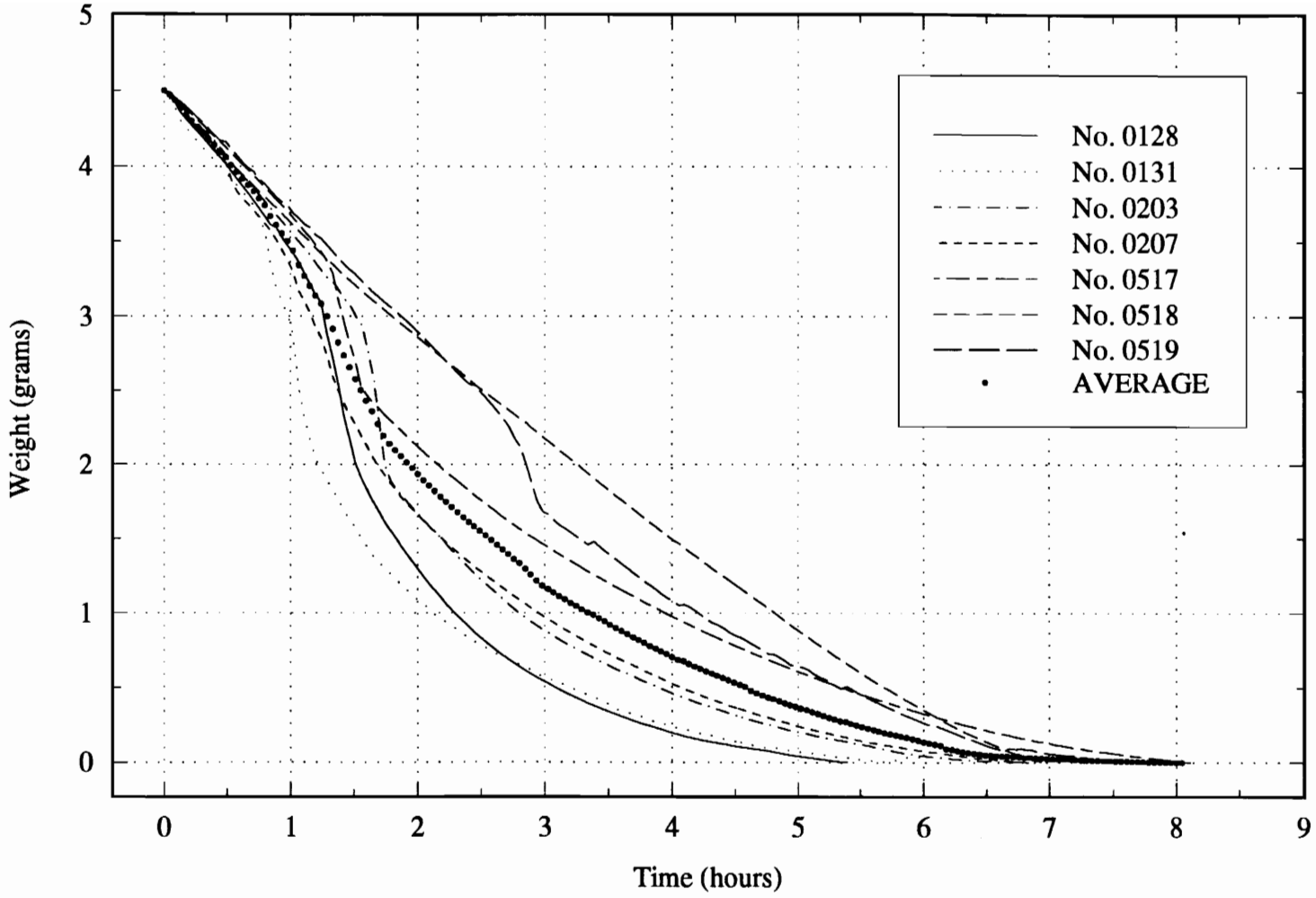

Figure B.3 Fast freezing rate average drying curve

APPENDIX C

AXUM HISTORY FILES

This section contains the AXUM technical graphics and data analysis history file programs used to make data calculations and to create data plots. Two programs are listed. The first, FRZDRY2.HST, is used to make calculations. The second, MAKEPLOT.HST, is used to generate plots of the data.

C.1 AXUM history file "FRZDRY2.HST"

```
Import FileName = C:\JIM\FREEZDRY\frzd0601.1, FileType = ASCII, DataSheet =
frzddata, ColNames = {Time,Temp,Pressure,IncPower,RefPower,Weight}, Format = {%f
%f %f %f %f %f };

Convert DataSheet = frzddata, {1} using subtract with args = { \1[1] };
Convert DataSheet = frzddata, {1} using divide with args = { 3600 };
Convert Datasheet = frzddata, {2..5} using realtomiss with args = { -10 };
Convert DataSheet = frzddata, {2} using multiply with args = { 20 };

ModifyColSpecs DataSheet = frzddata, Column = 7, NewColName = TotPower;
ModifyColSpecs DataSheet = frzddata, Column = 8, NewColName = PresTorr;
ModifyColSpecs DataSheet = frzddata, Column = 9, NewColName = PresEqva;
ModifyColSpecs DataSheet = frzddata, Column = 10, NewColName = deltaP;
ModifyColSpecs DataSheet = frzddata, Column = 11, NewColName = Pwater;

TotPower = IncPower - RefPower;
PresTorr = exp(1.236*Pressure - 2.577);
Pwater   = (min(Weight) - Weight)/min(Weight);
deltaP   = PresTorr - min(PresTorr);

LONG j;

for(j=1; j<length(Temp); j++ ){
     if( Temp[j] <= 0.000 )
       PresEqva[j] = 0.6113 + 0.050194*Temp[j] + 0.001875*Temp[j]^^2 +
       4.1679E-5*Temp[j]^^3 + 5.9516E-7*Temp[j]^^4 + 5.2622E-9*Temp[j]^^5;
     else
       PresEqva[j] = -11.1;
}

Convert DataSheet = frzddata, {PresEqva} using realtomiss with args = { -11.1 };
Convert Datasheet = frzddata, {PresEqva} using divide with args = { 0.1333 };

DeleteCol DataSheet = frzddata, {3..5};

SaveDS C:\JIM\DSF\frzd0601.DSF, DataSheet = frzddata;

CreateDS {frzd2};
CurrentDS {frzddata};

LONG i;
FLOATCOL Time, Temp, PresEqva, deltaP, Pwater;

     for(i=1; i<=length(Time)/20 + 1; i++ ){

      \\frzd2\Time[i] = Time[i*20-19];
      \\frzd2\Temp[i] = Temp[i*20-19];
      \\frzd2\PresEqva[i] = PresEqva[i*20-19];
      \\frzd2\deltaP[i] = deltaP[i*20-19];
      \\frzd2\Pwater[i] = Pwater[i*20-19];
   }

CurrentDS {frzd2};
ModifyColSpecs DataSheet = frzddata, Column = 9, NewColName = 1;
```

```
LONG y;
FLOATCOL MDOT,l;

l = 3.0 * (1.0 - Pwater);
Pwater = Pwater*4.5;
y = length(Pwater) - 1;
Mdot[1] = (Pwater[1] - Pwater[2]) / Time[2];

     for(i=1; i<y ; i++) {
     MDOT[i+1] = (Pwater[i] - Pwater[i+2]) / (Time[i+2]-Time[i]);
     }

MDOT[length(Pwater)] = (Pwater[y] - Pwater[length(Pwater)]) / Time[2];


for(i=1; i<=length(Mdot); i++ ){
     if( Mdot[i] < 0.0)
         Mdot[i] = 0.0;
}

     for (i=1; i<=length(MDOT); i++ ){
       if( Temp[i] < 0.00 ){
          if( MDOT[i] > 0.0000 )
              Rp[i] = (PresEqva[i] - deltaP[i])/MDOT[i];
          else
              Rp[i] = -111.1;
       }
     }

Convert DataSheet = frzd2, {Rp} using realtomiss with args = { -111.1 };

FLOATCOL Edot;

Edot = ( 2834.808 - 0.2131906*Temp + 0.01349646*Temp^^2 + 0.002924825*Temp^^3 +
0.0002551956*Temp^^4 + 1.241047E-7*Temp^^5 + 3.390218E-7*Temp^^7 )*Mdot/1000.0;

for(i=1; i<=length(Edot); i++ ){
     if(Edot[i] < 0.0 )
          Edot[i] = 0.0;
}
```

B.2 AXUM history file "MAKEPLOT.HST"

```
// ---------- Beginning of commands for graph RawDat ----------

CreateGraph Graph = RawDat, AxesType = "XY", Units = "Inches";

SetPageLayoutSpecs Graph = RawDat, RotatePage = No, DisplayWidth = 9,
DisplayHeight = 6.884, VerticalShift = 0, HorizontalShift = 0,
MaxDisplayBox = No, MaxBoxColor = "White", SelectedDisplayBox = No,
SelectedBoxColor = "Yellow";

// ----- plot information for 4 plots.

SetPlotItemSpecs Graph = RawDat, PlotNumber = 1, PlotType = "Line",
Projection = No, DataSheet = frzddata, xColumn = {Time},
yColumn = {Weight}, zColumn = {}, wColumn = {};

SetLineOtherInfo Graph = RawDat, PlotNumber = 1, BreakForMissing = Yes;

SetLinePlotAtt Graph = RawDat, PlotNumber = 1, SymbolColor = "Blue",
SymbolType = "Circle, Solid", SymbolHeight = 0, SymbolFreq = 0,
LineColor = "Blue", LineType = "Solid", LineWidth = 1, Crop = Yes;

SetPlotItemSpecs Graph = RawDat, PlotNumber = 2, PlotType = "Line",
Projection = No, DataSheet = frzddata, xColumn = {Time},
yColumn = {TotPower}, zColumn = {}, wColumn = {};

SetLineOtherInfo Graph = RawDat, PlotNumber = 2, BreakForMissing = Yes;

SetLinePlotAtt Graph = RawDat, PlotNumber = 2,
SymbolColor = "Bright White", SymbolType = "Triangle, Up, Solid",
SymbolHeight = 0, SymbolFreq = 0, LineColor = "Red", LineType = "Solid",
LineWidth = 1, Crop = Yes;

SetPlotItemSpecs Graph = RawDat, PlotNumber = 3, PlotType = "Line",
Projection = No, DataSheet = frzddata, xColumn = {Time},
yColumn = {PresTorr}, zColumn = {}, wColumn = {};

SetLineOtherInfo Graph = RawDat, PlotNumber = 3, BreakForMissing = Yes;

SetLinePlotAtt Graph = RawDat, PlotNumber = 3, SymbolColor = "Red",
SymbolType = "Box, Solid", SymbolHeight = 0, SymbolFreq = 0,
LineColor = "Black", LineType = "Solid", LineWidth = 1, Crop = Yes;

SetPlotItemSpecs Graph = RawDat, PlotNumber = 4, PlotType = "Line",
Projection = No, DataSheet = frzddata, xColumn = {Time}, yColumn = {Temp},
zColumn = {}, wColumn = {};

SetLineOtherInfo Graph = RawDat, PlotNumber = 4, BreakForMissing = Yes;

SetLinePlotAtt Graph = RawDat, PlotNumber = 4, SymbolColor = "Dark Gray",
SymbolType = "Diamond, Solid", SymbolHeight = 0, SymbolFreq = 0,
LineColor = "Yellow", LineType = "Solid", LineWidth = 1, Crop = Yes;

// ----- axes information

Set2DAxesSpecs Graph = RawDat, Height = @Auto, Width = @Auto,
yPlotOrigin = @Auto, xPlotOrigin = @Auto, xAxisOffset = 0, yAxisOffset = 0,
AxesColor = "Black", CrossAxes = No, DrawXAxis = Yes, DrawYAxis = Yes,
DrawRightYAxis = Yes, DrawFrame = "With ticks", RtYStartPlotNum = 4,
Thickness = @Auto;
```

```
Set2DAxesTicksSpecs Graph = RawDat, MajorTickLength = 0.08,
MinorTickLength = 0.04, MajorTickWidth = 1, MinorTickWidth = 1;

Set2DXAxisTicksSpecs Graph = RawDat, AxisMinType = "Auto",
AxisMin = -0.258043, AxisMaxType = "Auto", AxisMax = 6,
FirstTickType = "Auto", FirstTick = 0, LastTickType = "Auto", LastTick = 6,
MajorTickIntervalType = "Numbers", MajorTickIntSpec = "Auto",
MajorTickInterval = 6, MajorTickIntervalMax = 0, MinorTickInterval = @Auto,
TickPosition = "In";

Set2DYAxisTicksSpecs Graph = RawDat, AxisMinType = "Number", AxisMin = -5,
AxisMaxType = "Number", AxisMax = 2, FirstTickType = "Auto",
FirstTick = -5, LastTickType = "Auto", LastTick = 2,
MajorTickIntervalType = "Numbers", MajorTickIntSpec = "Auto",
MajorTickInterval = 7, MajorTickIntervalMax = 0, MinorTickInterval = @Auto,
TickPosition = "In";

Set2DRtYAxisTicksSpecs Graph = RawDat, AxisMinType = "Number",
AxisMin = -30, AxisMaxType = "Number", AxisMax = 40,
FirstTickType = "Auto", FirstTick = -30, LastTickType = "Auto",
LastTick = 40, MajorTickIntervalType = "Numbers",
MajorTickIntSpec = "Auto", MajorTickInterval = 7, MajorTickIntervalMax = 0,
MinorTickInterval = @Auto, TickPosition = "In";

Set2DAxesLabelsSpecs Graph = RawDat, LabelColor = "Black", Height = 0.15,
ShrinkFactor = 0.8, AdjustLabels = "None", xLabelType = "Numbers",
xFormat = "Auto", xPrecision = 1, xColumnName = "", yLabelType = "Numbers",
yFormat = "Auto", yPrecision = 1, yColumnName = "",
RtYLabelType = "Numbers", RtYFormat = "Auto", RtYPrecision = 1,
RtYColumnName = "", xLabelsAngle = 0, yLabelsAngle = 0, RtYLabelsAngle = 0,
xVerticalOffset = @Auto, yVerticalOffset = @Auto,
RtYVerticalOffset = @Auto, xHorizontalOffset = @Auto,
yHorizontalOffset = @Auto, RtYHorizontalOffset = @Auto,
xVerticalJustification = "Auto", yVerticalJustification = "Auto",
RtYVerticalJustification = "Auto", xHorizontalJustification = "Auto",
yHorizontalJustification = "Auto", RtYHorizontalJustification = "Auto",
AutoXSkipNumber = 0, xSkipNumber = 0, xOverlapHandling = "Auto",
AutoYSkipNumber = 0, ySkipNumber = 0, yOverlapHanding = "Auto",
AutoRtYSkipNumber = 0, RtYSkipNumber = 0, RtOverlapHandling = "Auto",
LabelMinorLogXTicks = Yes, LabelMinorLogYTicks = Yes;

Set2DAxesGridSpecs Graph = RawDat, MajorXGridType = "Dots",
MinorXGridType = "Dots", MajorXGridWidth = 1, MinorXGridWidth = 1,
MajorYGridType = "Dots", MinorYGridType = "Dots", MajorYGridWidth = 1,
MinorYGridWidth = 1, MajorRtYGridType = "None", MinorRtYGridType = "None",
MajorRtYGridWidth = 1, MinorRtYGridWidth = 1;

// ----- there are no reference lines.

// ---------- Color specifications ----------

SetColorSpecs Graph = RawDat, Background = "Cyan", Axes = "Black",
Title = "Black", SubTitle = "Black", xAxisTitle = "Black",
yAxisTitle = "Black", zAxisTitle = "Black", LegendBox = "Black",
MaxDisplayBox = "White", SelectedDisplayBox = "Yellow";

// ----- titles information

SetTitleSpecs Graph = RawDat,
Title = "Freeze-Dry Data - Slow Freezing Rate", TitleX = @Auto,
TitleY = @Auto, Color = "Black", FontNumber = 1, Height = 0.18, Hide = No,
OverrunProtectedArea = No;

SetSubTitleSpecs Graph = RawDat, Title = "10% (w/w) Mannitol Solution",
TitleX = @Auto, TitleY = @Auto, Color = "Black", FontNumber = 1,
Height = 0.15, Hide = No, OverrunProtectedArea = No;
```

```
SetXTitleSpecs Graph = RawDat, Title = "Time (hours)", TitleX = @Auto,
TitleY = @Auto, Color = "Black", FontNumber = 1, Height = 0.15, Hide = No,
OverrunProtectedArea = No;

SetYTitleSpecs Graph = RawDat,
Title = "Wt Loss (g), Power (W/100), Pressure (Torr)", TitleX = 0.5,
TitleY = @Auto, Color = "Black", FontNumber = 1, Height = 0.15, Hide = No,
OverrunProtectedArea = No;

SetZTitleSpecs Graph = RawDat, Title = "Temperature ([~199]C)",
TitleX = 9.7, TitleY = @Auto, Color = "Black", FontNumber = 1,
Height = 0.15, Hide = No, OverrunProtectedArea = No;

// ----- legend information

SetLegendSpecs Graph = RawDat, DrawLegend = No, AutoUpdate = Yes,
Protect = Yes, OverrunProtectedArea = Yes, TextHeight = 0.151195,
xPosition = 3.15, yPosition = 1.53084, Units = "Inches";

SetLegendBoxSpecs Graph = RawDat, DrawBox = Yes, BoxColor = "Black",
LineWidth = 1, BoxMargin = 0.201595, SampleLength = 0.604786,
VerticalSpacing = 1.6, MiddleSpacing = 0.201595;

// ----- legend item information for 4 legend items.

SetLegendItemSpecs Graph = RawDat, LegendNumber = 1, Text = "@Auto",
Color = "Black", FontNumber = 1, SampleColor = "Blue",
SampleLineColor = "Blue", SampleHeight = 0.15, LineWidth = 1,
Line = "Solid";

SetLegendItemSpecs Graph = RawDat, LegendNumber = 2, Text = "@Auto",
Color = "Black", FontNumber = 1, SampleColor = "Red",
SampleLineColor = "Red", SampleHeight = 0.15, LineWidth = 1,
Line = "Solid";

SetLegendItemSpecs Graph = RawDat, LegendNumber = 3, Text = "@Auto",
Color = "Black", FontNumber = 1, SampleColor = "Black",
SampleLineColor = "Black", SampleHeight = 0.15, LineWidth = 1,
Line = "Solid";

SetLegendItemSpecs Graph = RawDat, LegendNumber = 4, Text = "@Auto",
Color = "Black", FontNumber = 1, SampleColor = "Yellow",
SampleLineColor = "Yellow", SampleHeight = 0.15, LineWidth = 1,
Line = "Solid";

// ----- there are no comments.

// ----- there are no extra symbols.

// ----- there are no extra lines.

// ----- there are no arcs.

// ----- there are no radial lines.

// ----- there are no arrows.

// ----- there are no error bars.

// ------ font, text, and date stamp information

SetFontSelections Graph = RawDat, FontChoice = "PostScript", Font1 = "Times -
Roman",
Font2 = "Times - Roman", Font3 = "Times - Roman", Font4 = "Times - Roman";
```

```
SetTextSpacingSpecs Graph = RawDat, WideningFactor = 1.3,
SkewingFactor = 0.3, AutoThick = No, ThicknessFactor = 3,
CharacterSpacing = 0, HeightMultiplier = 0.75, ShiftMultiplier = 0.6;

SetDateStampSpecs Graph = RawDat, Text = "@Auto", Color = "Black",
FontNumber = 1, UseDate = Yes, UseTime = No, Hide = Yes,
OverrunProtectedArea = No, xPosition = 0.2, yPosition = 6.784,
TextHeight = 0.075;

// ------ protected area information

SetUserProtectSpecs Graph = RawDat, WindowOn = No, Units = "Inches",
xPosition = 4, yPosition = 4, Height = 2, Width = 2, DrawBox = No,
Color = "Black";

// ----- there are no overlay images.

SaveGraph Graph = RawDat, File = "fzd0309A.GRF";
SaveGraphImage Graph = RawDat, File = RawDat.IMF;
RemoveGraph "RawDat";

// ---------- End of commands for graph RawDat ----------

// ---------- Beginning of commands for graph Mdot ----------

CreateGraph Graph = Mdot, AxesType = "XY";

SetPlotItemSpecs Graph = Mdot, PlotNumber = 1, PlotType = "Line",
DataSheet = frzd2, xColumn = {Time}, yColumn = {MDOT};

SetTitleSpecs Graph = Mdot, Title = "Water Vapor Mass Flux";

SetSubTitleSpecs Graph = Mdot, Title = "9% (w/w) Mannitol Solution";

SetXTitleSpecs Graph = Mdot, Title = "Time (hours)";

SetYTitleSpecs Graph = Mdot, Title = "Mass Flux (grams/hr)";
SetFontSelections Graph = Mdot, FontChoice = "PostScript", Font1 = "Times - Roman",

Font2 = "Times - Roman", Font3 = "Times - Roman", Font4 = "Times - Roman";

SaveGraphImage Graph = Mdot, File = "Mdot.IMF";
RemoveGraph "Mdot";

// ---------- End of commands for graph Mdot ----------

// ---------- Beginning of commands for graph Rp ----------

CreateGraph Graph = Rp, AxesType = "XY";

SetPlotItemSpecs Graph = Rp, PlotNumber = 1, PlotType = "Line",
DataSheet = frzd2, xColumn = {l}, yColumn = {Rp};

SetTitleSpecs Graph = Rp, Title = "Mass Transfer Resistance of Dried Layer";

SetSubTitleSpecs Graph = Rp, Title = "9% (w/w) Mannitol Solution";

SetXTitleSpecs Graph = Rp, Title = "Thickness of Dried Layer (cm)";

SetFontSelections Graph = Rp, FontChoice = "PostScript", Font1 = "Times - Roman",
Font2 = "Times - Roman", Font3 = "Times - Roman", Font4 = "Times - Roman";
SetYTitleSpecs Graph = Rp, Title = "Resistance (mmHg*hr/grams)";

SaveGraphImage Graph = Rp, File = "Rp.IMF";
RemoveGraph "Rp";

// ---------- End of commands for graph Rp ----------
```

```
// ---------- Beginning of commands for graph Edot ----------

CreateGraph Graph = Edot, AxesType = "XY";

SetPlotItemSpecs Graph = Edot, PlotNumber = 1, PlotType = "Line",
DataSheet = frzd2, xColumn = {Time}, yColumn = {Edot};

SetTitleSpecs Graph = Edot, Title = "Energy Required for Sublimation";

SetSubTitleSpecs Graph = Edot, Title = "9% (w/w) Mannitol Solution";

SetXTitleSpecs Graph = Edot, Title = "Time (hours)";

SetYTitleSpecs Graph = Edot, Title = "Heat Generated (Watts)";
SetFontSelections Graph = Edot, FontChoice = "PostScript", Font1 = "Times - Roman",

Font2 = "Times - Roman", Font3 = "Times - Roman", Font4 = "Times - Roman";

SaveGraphImage Graph = Edot, File = "Edot.IMF";
RemoveGraph "Edot";

// ---------- End of commands for graph Edot ----------

// ---------- Beginning of commands for graph Weight ----------

CreateGraph Graph = Wt, AxesType = "XY";

SetPlotItemSpecs Graph = Wt, PlotNumber = 1, PlotType = "Line",
DataSheet = frzd2, xColumn = {Time}, yColumn = {Pwater};

SetTitleSpecs Graph = Wt, Title = "Water Mass";

SetSubTitleSpecs Graph = Wt, Title = "9% (w/w) Mannitol Solution";

SetXTitleSpecs Graph = Wt, Title = "Time (hours)";

SetYTitleSpecs Graph = Wt, Title = "Water Mass (grams)";
SetFontSelections Graph = Wt, FontChoice = "PostScript", Font1 = "Times - Roman",
Font2 = "Times - Roman", Font3 = "Times - Roman", Font4 = "Times - Roman";

SaveGraphImage Graph = Wt, File = "Wt.IMF";
RemoveGraph "Wt";

// ---------- End of commands for graph Weight ----------

CreateDS Graphs;
CurrentDS Graphs;

STRINGCOL Overlay_Names;
Overlay_Name[1] = "RawDat.IMF";
Overlay_Name[2] = "Mdot.IMF";
Overlay_Name[3] = "Rp.IMF";
Overlay_Name[4] = "Edot.IMF";
Overlay_Name[5] = "Wt.IMF";

STRINGCOL Current_Batch;
Current_Batch[1] = "RawData";
Current_Batch[2] = "Mdot";
Current_Batch[3] = "Rp";
Current_Batch[4] = "Edot";
Current_Batch[5] = "Wt";

CreateGraph Graph = CATALOG, AxesType = Text, Units = Inches;
```

```
//  Loop through the six save images, overlaying them on the
//  graph, and placing the Graph file name directly below the image.
for(j=1;j<=5; j++)
{
     STRING Current_Image = \\Graphs\Overlay_Name[j];

     //  Calculate coordinates for current image.
     FLOAT Current_X = (j-1)%3 * 3 + .1;
     FLOAT Current_Y = 3.8 - trunc((j-1)/3) * 3;

     //  Overlay the images on the page.
     SetOverlayImageSpecs Graph = CATALOG,
                          OverlayNumber = *j,
                          FileName = *Current_Image,
                          Units = "Inches",
                          xPosition = *Current_X,
                          yPosition = *Current_Y,
                          Height = 2.1, Protect = No,
                          Rotate = No, Hide = No;

     //  Determine Graph name, and coordinates for placing graph name.
     Current_Graph = \\Graphs\Current_Batch[j];
     Current_X += .3;
     Current_Y -= .3;

     //  Place graph name under the overlaid image.
     SetCommentItemSpecs Graph = CATALOG,
                         CommentNumber = *j,
                         Text = *Current_Graph,
                         Units = "Inches",
                         xPosition = *Current_X,
                         yPosition = *Current_Y,
                         Height = 0.15, Angle = 0,
                         FontNumber = 1, Color = "Black",
                         Hide = No, OverrunProtectedArea = No;
}
ViewGraph Graph = CATALOG, Duration = 5;
```

APPENDIX D

DATA ACQUISITION PROGRAM

This section contains the data acquisition program FRZDRY2.C. This program uses the SCXI module 2 to scan SCXI channels 18 through 21 every 8 seconds. The gain is 1. Additional channels can be added by increasing *numChans*, *voltArray*, *binArray* and *buffer*. Output is to the standard i/o screen using FmtOut and to a user specified file using FmtFile. The program terminates when the user hits a key. Channel 8 on the SCXI terminal block should be shorted and grounded for determining the offset voltage of the SCXI.

```
/*                        C:\LW\JIMDAQ\FRZDRY2.C                              */
/*                                                                            */
/*  This program uses SCXI module 2 to scan SCXI channels 18 thru 21 every    */
/*  8 seconds. The gain is 1. Additional channels can be added by increasing  */
/*  numChans, voltArray, binArray, and buffer. Output is to the standard i/o  */
/*  screen using FmtOut and to a user specified file using FmtFile.           */
/*  Data taken by the RS-232 is also written to the user specified file.      */
/*  Time is recorded by using the function "Timer()", which returns the       */
/*  number of seconds since midnight.  The program terminates when the user   */
/*  hits a key.  At that point a  file name should be entered if the data is  */
/*  to be saved. Channel 8 should be shorted and grounded to determine        */
/*  the offset voltage. At two hours the program will exit the DAQ loop and   */
/*  require either the data to be saved or over written in order to continue.*/


void error_check (char *, int);


void file_name (double time[], double temp[], double pressure[], double incident[],
                double reflected[], double scaleData[], int n);


static double scanRateDesired;      /*  Scan rate in seconds.     */
static double sampleRateDesired;    /*  Sample rate in Hz.        */
static int scanInterval;
static int scanTimebase;
static int sampInterval;
static int sampTimebase;
static int numChans[1];
static int startChans[1];
static int moduleList[1];
static int boardcode;
static int ptsTfr;
static int numpts;
static double voltArray[4];
static int binArray[4];
static int buffer[8];
static int daqStopped;
static int halfReady;
static int gain[1];
static int chans[1];
static char msg[100];
static int err, i, n, count;
static char buf[50];
static double voltage, volts, v, weight;
static double time[900], temp[900], pressure[900];
static double incident[900], reflected[900], scaleData[900];


main()

{
    numpts             = 8;       /* Twice the number actually desired      */
    numChans[0]        = 4;       /* Number of SCXI channels to scan        */
    count              = 4;       /* Length of binArray and voltArray       */
    moduleList[0]      = 2;       /* Module to scan                         */
    startChans[0]      = 18;      /* First SCXI channel to scan             */
    chans[0]           = 0;       /* MIO channel to scan                    */
    gain[0]            = 1;       /* MIO gain                               */
    sampleRateDesired  = 100.0;   /* A/D conversion rate (pts/sec.)         */
    scanRateDesired    = 2.0;     /* 1/numChans the amount of delay desired */
                                  /*    between acquisitions   (sec/pt.)    */
```

```
    cls();

    err = Init_DA_Brds (1, &boardcode);
        if (err < 0)
            error_check ("Init_DA_Brds", err);

    err = SCXI_Load_Config (1);
        if (err < 0)
            error_check ("SCXI_Load_Config", err);

/*----------- find voltage offset to be subtracted from reading ------------*/

    err = SCXI_Reset (1, -1);
        if (err < 0)
            error_check ("SCXI_Reset1", err);

    err = SCXI_Single_Chan_Setup (1, 2, 8, 1);
        if (err < 0)
            error_check ("SCXI_Single_Chan_Setup", err);

    err = SCXI_Set_Module_Gain (1, 2, 1);
        if (err <  0)
            error_check ("SCXI_Set_Module_Gain", err);

    err = SCXI_Calibrate_Setup (1, 2, 1);
        if (err < 0)
            error_check ("SCXI_Calibrate_Setup1", err);

    voltage = 0;
    for ( i = 1; i<=1000; i++ ) {

        err = AI_VRead (1, 0, 1, &volts);
            if (err < 0)
                error_check ("AI_VRead", err);

       voltage = volts + voltage;
    }
    v = voltage/1000;
    FmtOut ( " \n offset = %f\n", v);

    err = SCXI_Calibrate_Setup (1, 2, 0);
        if (err < 0)
            error_check ("SCXI_Calibrate_Setup2", err);

/*----------------------------------------------------------------------------*/

    err = SCXI_Reset (1, -1);
        if (err < 0)
            error_check ("SCXI_Reset", err);

    err = SCXI_SCAN_Setup (1, 1, moduleList, numChans, startChans, 1, 0);
        if (err < 0)
           error_check ("SCXI_SCAN_Setup", err);
```

```
    err = SCAN_Setup (1, 1, chans, gain);
        if (err < 0)
           error_check ("SCAN_Setup", err);


    err = DAQ_DB_Config (1, 1);
        if (err < 0)
           error_check ("DAQ_DB_Config", err);
                                        .
    err = DAQ_Rate (sampleRateDesired, 0, &sampTimebase, &sampInterval);
        if (err < 0)
            error_check ("Samp_DAQ_Rate", err);


    err = DAQ_Rate (scanRateDesired, 1, &scanTimebase, &scanInterval);
        if (err < 0)
            error_check ("Scan_DAQ_Rate", err);


    err = SCAN_Start (1, buffer, numpts, sampTimebase, sampInterval, scanTimebase,
scanInterval);
        if (err < 0)
            error_check ("SCAN_Start", err);


     OpenComConfig (2, 2400L, 2, 7, 1, 512, 512, 0, 0);
     ComWrt (2,"T\15\12",3);

     n = 0;

    while (keyhit() != 1)
    {

        err = DAQ_DB_HalfReady (1, &halfReady, &daqStopped);
            if (err < 0)
                error_check ("DAQ_DB_HalfReady", err);


        if ( halfReady == 1 ) {


/*---------- use RS-232 functions to get data from the balance---------------*/

           ComWrt (2,"SI\15\12",4);
           Delay (1.0);
           ComRd (2, buf, 16);
           Scan (buf, "%s>%s[dt#]%f", &weight);
           scaleData[n] = weight;

/*-------------------------------------------------------------------------*/


            err = DAQ_DB_Transfer (1, binArray, &ptsTfr, &daqStopped);
                if (err < 0)
                    error_check ("DAQ_DB_Transfer", err);


            err = DAQ_VScale (1, chans[0], gain[0], 1.0, 0.0, count, binArray,
voltArray);
                if (err < 0)
                    error_check ("DAQ_VScale", err);
```

```
            time[n]       = Timer();
            temp[n]       = voltArray[0]-v;
            pressure[n]   = voltArray[1]-v;
            incident[n]   = voltArray[2]-v;
            reflected[n]  = voltArray[3]-v;
            FmtOut ("%s<%f[p3]   %f[p3]   %f[p3]   %f[p3]   %f[p3]   %f\n",
                    time[n], temp[n], pressure[n], incident[n], reflected[n],
scaleData[n]);
            n=n+1;


            if ( n == 900 ){
              while (keyhit() != 1){
                 Beep ();
                 Delay(0.5);
              }

              file_name (time, temp, pressure, incident, reflected, scaleData, n);
              CloseInterfaceManager ();
              n = 0;

            }
        }
    }

    CloseCom (2);
    file_name (time, temp, pressure, incident, reflected, scaleData, n);
}


void error_check (func, err)

char func[];
int err;

{
    Fmt(msg, "%s<Function %s returned error %i", func, err);
    MessagePopup (msg);
    exit(1);
}

void file_name (double time[], double temp[], double pressure[], double incident[],
                double reflected[], double scaleData[], int n)
{
    long size;
    int response, result;
    char buffer[20];
    int handle, l, flag;
    char filename[15];

    response = ConfirmPopup ("Do you want to save the data?");
    while ( response == 1 )
    {
        PromptPopup ("Enter file name for freeze dry data:", buffer, 12);
        Fmt(filename, "%s<%s", buffer);
        l = NumFmtdBytes ();
        if ( l != 0 ) {
            result = GetFileSize (filename, &size);
            if ( result == 0 ) {
                response = ConfirmPopup ("File already exists.  Do you want to
replace it?");
                if ( response == 0 ) {
                    l = 0;
                    response = 1;
                }
            }
        }
```

```
        if (l != 0) {
            handle = OpenFile (filename, 2, 0, 1);
            for (i=0; i< n; i++)
                FmtFile (handle,"%s<%f[p3]   %f[p3]   %f[p3]   %f[p3]   %f[p3]
%f[p3]\n",
                  time[i],  temp[i],  pressure[i],  incident[i],  reflected[i],
scaleData[i]);

            CloseFile (handle);
            FmtOut ("%s<Freeze dry data is saved in C:\\LW\\%s\n",filename);
            response = 0;
        }
    }
}
```

VITA

The author, James Dolan, the son of Thomas E. Dolan and Sandra J. Dolan, was born on December 5th, 1968, in Teeneck, New Jersey. He obtained his high school diploma Southington, Connecticut in June 1987. He then attended the University of North Carolina at Charlotte where he received a Bachelor of Science in Mechanical Engineering in May, 1992. After receiving his undergraduate degree, he moved to Blacksburg, Virginia where he attended Virginia Polytechnic Institute and State University. There he completed the requirements for the degree of Master of Science in Mechanical Engineering on September 20th, 1994.